DESIGN METHOD FOR CENTRIFUGAL COMPRESSOR AND CENTRIPETAL TURBINE IMPELLERS

by

RAYMOND E. HOLTHE

S.B., University of Illinois

(1951)

SUBMITTED IN PARTIAL FULFILLMENT OF THE REQUIREMENTS FOR THE DEGREE OF MASTER OF SCIENCE

at the

MASSACHUSETTS INSTITUTE OF TECHNOLOGY

June, 1957

Signature of Author . . . .
Department of Mechanical Engineering, May 20, 1957

Certified by . . . .
Thesis Supervisor

Accepted by . . . .
Chairman, Departmental Committee on Graduate Students

Design Method for Centrifugal Compressor and Centripetal Turbine Impellers

Raymond E. Holthe

Submitted to the Department of Mechanical Engineering on May 20, 1957, in partial fulfillment of the requirements for the degree of Master of Science in Mechanical Engineering.

The design method presented in this thesis in intended to satisfy the need for a simple, rapid, approximate means of obtaining hub and casing shapes for compressor and turbine impellers with straight radial blades.

The method consists of three separate one-dimensional solutions of the equations of motion in a rotating impeller channel. Two solutions are made assuming axial symmetry and the third accounts for variations in fluid properties from blade to blade.

In the first solution, isentropic and axisymmetric flow is assumed and the concept of a mean streamline is introduced. The mean streamline is defined as that streamline which is representative of the flow in the meridional plane. The designer then specifies a velocity distribution along the mean streamline and uses influence equations, developed in this thesis, to compute the corresponding flow area. This solution gives no information as to the shape of the mean streamline.

In the second solution, irrotational, isentropic, and axisymmetric flow is assumed. The designer selects a particular mean streamline and computes the hub and casing shapes, using the flow areas from the first solution. A second set of influence equations is used to determine the variation in fluid properties from hub to casing. The combination of the first and second solutions completely determines the flow in the meridional plane.

The third solution considers the flow in the blade-to-blade plane. Blade surface velocities are computed to investigate blade loading and to examine the possibility of a stagnation area on the pressure surface of the blade.

Combining all three solutions results in a quasi three-dimensional solution which gives a clear physical understanding of the main flow in the impeller channel.

The design method is completely analytic and all calculations may be made by a digital computing machine.

Thesis Supervisor: Ascher H. Shapiro
Title: Professor of Mechanical Engineering

PREFACE

In writing this thesis, I have tried to keep in mind the need for a simple impeller design method suitable for designers with no more than four years of formal engineering training. However, calculus has been used extensively. Mathematics is such a powerful tool that any designer worth his salt should be willing to sit down with pencil, paper, and eraser and calculate before he begins to speculate.

The model of the flow has been based on the one-dimensional approach in order to give a clear physical picture of what is going on in the impeller channel. This means that impellers designed by this method will not be the best impellers it is possible to make -- they must be regarded only as first approximations which are to be modified after performance tests have been run.

My first acknowledgment is to Professor Ascher H. Shapiro, my thesis supervisor, who has generously donated his limited time and unlimited talents in maintaining the technical accuracy and readability of this work. For her accurate typing, I wish to thank Dorothy Mastrorillo. Caterpillar Tractor Co., Peoria, Illinois, has generously provided both the leave of absence and the financial arrangements which were necessary that I might devote full time to graduate study. Finally, and most important, I express my appreciation to Donna, surely the most patient and understanding of wives.

TABLE OF CONTENTS

TABLE OF CONTENTS

I. INTRODUCTION

A. Need for a design method

The ability of centrifugal compressors and centripetal turbines to handle a large pressure ratio in a single stage is being exploited fully at the present time. Small gas turbine engines for road vehicles and helicopters appear to be the most promising applications. At high pressure ratios, compressor and turbine impellers are highly stressed and the trend has been toward impellers with straight radial blades. Radial blades have no bending stresses due to centrifugal force and straight blades are the least expensive to manufacture. I believe that this trend will continue and that the majority of the small gas turbine engines of the future will use single stage impellers with straight radial blades. It is for this reason that a simple, rapid, design method for determining hub and casing shapes for centrifugal compressor and centripetal turbine impellers with straight radial blades will be a valuable addition to the turbomachinery literature.

B. Literature survey with comments

The following is a list of those published books and papers relating specifically to compressors and turbines which I have found to be the most useful in writing this thesis.

Reference 3- "Steam and Gas Turbines" by Stodola

This is certainly a classic and is the logical starting point for any investigation in the turbomachinery field. The Lorenz axial symmetry analysis, basic to most impeller design methods, is developed on pages 990 and 991.

Reference 4- "A Rapid Approximate Method for the Design of Hub-Shroud Profiles of Centrifugal Impellers of Given Blade Shape", NACA TN 3399.

This reference presents a graphical design method which requires about 40 hours for a solution. The flow is assumed to be isentropic, steady, non-viscous, and compressible. The method consists in specifying a blade shape, hub shape, and hub velocity distribution and then drawing, by experience, a streamline adjacent to the hub. The analysis of reference 7 is used to compute the velocity and density along the assumed streamline. The one-dimensional continuity equation, based on the velocity and density at the midpoint of the streamtube formed by the two streamlines, is used to check the mass flow along the streamtube. If the mass flows at each station are not equal (within prescribed limits), a new streamline is assumed and the process is repeated. The final streamline becomes the base line for a new streamtube. The casing shape is determined by the streamline which finally passes the design mass flow.

The method was used with 3, 5, and 9 streamtubes and it was found that more than 3 streamtubes did not appreciably affect the resulting casing shape. This result leads me to believe that using just 1 streamtube (the basis of this thesis) will result in acceptable hub and casing shapes with a specified velocity distribution along the mean streamline. Also, the method of this thesis can be set up for a digital computer and 40 hours of hand calculations and graphical measurements are eliminated.

Reference 5- "A Rapid Approximate Method for Determining Velocity Distribution on Impeller Blades of Centrifugal Compressors", NACA TN 2421.

This reference presents a method for computing blade surface velocities after the impeller is completely designed. The method is essentially an extension of that given in Appendix D of reference 7. The effect of slip is included here but not in reference 7. It was shown in reference 4 that including slip did not appreciably affect the casing shape but did affect the blade surface velocities. However, neglecting slip is conservative as the blade loading is decreased by slip (good), as shown in reference 4.

Reference 6- "A General Theory of Three-Dimensional Flow in Subsonic and Supersonic Turbomachines of Axial, Radial, and Mixed Flow Types", NACA TN 2604.

Wu's analyses and design methods are the most comprehensive that I know. He treats the flow as being 3 dimensional in the analyses and as quasi-3 dimensional in the design methods. His methods would yield very accurate hub and casing shapes but are so long and complex that, as far as I know, no one uses them.

Reference 7- "Method of Analysis for Compressible Flow Through Mixed-Flow Centrifugal Impellers of Arbitrary Design", NACA Report 1082.

The analysis developed in this reference is the basis of the most recent NACA publication on impeller design (reference 4). The analysis can be applied to any impeller with radial blade elements (the blades are otherwise arbitrary). Appendices B, C, and D develop equations for pressure and velocity variations from hub to casing and from blade to blade for these arbitrary blades. These equations reduce to the equations presented in this thesis when straight radial blades are used.

Reference 14- "Two-Dimensional Compressible Flow in Centrifugal Compressors with Straight Blades", NACA Report 954.

This is an early (1949) analysis of compressible, non-viscous, steady, isentropic flow which is assumed to lie on the surface of a cone. The flow is assumed to be uniform normal to the cone (from hub to casing). This reference derives the commonly used slip factor equation:

$$f_s = 1 - \frac{2}{Z}$$

where Z is the number of blades at the outlet.

Reference 15- "Some Elements of Gas Turbine Performance", paper presented at SAE meeting, March 6-8, 1956.

The centrifugal compressor and centripetal turbine appear to have a bright future in small gas turbine engines, such as engines for road vehicles. This reference presents a clear, detailed discussion of gas turbines in general and gas turbines for road vehicles in particular.

Reference 16- "Approximate Design Method for High Solidity Blade Elements in Compressors and Turbines", NACA TN 2408.

The design method developed here leads to a blade shape for a prescribed surface of revolution about the axis of rotation and prescribed blade surface velocities. It does not determine the hub and casing shapes. The method may lead to blade shapes which are not acceptable for high tip speeds.

Reference 17- "Some NACA Research on Centrifugal Compressors", ASME Transactions, 1953.

A concise resume of the extensive work done by NACA up to 1952 and covers inducer, impeller, and diffuser research. It is an extremely valuable summary of all phases of compressor research by the leading U. S. agency in this field.

Reference 18- "Theoretical and Experimental Analysis of One-Dimensional Compressible Flow in a Rotating Radial-Inlet Impeller Channel", NACA TN 2691.

An excellent discussion of one-dimensional flow in a rotating channel. Effects of friction, choking, and shock formation are included. The effect of losses was found to be similar to the effect of a reduction of flow area. The losses in a rotating channel were placed in four catagories:

1. Friction loss due to the viscosity of the fluid. Friction loss is proportional to the square of the relative velocity and increases rapidly with flow rate.

2. Incidence loss due to a sudden enlargement or contraction of the inlet flow area. Incidence loss occurs at flow rates different from the design flow rate. At flow rates less than design, the situation is as shown by Figure A.

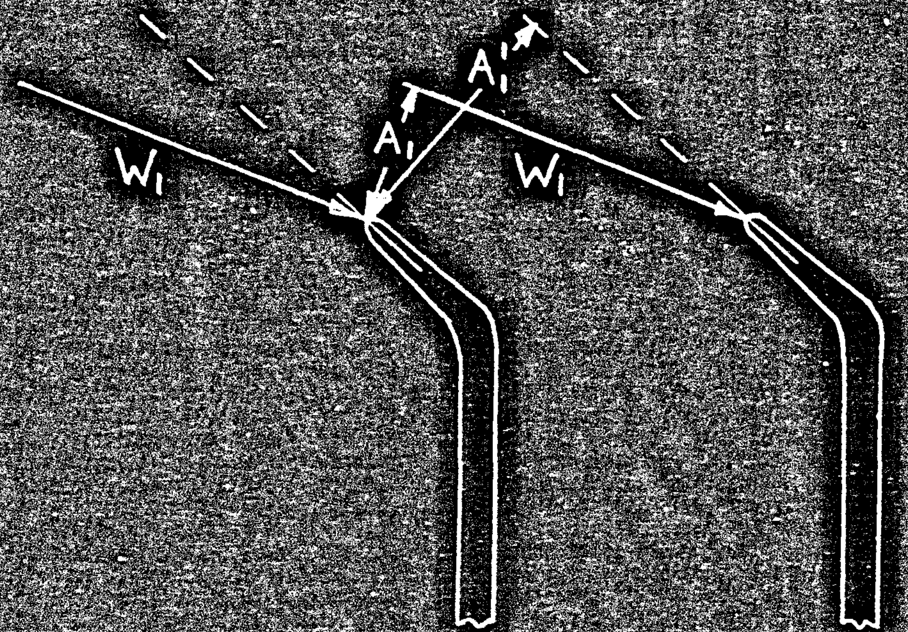

Figure A

Inlet condition at flow rate less than design

The actual flow area A_1 is less than the geometric flow area A_1' and a sudden expansion loss occurs as W_1 decreases suddenly to the value W_1'. This loss is proportional to the product

$$\frac{W_1^2}{2g_o}(1 - A_1/A_1')^2$$

and is approximately constant at all flow rates less than design because W_1 and A_1 both decrease. At flow rates greater than design the situation is as shown by Figure B.

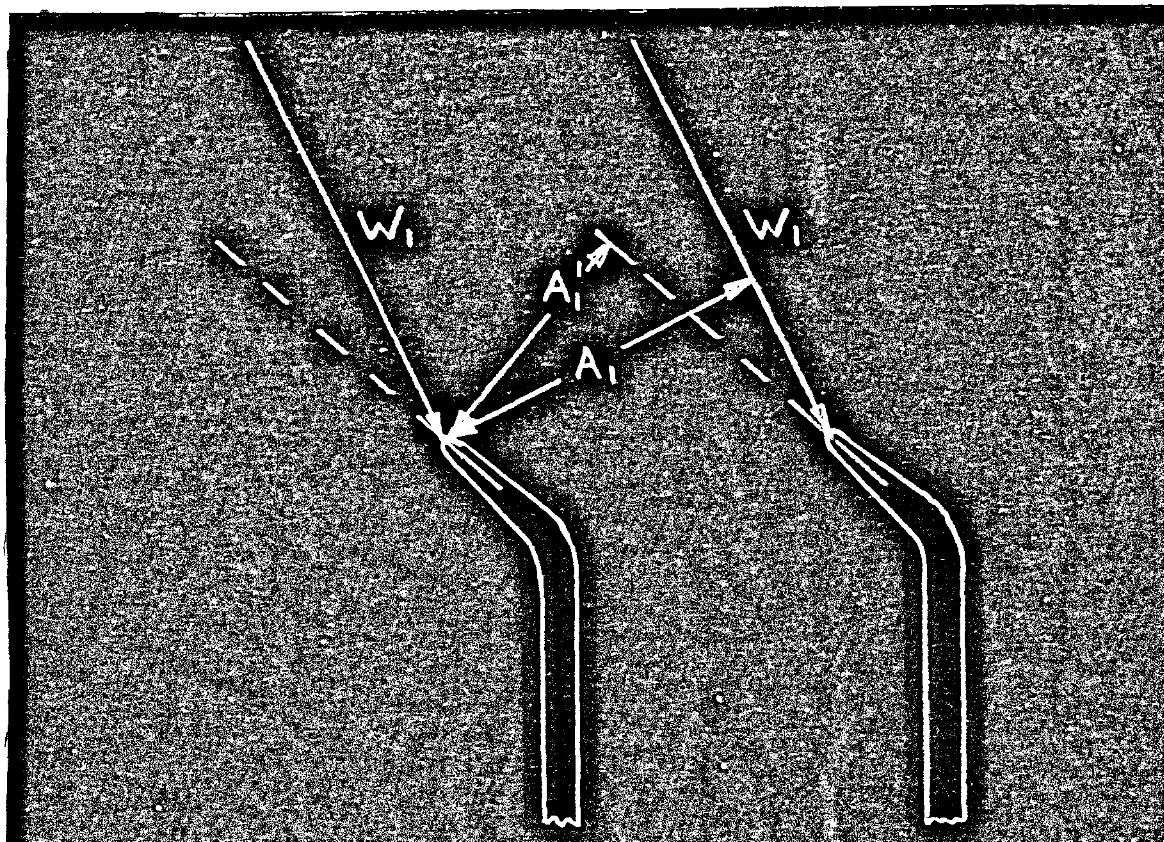

Figure B

Inlet condition at flow rate greater than design

The actual flow area A_1 is greater than the geometric flow area A_1' and a sudden contraction loss occurs as W_1 increases suddenly to the value W_1'. This loss is proportional to the product

$$\frac{W_1'^2}{2g_o}(1 - A_1'/A_1)^2$$

and increases rapidly as the flow rate exceeds design because W_1' and A_1 both increase.

3. Blade loading loss due to boundry layer separation and secondary flow on the blade surfaces. This loss decreases as the flow rate is increased because the greater momentum in the main flow delays boundry layer separation.

4. Shock loss when operating in the range of supersonic relative velocities. This loss occurs at large flow rates if the static pressure at the channel outlet is too great for completely supersonic flow to the outlet.

Reference 19- "Centrifugal Compressors"
Reference 20- "Design of Radial Flow Turbines"

For complete, up to date information on centrifugal compressors and centripetal turbines, I recommend references 19 and 20. These references are the most complete that I know.

Units and dimensions

Seven independent physical units of measure are used in this thesis:

1. Force measured in pounds of force, lbf
2. Mass, measured in pounds of mass, lbm
3. Length, measured in feet, ft
4. Time, measured in seconds, sec
5. Heat, measured in British thermal units, BTU
6. Temperature, measured in degrees Rankine, R
7. Angle, measured in radians, rad

As the equations derived in this thesis are valid only in Newtonian reference frames (inertial or accelerating) and thus relativity and nuclear reactions are excluded, we may use Newton's second law of motion to relate the first four of the above units of measure:

$$F = \frac{Ma}{g_o}$$

where F is the unbalanced force acting on a system of fixed identity, lbf; M is the total mass of the system, lbm; a is the acceleration of the mass-center of the system, ft/sec^2; and g_o is a constant of proportionality whose numerical value must be determined by experiment. It has been found by countless experiments that a one pound unbalanced force when acting on a mass of 32.174 lbm will produce an acceleration of one ft/sec^2, irregardless of the location where the experiments are performed. Thus, Newton's second law may be written

$$1 \text{ lbf} = \frac{32.174 \text{ lbm} \times 1 \text{ ft/sec}^2}{g_o}$$

$$1 = 32.174 \text{ lbm ft/sec}^2 \text{ lbf} \equiv g_o$$

g_o, being really equal to the pure number unity, may be introduced into <u>any</u> equation to cancel units, whether Newton's law is used or not and, indeed, if motion is involved or not.

Similarly, experiments by Joule and others have shown that, in Newtonian reference frames, heat and work are related by Joules law:

$$Q = \frac{W}{J}$$

where Q is the heat flowing into a system of fixed identity, BTU; W is the work flowing out of the system so as to maintain the system at its initial temperature, ft lbf; and J is a constant of proportionality whose value is determined by experiment. Again, countless experiments, irregardless of location, have shown that one BTU of heat flowing into a system results in 778.2 ft lbf of work flowing out of the system to maintain the temperature of the system constant. Thus, Joules' law may be written

$$1 \text{ BTU} = \frac{778.2 \text{ ft lbf}}{J}$$

$$1 = 778.2 \text{ ft lbf/BTU} \equiv J$$

J, like g_o, is really a pure number having the value unity, and may be introduced into any equation to cancel units, whether heat or work is involved or not.

II. EXPLANATION OF THE DESIGN METHOD

A. List of assumptions

The design method presented in this thesis is based on the following assumptions:

1. The impeller has straight radial blades.
2. The impeller rotates with constant angular velocity about a fixed (Z) axis.
3. The fluid flowing through the impeller is a perfect gas with zero viscosity.
4. The flow within the impeller has these characteristics:
    a. It may be represented by a mean streamline which follows the approximate geometric center of the impeller channel.
    b. It is isentropic, that is, there is no heat transfer and the flow is perfectly reversible.
    c. It is irrotational, that is, its total energy is constant both along the mean streamline and normal to the mean streamline.
    d. It is steady, that is, values of flow properties at a fixed point in the channel do not change with time.
    e. It is axisymmetric, that is, values of flow properties are the same in all meridional (axial-radial) planes.

5. Gravity effects are negligible.

6. The absolute acceleration of the earth with respect to the fixed stars is negligible.

B. Flow along the mean streamline

It is well known that the relative flow in an impeller channel, although steady, is three-dimensional in nature. Fluid properties vary with distance in all three coordinate directions. The solution of a three-dimensional flow is extremely complex (reference 6) and, for engineers with no more than undergraduate calculus, practically impossible. It is for this reason that one and two-dimensional approximations are commonly used.

The one-dimensional approximation, that is, assuming that the rates of change of fluid properties in all directions other than along a streamline are negligible compared with the rates of change along the streamline, has several extremely important advantages. Simply and rapidly, it yields results which are valid in the engineering sense and which present a clear physical understanding of the significant features of the flow.

Using the one-dimensional approach, we assume that the flow in an impeller channel is characterized by one particular streamline, which we call the "mean" streamline. Values of fluid properties along the mean streamline are assumed to be the mean values from hub to casing and from blade to blade.

This assumption, to be valid, restricts the position of the mean streamline -- it must lie (approximately) along the centerline of the channel.

Appendix J presents the results of a one-dimensional analysis of impeller relative flow, within the assumptions presented previously. Using these results (collected in Table 1), we specify, by experience or by fluid mechanics theory, a velocity distribution along the mean streamline. If this distribution is linear with radius, or constant, the required flow area at any radius is computed in closed form, as shown in Appendix J. Otherwise, numerical integration must be used. <u>All</u> channels having this calculated area-radius relationship are equivalent as far as the one-dimensional analysis is concerned. We must turn to a two-dimensional analysis to select one particular channel from the infinite number which are satisfied by the calculated area-radius relationship.

C. <u>Property changes normal to the mean streamline</u>

Table 2, in Appendix K, presents the results of a one-dimensional analysis of property changes normal to a relative streamline. By combining these results with those summarized in Table 1, we have a quasi two-dimensional solution of the flow in the meridional plane, since, with straight radial blades and axial symmetry, the mean streamline must lie in this plane. This quasi two-dimensional solution enables us to select the one particular channel which fulfills our design requirements (such as space or weight limitations or the need for highest possible efficiency). The selection is accomplished by assuming a mean streamline and then computing the corresponding hub and casing profiles and velocities. If these profiles or velocities are unacceptable, a new mean streamline is assumed and the calculations are repeated. Originally, I had planned to develop a design method in which the hub and casing velocities are specified and the corresponding hub, mean streamline, and casing shapes are computed. This procedure was found to be unacceptable as the calculated mean streamline would not, in general, lie on the (approximate) centerline of the channel. In the proposed method, all computations may be done on an automatic computer and, for a fixed set of design parameters, several assumed mean streamlines may be fed into the computer and the designer (or technician) merely plots the results. This procedure also gives a clear picture of the effects of mean streamline shape on the flow in the meridional plane.

D. Property changes from blade to blade

Having an approximate picture of the flow in the meridional plane, we use the analysis of Appendix N to compute property variations from blade to blade. These variations are intimately associated with the number of impeller blades and the analysis of Appendix N helps us to understand the influence of blade number on blade loading and behavior of the boundry layer. By combining the two-dimensional meridional plane solution with the one-dimensional blade to blade solution, we obtain a quasi three-dimensional solution throughout the entire impeller. Thus, with the aid of this quasi three-dimensional solution, we can evaluate the gross effects of hub shape, casing shape, and blade number on size, weight, and efficiency.

E. <u>Design procedure for a compressor</u>

A. Preliminary steps:

1. Specify the properties of the perfect gas which is to be used
    a. Inlet stagnation pressure and temperature
    b. Outlet stagnation pressure
    c. Mass flow
    d. Ratio of specific beats
    e. Molecular weight
2. Compute the following:
    a. Tip speed
    b. Casing radius, tip radius, and angular velocity
    c. Hub radius for known (or assumed) blade number and thickness at inducer inlet
    d. Properties at the inducer inlet
    e. Properties at the impeller inlet, including the radius to the mean streamline.

B. Hub and casing design:

1. Specify the relative velocity distribution along the mean streamline
2. Using the analysis given in Appendix J, compute the corresponding area distribution normal to the mean streamline at specified stations on the mean streamline
3. Specify the shape of the mean streamline (its angle with the Z axis) and compute its radius of curvature at all stations
4. Divide the areas computed in step B2 into two parts -- one area extending from the hub (as yet undetermined) to the mean streamline, the other area from the mean streamline to the casing (also not yet determined). This step is necessary to be certain that the mean streamline will lie approximately midway between the hub and casing
5. Using the angles specified in step B3 and the areas of step B4, compute the hub and casing radii at all stations. The hub and casing are now completely determined.

C. Evaluation of the hub and casing design:

1. Using the mean streamline velocities specified in step B1, the radii of curvature of the mean streamline computed in step B3, the hub and casing radii from step B5, and the analysis of

Appendix K, compute the hub and casing relative velocities at all stations.

2. Plot the results of steps B3 and C1. On the basis of space or weight limitations and boundry layer theory (or experience) evaluate the hub and casing design. If unacceptable, repeat the design, beginning with step B3, until satisfactory shapes and velocities are produced. This completes the design in the meridional plane.

D. Checking blade loading

1. Using the following:
   a. Properties at the impeller inlet from step A2e
   b. Velocities along the mean streamline from step B1
   c. Areas normal to the mean streamline from step B2
   d. Mean streamline angles from step B3
   e. Known (or assumed) blade number and thickness at all stations
   f. The analysis of Appendix N,

   compute the blade surface velocities.

2. Plot the results of step D1. On the basis of boundry layer theory (or experience) evaluate the choice of blade number and

thickness made in step D1e. If unacceptable, repeat the design, beginning with step D1e until satisfactory velocities are produced. Since blade number and thickness have only second-order effects on the hub and casing shapes, it is not necessary to redesign the hub and casing until step D2 is considered satisfactory. The final design is then made, beginning with step A2e.

A detailed numerical example is given in Appendices M and N.

III. SUGGESTIONS FOR FUTURE WORK

Time limitations prevented my working out a detailed turbine design. The equations developed in this thesis are based on first principles and are valid for turbines as well as compressors. The details of design, however, will be different. The flow enters a turbine impeller after leaving a set of nozzles (rather than an inducer) and leaves the impeller by entering an exducer (rather than a diffuser). Thus, the <u>leaving</u> flow must be analyzed, rather than the entering flow as was done in Appendix L. Centripetal turbine design methods are even more scarce than compressor design methods and I hope that this thesis will be the starting point for a similar detailed turbine design.

IV. APPENDICES

Appendix A

$\bar{a}_P$	vector absolute acceleration of P
$\bar{i}$, $\bar{j}$, $\bar{k}$	unit vectors in the x, y, z directions
O_A	origin of accelerating reference frame
O_I	origin of inertial reference frame
P	a particle of fixed identity moving in any manner in an accelerating reference frame
$\bar{R}_A$	position vector of P from O_A
$\bar{R}_I$	position vector of P from O_I
$\bar{R}_O$	position vector of O_A from O_I
t_A	time as measured in the accelerating reference frame
t_I	time as measured in the inertial reference frame
$\bar{V}_P$	vector absolute velocity of P
$\bar{W}$	vector relative velocity of P
W_x, W_y, W_z	scalar components of $\bar{W}$ in the x, y, z directions
X_A, Y_A, Z_A	orthogonal directions defining an arbitrarily accelerating reference frame
X_I, Y_I, Z_I	orthogonal directions defining an inertial reference frame which is fixed in outer space

x

y instantaneous scalar coordinates of P with respect to

z O_A in the X_A Y_A Z_A accelerating reference frame

∇ vector operator defined by equation (16)

$\bar{\omega}$ vector absolute rotation of the accelerating reference frame

ω_x

ω_y scalar components of $\bar{\omega}$ in the x, y, z directions

ω_z

Appendix A

MOTION OF A PARTICLE IN AN ACCELERATING REFERENCE FRAME

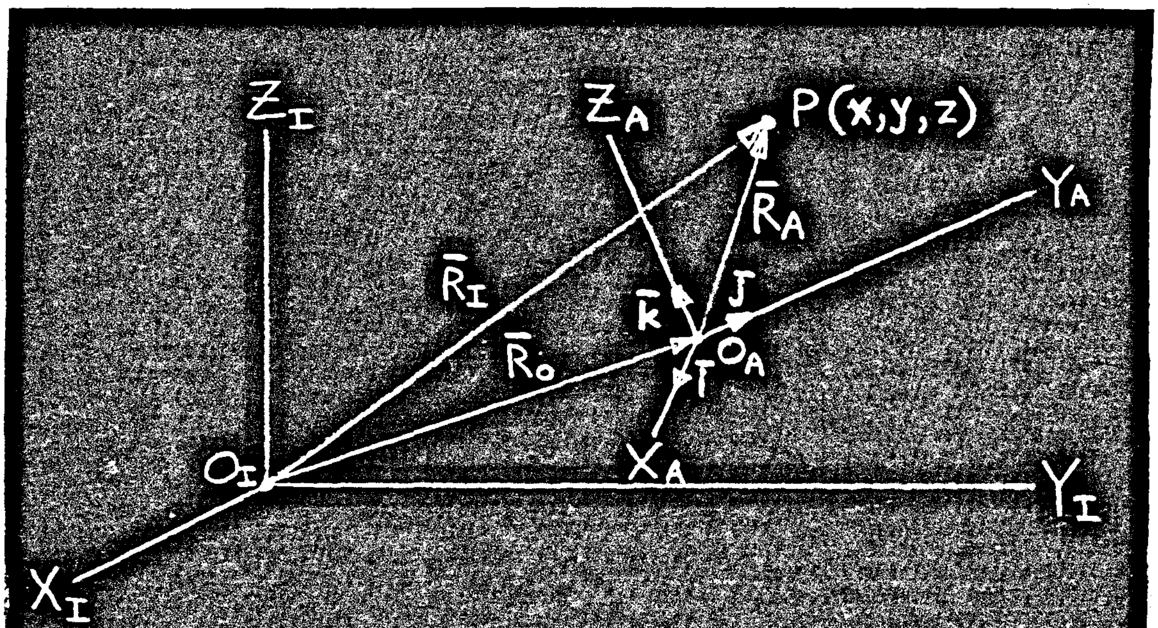

Figure 1

Inertial (I) frame and accelerating (A) frame

X_I Y_I Z_I determine an orthogonal inertial reference frame, fixed in outer space (not fixed to the earth).

X_A Y_A Z_A determine an orthogonal reference frame, accelerating in any manner with respect to the inertial (I) frame.

P is a particle moving in any manner in the accelerating (A) frame and instantaneously located at the point (x, y, z) in the A frame.

$\bar{R}_I$ is the position vector of P with respect to O_I.

$\bar{R}_A$ is the position vector of P with respect to O_A.

$\bar{R}_o$ is the position vector of O_A with respect to O_I.

$\bar{I}$, $\bar{J}$, and $\bar{K}$ are unit orthogonal vectors in the X_A, Y_A, Z_A directions. $\bar{I}$, $\bar{J}$, and $\bar{K}$ are constant in magnitude <u>and</u> direction in the A frame. In general, they are constant <u>only in magnitude</u> in the I frame since the A frame may be rotating with respect to the I frame and, in that case, the directions of $\bar{I}$, $\bar{J}$, and $\bar{K}$ would be changing in the I frame.

From Figure 1,

$$\bar{R}_I = \bar{R}_o + \bar{R}_A$$

The derivative of $\bar{R}_I$ with respect to time in the I frame is the velocity of P in the I frame (the "absolute" velocity of P), $\bar{V}_P$.

$$\bar{V}_P = \frac{d\bar{R}_I}{dt_I} = \frac{d\bar{R}_o}{dt_I} + \frac{d\bar{R}_A}{dt_I} \tag{1}$$

From Figure 1,

$$\bar{R}_A = \bar{I}x + \bar{J}y + \bar{K}z \tag{2}$$

Differentiating (2),

$$\frac{d\bar{R}_A}{dt_I} = \bar{I}\frac{dx}{dt_I} + \frac{d\bar{I}}{dt_I}x + \bar{J}\frac{dy}{dt_I} + \frac{d\bar{J}}{dt_I}y + \bar{K}\frac{dz}{dt_I} + \frac{d\bar{K}}{dt_I}z$$

Grouping terms,

$$\frac{d\bar{R}_A}{dt_I} = [\bar{I}\frac{dx}{dt_I} + \bar{J}\frac{dy}{dt_I} + \bar{K}\frac{dz}{dt_I}] + [\frac{d\bar{I}}{dt_I}x + \frac{d\bar{J}}{dt_I}y + \frac{d\bar{K}}{dt_I}z] \tag{3}$$

Since x, y, and z are scalars, they have identical time derivatives in both the I and A frames. The first bracket in (3) may be written:

$$\left[\bar{i}\frac{dx}{dt_I} + \bar{j}\frac{dy}{dt_I} + \bar{k}\frac{dz}{dt_I}\right] = \left[\bar{i}\frac{dx}{dt_A} + \bar{j}\frac{dy}{dt_A} + \bar{k}\frac{dz}{dt_A}\right] \qquad (4)$$

The derivatives of the unit vectors in the second bracket of (3) are perpendicular to these vectors and may be written:

$$\frac{d\bar{i}}{dt_I} = \bar{\omega} \times \bar{i}, \quad \frac{d\bar{j}}{dt_I} = \bar{\omega} \times \bar{j}, \quad \frac{d\bar{k}}{dt_I} = \bar{\omega} \times \bar{k} \qquad (5)$$

where $\bar{\omega}$ is the vector rotation of the A frame with respect to the I frame.

$$\bar{\omega} = \bar{i}\,\omega_x + \bar{j}\,\omega_y + \bar{k}\,\omega_z \qquad (6)$$

Expanding (5), we have, using (6),

$$\frac{d\bar{i}}{dt_I} = -\bar{k}\,\omega_y + \bar{j}\,\omega_z \qquad (7a)$$

$$\frac{d\bar{j}}{dt_I} = \bar{k}\,\omega_x - \bar{i}\,\omega_z \qquad (7b)$$

$$\frac{d\bar{k}}{dt_I} = -\bar{j}\,\omega_x + \bar{i}\,\omega_y \qquad (7c)$$

Combining (3), (4), and (7):

$$\frac{d\bar{R}_A}{dt_I} = \left[\bar{i}\frac{dx}{dt_A} + \bar{j}\frac{dy}{dt_A} + \bar{k}\frac{dz}{dt_A}\right]$$

$$+ \left[-\bar{k}\,\omega_y\,x + \bar{j}\,\omega_z\,x + \bar{k}\,\omega_x\,y - \bar{i}\,\omega_z\,y - \bar{j}\,\omega_x\,z + \bar{i}\,\omega_y\,z\right] \qquad (8)$$

The first bracket of (8) is the expansion of $\frac{d\bar{R}_A}{dt_A}$, the velocity of P in the A frame (the "relative" velocity of P), since $\bar{i}$, $\bar{j}$, and $\bar{k}$ are constant in magnitude and direction in the A frame. The second bracket of (8) is the expansion of $\bar{\omega} \times \bar{R}_A$. Inserting these equivalents into (8), we have:

$$\frac{d\bar{R}_A}{dt_I} = \frac{d\bar{R}_A}{dt_A} + \bar{\omega} \times \bar{R}_A \qquad (9)$$

Combining (1) and (9):

$$\bar{V}_P \equiv \frac{d\bar{R}_I}{dt_I} = \frac{d\bar{R}_o}{dt_I} + \frac{d\bar{R}_A}{dt_A} + \bar{\omega} \times \bar{R}_A \qquad (10)$$

From (9) we see that the derivative of <u>any</u> vector in the A frame with respect to time in the I frame is equal to the derivative of that vector with respect to time in the A frame plus the vector product of that vector with $\bar{\omega}$. We now make use of this fact in differentiating $\bar{V}_P$ to obtain $\bar{a}_P$, the acceleration of P in the I frame (the absolute acceleration of P). From (10),

$$\bar{a}_P \equiv \frac{d\bar{V}_P}{dt_I} = [\frac{d^2\bar{R}_o}{dt_I^2}] + [\frac{d}{dt_I}(\frac{d\bar{R}_A}{dt_A} + \bar{\omega} \times \bar{R}_A)] \qquad (11)$$

From (9), the second bracket of (11) is:

$$\frac{d}{dt_I}(\frac{d\bar{R}_A}{dt_A} + \bar{\omega} \times \bar{R}_A) = [\frac{d^2\bar{R}_A}{dt_A^2}] + [\bar{\omega} \times \frac{d\bar{R}_A}{dt_A}]$$

$$+ [\frac{d}{dt_A}(\bar{\omega} \times \bar{R}_A)] + [\bar{\omega} \times \bar{\omega} \times \bar{R}_A] \qquad (12)$$

Defining the relative velocity of P as $\bar{W}$, the first bracket of (12) is:

$$\frac{d^2\bar{R}_A}{dt_A{}^2} \equiv \frac{d}{dt_A}\left(\frac{d\bar{R}_A}{dt_A}\right) \equiv \frac{d\bar{W}}{dt_A} = \frac{D\bar{W}}{Dt_A} \qquad (13)$$

Since $\bar{W}$ is the relative velocity of a particle of <u>fixed identity</u>, we use the special notation capital D to denote substantial differentiation while following the motion of this particle. $\bar{W}$ is a function of space and time (x, y, z, and t_A), thus:

$$\frac{D\bar{W}}{Dt_A} = \frac{\partial \bar{W}}{\partial x}\frac{Dx}{Dt_A} + \frac{\partial \bar{W}}{\partial y}\frac{Dy}{Dt_A} + \frac{\partial \bar{W}}{\partial z}\frac{Dz}{Dt_A} + \frac{\partial \bar{W}}{\partial t_A} \qquad (14)$$

But, $\frac{Dx}{Dt_A}$, $\frac{Dy}{Dt_A}$, and $\frac{Dz}{Dt_A}$ are the scalar components of $\bar{W}$ in the x, y, and z directions, respectively.

$$\frac{D\bar{W}}{Dt_A} = W_x\frac{\partial \bar{W}}{\partial x} + W_y\frac{\partial \bar{W}}{\partial y} + W_z\frac{\partial \bar{W}}{\partial z} + \frac{\partial \bar{W}}{\partial t_A} \qquad (15)$$

(15) may be written in more compact form by introducing the vector operator, ∇. In x, y, z coordinates,

$$\nabla = \bar{i}\frac{\partial}{\partial x} + \bar{j}\frac{\partial}{\partial y} + \bar{k}\frac{\partial}{\partial z} \qquad (16)$$

$$\bar{W}\cdot\nabla = (\bar{i}\,W_x + \bar{j}\,W_y + \bar{k}\,W_z)\cdot\left(\bar{i}\frac{\partial}{\partial x} + \bar{j}\frac{\partial}{\partial y} + \bar{k}\frac{\partial}{\partial z}\right)$$

$$= W_x\frac{\partial}{\partial x} + W_y\frac{\partial}{\partial y} + W_z\frac{\partial}{\partial z} \qquad (\text{NOTE: } \bar{W}\cdot\nabla \neq \nabla\cdot\bar{W})$$

$$(17)$$

Thus, (15) may be written,

$$\frac{D\bar{W}}{Dt_A} = (\bar{W} \cdot \nabla)\, \bar{W} + \frac{\partial \bar{W}}{\partial t_A} \qquad (18)$$

The second bracket of (12), from (13), is:

$$\bar{\omega} \times \frac{d\bar{R}_A}{dt_A} \equiv \bar{\omega} \times \bar{W} \qquad (19)$$

The third bracket of (12), from (13), is:

$$\frac{d}{dt_A}(\bar{\omega} \times \bar{R}_A) = \bar{\omega} \times \bar{W} + \frac{d\bar{\omega}}{dt_A} \times \bar{R}_A \qquad (20)$$

Introducing (12), (13), (18), (19), and (20) into (11):

$$\bar{a}_P = [\frac{d^2\bar{R}_o}{dt_I^2}] + [(\bar{W} \cdot \nabla)\, \bar{W} + \frac{\partial \bar{W}}{\partial t_A}]$$

$$+ [\frac{d\bar{\omega}}{dt_A} \times \bar{R}_A + \bar{\omega} \times \bar{\omega} \times \bar{R}_A] + [2\bar{\omega} \times \bar{W}] \qquad (21)$$

(21) is the basic kinematic equation of motion of a particle moving in any manner in a reference frame (the A frame) which is itself accelerating in any manner with respect to an inertial frame (the I frame). In words, the absolute acceleration of P equals the absolute acceleration of the origin of the A frame (first bracket) plus the total acceleration of P if the A frame were <u>not</u> accelerating (the total acceleration of P as seen by an observer stationed <u>in</u> the A frame and thus unaware

of the acceleration of the A frame)(second bracket) plus the sum of the tangential and normal accelerations of P about O_A due to the rotation of the A frame if P were <u>fixed</u> in the A frame (third bracket) plus the "Coriolis" acceleration of P (fourth bracket). All of the above was adapted from reference 1, p. 249-252.

For our purposes, we consider the inertial frame as being fixed to the earth, with O_I at the center of the earth. This means we are neglecting the absolute acceleration of the earth with respect to the fixed stars. This leads to insignificant errors for the present work since the angular velocity of the earth is only about 7×10^{-5} rad per sec (reference 1, p. 269). Our A frame is defined as being attached to the surface of the earth and rotating with an angular velocity $\bar{\omega}$ about the Z_A axis only. Thus, $\bar{\omega}$ has no components in the X_A and Y_A directions and

$$\bar{\omega} \equiv \bar{k}\,\omega_z \equiv \bar{k}\,\omega$$

The distance $|\bar{R}_o|$ is assumed to be constant and we neglect the angular velocity of $\bar{R}_o$ (the angular velocity of the earth). Thus,

$$\frac{d^2\bar{R}_o}{dt_I^{\,2}} \equiv 0$$

We also assume that $\bar{\omega}$ is constant in magnitude, thus

$$\frac{d\bar{\omega}}{dt_A} = \bar{k}\,\frac{d\omega}{dt_A} \equiv 0$$

Equation (21) reduces to:

$$\bar{a}_P = (\bar{W} \cdot \nabla)\,\bar{W} + \frac{\partial \bar{W}}{\partial t_A} + \bar{k}\omega \times (\bar{k}\omega \times \bar{R}_A) + 2\bar{k}\omega \times \bar{W} \qquad (22)$$

Appendix B

h_1
h_2 lengths of $\bar{U}$ vectors in the u_1, u_2, u_3 directions
h_3

$\bar{i}$
$\bar{j}$ unit vectors in x, y, z directions
$\bar{k}$

O_A origin of accelerating reference frame

P a particle of fixed identity moving in any manner in an accelerating reference frame

$\bar{R}_A$ position vector of P from O_A

$\bar{U}_1$
$\bar{U}_2$ vectors tangent to arbitrary orthogonal curvilinear surfaces at the instantaneous location of P
$\bar{U}_3$

$\bar{u}_1$
$\bar{u}_2$ unit vectors tangent to arbitrary orthogonal curvilinear surfaces at the instantaneous location of P
$\bar{u}_3$

u_1
u_2 scalar coordinates of P in an arbitrary orthogonal reference frame
u_3

$\bar{W}$ vector relative velocity of P

W_1
W_2 scalar components of $\bar{W}$ in the u_1, u_2, u_3 directions
W_3

X_A, Y_A, Z_A	orthogonal directions defining an accelerating reference frame
x, y, z	scalar coordinates of P in the X_A Y_A Z_A accelerating reference frame
∇	vector operator using u_1, u_2, u_3 coordinates - defined by equation (28)
$\bar{\omega}$	vector absolute rotation of the accelerating reference frame
ω_1, ω_2, ω_3	scalar components of $\bar{\omega}$ in the u_1, u_2, u_3 directions

Appendix B

VECTORS IN GENERAL CURVILINEAR COORDINATES

Let u_1, u_2, and u_3 be any orthogonal curvilinear coordinates which form a <u>right-handed system</u>. For example, x, y, and z in Appendix A form a right-handed system. If $\bar{R}_A$ is the position vector of P from O_A,

$$\bar{R}_A = \bar{i}x + \bar{j}y + \bar{k}z \tag{23}$$

We now define the following:

$$\bar{U}_1 \equiv \frac{\partial \bar{R}_A}{\partial u_1} \tag{24a}$$

$$\bar{U}_2 \equiv \frac{\partial \bar{R}_A}{\partial u_2} \tag{24b}$$

$$\bar{U}_3 \equiv \frac{\partial \bar{R}_A}{\partial u_3} \tag{24c}$$

$$h_1 \equiv |\bar{U}_1| \tag{25a}$$

$$h_2 \equiv |\bar{U}_2| \tag{25b}$$

$$h_3 \equiv |\bar{U}_3| \tag{25c}$$

$$\bar{u}_1 \equiv \frac{\bar{U}_1}{h_1} \tag{26a}$$

$$\bar{u}_2 \equiv \frac{\bar{U}_2}{h_2} \tag{26b}$$

$$\bar{u}_3 \equiv \frac{\bar{U}_3}{h_3} \tag{26c}$$

The $\overline{U}$'s are vectors tangent to the coordinate surfaces; the h's are the lengths of the $\overline{U}$'s; and the $\overline{u}$'s are unit vectors tangent to the coordinate surfaces.

In these general coordinates:

$$\overline{W} = \overline{u}_1 W_1 + \overline{u}_2 W_2 + \overline{u}_3 W_3 \qquad (27a)$$

$$\overline{\omega} = \overline{u}_1 \omega_1 + \overline{u}_2 \omega_2 + \overline{u}_3 \omega_3 \qquad (27b)$$

$$\nabla = \frac{\overline{u}_1}{h_1} \frac{\partial}{\partial u_1} + \frac{\overline{u}_2}{h_2} \frac{\partial}{\partial u_2} + \frac{\overline{u}_3}{h_3} \frac{\partial}{\partial u_3} \qquad (28)$$

$$\nabla \cdot \overline{W} = \frac{1}{h_1 h_2 h_3} \left[\frac{\partial (h_2 h_3 W_1)}{\partial u_1} + \frac{\partial (h_1 h_3 W_2)}{\partial u_2} + \frac{\partial (h_1 h_2 W_3)}{\partial u_3} \right] \qquad (29)$$

$$\nabla \times \overline{W} = \frac{1}{h_1 h_2 h_3} \begin{vmatrix} h_1 \overline{u}_1 & h_2 \overline{u}_2 & h_3 \overline{u}_3 \\ \frac{\partial}{\partial u_1} & \frac{\partial}{\partial u_2} & \frac{\partial}{\partial u_3} \\ h_1 W_1 & h_2 W_2 & h_3 W_3 \end{vmatrix} \qquad (30)$$

Appendix B adapted from reference 2, p. 321-327.

Appendix C

$\bar{a}_P$ vector absolute acceleration of P

a_r

a_θ scalar components of $\bar{a}_P$ in the r, θ, z directions

a_z

h_r

h_θ lengths of $\bar{U}$ vectors in the r, θ, z directions

h_z

$\bar{i}$

$\bar{j}$ unit vectors in the x, y, z directions

$\bar{k}$

$\bar{\ell}$ unit vector in the r direction

$\bar{m}$ unit vector in the θ direction

O_A origin of accelerating reference frame

P a particle of fixed identity moving in any manner in an accelerating reference frame

$\bar{R}_A$ position vector of P from O_A

r

θ scalar cylindrical coordinates of P in the X_A Y_A Z_A accelerating reference frame

z

t_A time as measured in the accelerating reference frame

$\bar{U}_1$

$\bar{U}_2$ vectors tangent to arbitrary orthogonal curvilinear surfaces at P

$\bar{U}_3$

$\bar{U}_r$

$\bar{U}_\theta$ vectors tangent to the r, θ, z orthogonal curvilinear surfaces at P

$\bar{U}_z$

$\bar{u}_r$

$\bar{u}_\theta$ unit vectors tangent to the r, θ, z orthogonal curvilinear surfaces at P

$\bar{u}_z$

u_1

u_2 scalar coordinates of P in an arbitrary orthogonal reference frame

u_3

$\bar{W}$ vector relative velocity of P

W_r

W_θ scalar components of $\bar{W}$ in the r, θ, z directions

W_z

X_A

Y_A orthogonal directions defining an arbitrarily accelerating reference frame

Z_A

x

y scalar coordinates of P in the X_A Y_A Z_A accelerating reference frame

z

∇ vector operator using r, θ, z coordinates - defined by equation (45)

$\bar{\omega}$ vector absolute rotation of the accelerating reference frame

ω_r	
ω_θ	scalar components of $\bar{\omega}$ in the r, θ, z directions
ω_z	
ω	resultant scalar component of $\bar{\omega}$ - defined by equation (44)

Appendix C

$\bar{a}_p$ IN CYLINDRICAL COORDINATES, r, θ, AND z

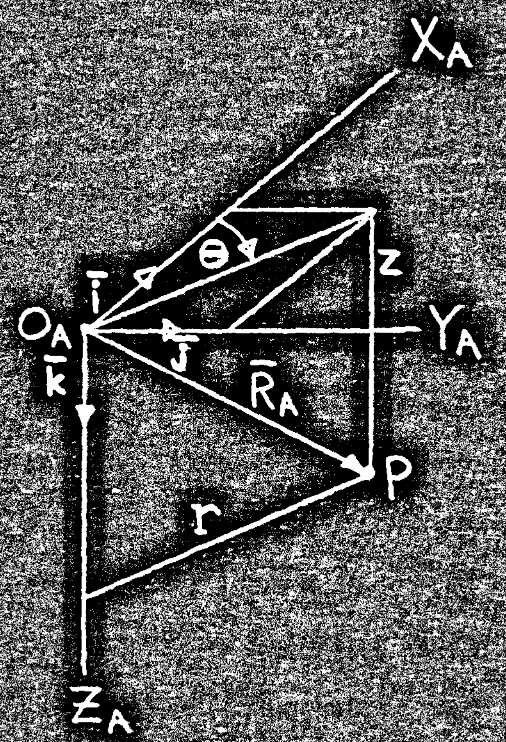

Figure 2

Cylindrical coordinate system for a compressor

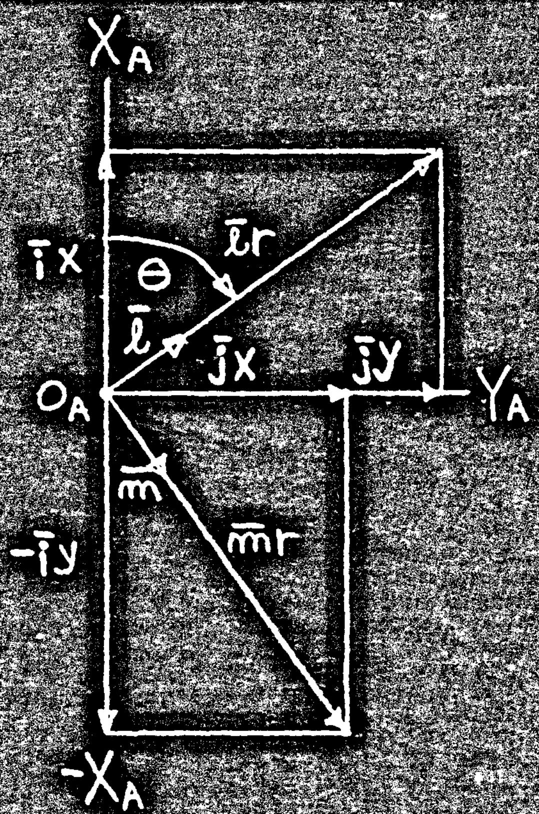

Figure 3

X_AY_A plane showing unit vectors $\bar{l}$ and $\bar{m}$

We refer to Appendix B for the equations for u, $\bar{R}_A$, $\bar{U}$, h, $\bar{u}$, $\bar{W}$, and ∇. As given,

$$u_1 \equiv r, \; u_2 \equiv \theta, \; u_3 \equiv z$$

From (23), Appendix B,

$$\bar{R}_A = \bar{I}x + \bar{J}y + \bar{K}z \tag{23}$$

From Figure 3,

$$x \equiv |\bar{I}x| = |\bar{\ell}r| \cos\theta = r\cos\theta \tag{31}$$

$$y \equiv |\bar{J}y| = |\bar{\ell}r| \sin\theta = r\sin\theta \tag{32}$$

Introducing (31) and (32) into (23),

$$\bar{R}_A = \bar{I}r\cos\theta + \bar{J}r\sin\theta + \bar{K}z \tag{33}$$

From (24a), Appendix B, and (33),

$$\bar{U}_1 \equiv \bar{U}_r \equiv \frac{\partial \bar{R}_A}{\partial r} = \bar{I}\cos\theta + \bar{J}\sin\theta \tag{34}$$

From (34), (31) and (32),

$$\bar{U}_r = \bar{I}\frac{x}{r} + \bar{J}\frac{y}{r} = \frac{1}{r}(\bar{I}x + \bar{J}y) \tag{35}$$

From Figure 3,

$$\bar{I}x + \bar{J}y = \bar{\ell}r \tag{36}$$

From (35) and (36),

$$\bar{U}_r = \bar{\ell} \tag{37}$$

From (24b) and (33),

$$\bar{U}_2 \equiv \bar{U}_\theta \equiv \frac{\partial \bar{R}_A}{\partial \theta} = -\bar{I}r\sin\theta + \bar{J}r\cos\theta \tag{38}$$

From (38), (31), and (32),

$$\bar{U}_\theta = -\bar{i}y + \bar{j}x \tag{39}$$

From Figure 3,

$$-\bar{i}y + \bar{j}x = \bar{m}r \tag{40}$$

From (39) and (40),

$$\bar{U}_\theta = \bar{m}r \tag{41}$$

From (24c) and (23),

$$\bar{U}_3 \equiv \bar{U}_z \equiv \frac{\partial \bar{R}_A}{\partial z} = \bar{k} \tag{42}$$

From (25), (26), (27), and (28) in Appendix B, and from (37), (41), and (42),

$$h_r = |\bar{U}_r| = 1$$

$$h_\theta = |\bar{U}_\theta| = r$$

$$h_z = |\bar{U}_z| = 1$$

$$\bar{u}_r = \frac{\bar{U}_r}{h_r} = \bar{\ell}$$

$$\bar{u}_\theta = \frac{\bar{U}_\theta}{h_\theta} = \bar{m}$$

$$\bar{u}_z = \frac{\bar{U}_z}{h_z} = \bar{k}$$

$$\bar{W} = \bar{\ell}\, W_r + \bar{m}\, W_\theta + \bar{k}\, W_z \qquad (43)$$

$$\bar{\omega} = \bar{\ell}\, \omega_r + \bar{m}\, \omega_\theta + \bar{k}\, \omega_z \equiv \bar{k}\, \omega \qquad (44)$$

$$\nabla = \bar{\ell}\, \frac{\partial}{\partial r} + \frac{\bar{m}}{r}\, \frac{\partial}{\partial \theta} + \bar{k}\, \frac{\partial}{\partial z} \qquad (45)$$

We now expand $\bar{a}_P$ in r, θ, z coordinates. From Appendix A, equation (22),

$$\bar{a}_P = (\bar{W} \cdot \nabla)\, \bar{W} + \frac{\partial \bar{W}}{\partial t_A} + \bar{k}\, \omega \times (\bar{k}\, \omega \times \bar{R}_A) + 2\bar{k}\, \omega \times \bar{W} \qquad (22)$$

We expand the terms in (22). From (43) and (45),

$$\bar{W} \cdot \nabla = (\bar{\ell}\, W_r + \bar{m}\, W_\theta + \bar{k}\, W_z)$$

$$\cdot (\bar{\ell}\, \frac{\partial}{\partial r} + \frac{\bar{m}}{r}\, \frac{\partial}{\partial \theta} + \bar{k}\, \frac{\partial}{\partial z}) = W_r\, \frac{\partial}{\partial r} + \frac{W_\theta}{r}\, \frac{\partial}{\partial \theta} + W_z\, \frac{\partial}{\partial z}$$

$$(\bar{W} \cdot \nabla)\, \bar{W} = W_r\, \frac{\partial \bar{W}}{\partial r} + \frac{W_\theta}{r}\, \frac{\partial \bar{W}}{\partial \theta} + W_z\, \frac{\partial \bar{W}}{\partial z} \qquad (47)$$

Before expanding (47), we notice that all partial derivatives of the unit vectors $\bar{\ell}$, $\bar{m}$, and $\bar{k}$ with respect to the r, θ, z, coordinate directions are zero because the unit vectors are always of unit length and orthogonal. $\bar{\ell}$ and $\bar{m}$ rotate about the Z axis as P moves in the A frame and these rotations will produce partial derivatives with respect to time, as we shall see later. Returning to (47) and using (43),

$$(\bar{W} \cdot \nabla)\ \bar{W} = W_r\ (\bar{\ell}\frac{\partial W_r}{\partial r} + \bar{m}\frac{\partial W_\theta}{\partial r} + \bar{k}\frac{\partial W_z}{\partial r})$$

$$+ \frac{W_\theta}{r}\ (\bar{\ell}\frac{\partial W_r}{\partial \theta} + \bar{m}\frac{\partial W_\theta}{\partial \theta} + \bar{k}\frac{\partial W_z}{\partial \theta})$$

$$+ W_z\ (\bar{\ell}\frac{\partial W_r}{\partial z} + \bar{m}\frac{\partial W_\theta}{\partial z} + \bar{k}\frac{\partial W_z}{\partial z}) \qquad (48)$$

Expanding $\frac{\partial \bar{W}}{\partial t_A}$ and using (43),

$$\frac{\partial \bar{W}}{\partial t_A} = \bar{\ell}\frac{\partial W_r}{\partial t_A} + \frac{\partial \bar{\ell}}{\partial t_A} W_r + \bar{m}\frac{\partial W_\theta}{\partial t_A} + \frac{\partial \bar{m}}{\partial t_A} W_\theta$$

$$+ \bar{k}\frac{\partial W_z}{\partial t_A} + \frac{\partial \bar{k}}{\partial t_A} W_z \qquad (49)$$

$\frac{\partial \bar{\ell}}{\partial t_A}$ = time rate of change of $\bar{\ell}$ in the A frame = $\bar{m}\frac{W_\theta}{r}$ where $\bar{m}$ gives the direction of the change (normal to $\bar{\ell}$ and in the positive θ direction) and $\frac{W_\theta}{r}$ is the instantaneous angular velocity of $\bar{\ell}$ (and $\bar{m}$) about the Z axis. Thus,

$$\frac{\partial \bar{\ell}}{\partial t_A} = \bar{m}\frac{W_\theta}{r} \qquad (50)$$

Similarly, $\frac{\partial \bar{m}}{\partial t_A} = -\bar{\ell}\frac{W_\theta}{r}$ where $-\bar{\ell}$ gives the direction of the change (normal to $\bar{m}$ and in the positive θ direction). Thus,

$$\frac{\partial \bar{m}}{\partial t_A} = -\bar{\ell}\frac{W_\theta}{r} \qquad (51)$$

$\frac{\partial \bar{k}}{\partial t_A} = 0$ since $\bar{k}$ does not rotate and is constant in magnitude, Thus,

$$\frac{\partial \bar{k}}{\partial t_A} = 0 \tag{52}$$

Combining (49), (50), (51), and (52),

$$\frac{\partial \bar{W}}{\partial t_A} = \bar{\ell}\,\frac{\partial W_r}{\partial t_A} + \bar{m}\,\frac{W_\theta\, W_r}{r} + \bar{m}\,\frac{\partial W_\theta}{\partial t_A}$$

$$-\bar{\ell}\,\frac{W_\theta^{\,2}}{r} + \bar{k}\,\frac{\partial W_z}{\partial t_A} \tag{53}$$

Expanding $\bar{k}\omega \times (\bar{k}\omega \times \bar{R}_A)$, we have, using (33),

$$\bar{k}\omega \times [\bar{k}\omega \times (\bar{i}r\cos\theta + \bar{j}r\sin\theta + \bar{k}z)]$$

$$= \bar{k}\omega \times (\bar{j}\,\omega r\cos\theta - \bar{i}\,\omega r\sin\theta)$$

$$= -\bar{i}\,\omega^2 r\cos\theta - \bar{j}\,\omega^2 r\sin\theta$$

$$= \omega^2(-\bar{i}r\cos\theta - \bar{j}r\sin\theta) \tag{54}$$

Using (54), (31), (32) and (36),

$$\bar{k}\omega \times (\bar{k}\omega \times \bar{R}_A) = \omega^2(-\bar{i}x - \bar{j}y) = -\bar{\ell}\,\omega^2 r \tag{55}$$

Expanding $2\bar{k}\omega \times \bar{W}$, we have, using (43),

$$2\bar{k}\omega \times (\bar{\ell}\,W_r + \bar{m}\,W_\theta + \bar{k}\,W_z)$$

$$= 2\bar{m}\,\omega W_r - 2\bar{\ell}\,\omega W_\theta \tag{56}$$

Combining (22), (48), (53), (55), and (56),

$$\bar{a}_P = [W_r \left(\bar{\ell} \frac{\partial W_r}{\partial r} + \bar{m} \frac{\partial W_\theta}{\partial r} + \bar{k} \frac{\partial W_z}{\partial r}\right)$$

$$+ \frac{W_\theta}{r} \left(\bar{\ell} \frac{\partial W_r}{\partial \theta} + \bar{m} \frac{\partial W_\theta}{\partial \theta} + \bar{k} \frac{\partial W_z}{\partial \theta}\right)$$

$$+ W_z \left(\bar{\ell} \frac{\partial W_r}{\partial z} + \bar{m} \frac{\partial W_\theta}{\partial z} + \bar{k} \frac{\partial W_z}{\partial z}\right)$$

$$+ \bar{\ell} \frac{\partial W_r}{\partial t_A} + \bar{m} \frac{\partial W_\theta}{\partial t_A} + \bar{k} \frac{\partial W_z}{\partial t_A} - \bar{\ell} \frac{W_\theta^{\,2}}{r} + \bar{m} \frac{W_\theta W_r}{r}]$$

$$-[\bar{\ell} \omega^2 r] + [2\bar{\ell} \omega W_\theta + 2\bar{m} \omega W_r] \qquad (57)$$

The first bracket in (57) is the relative acceleration of P (if the A frame were <u>not</u> rotating), the second bracket is the centripetal acceleration of P due to the rotation of the A frame, and the last bracket is the Coriolis acceleration of P, also due to the rotation of the A frame.

Equation (57) is the kinematic equation of motion of a particle of fixed identity moving in a rotating reference frame under the following conditions:

1. The inertial reference frame is attached to the surface of the earth with its center at the center of the earth. We neglect the angular velocity of the earth.

2. The origin of the rotating reference frame remains a constant distance from the center of the earth.

3. The rotating reference frame rotates with constant angular velocity about the Z axis.

We may write (57) in scalar form in the r, θ, and z directions:

$$a_r = W_r \frac{\partial W_r}{\partial r} + \frac{W_\theta}{r} \frac{\partial W_r}{\partial \theta} + W_z \frac{\partial W_r}{\partial z} + \frac{\partial W_r}{\partial t_A}$$

$$- \frac{{W_\theta}^2}{r} - \omega^2 r - 2\omega W_\theta \tag{57a}$$

$$a_\theta = W_r \frac{\partial W_\theta}{\partial r} + \frac{W_\theta}{r} \frac{\partial W_\theta}{\partial \theta} + W_z \frac{\partial W_\theta}{\partial z} + \frac{\partial W_\theta}{\partial t_A}$$

$$+ \frac{W_\theta W_r}{r} + 2\omega W_r \tag{57b}$$

$$a_z = W_r \frac{\partial W_z}{\partial r} + \frac{W_\theta}{r} \frac{\partial W_z}{\partial \theta} + W_z \frac{\partial W_z}{\partial z} + \frac{\partial W_z}{\partial t_A} \tag{57c}$$

Appendix D

a_r
a_θ scalar accelerations of P in r, θ, z directions, ft/sec^2
a_z

F_r
F_θ distributed body forces per unit mass in the r, θ, z directions, lbf/lbm
F_z

g_o universal constant relating force and mass, 32.174 lbm ft/sec^2 lbf

O origin of accelerating reference frame

P a particle of mass of fixed identity, lbm

p_r static pressure exerted by other fluid particles on P - in positive r direction, lbf/ft^2

p_z static pressure exerted by other fluid particles on P - in positive z direction, lbf/ft^2

p static pressure, lbf/ft^2 (for non-viscous fluids, $p = p_r = p_z$ = same in all directions at a given point in the fluid)

R force exerted by other fluid particles on P - in positive r direction, lbf

R' force exerted by other fluid particles on P - in negative r direction, lbf

S force exerted by impeller blade on P - in direction of ω, lbf

S' force exerted by impeller blade on P - in direction opposite to ω, lbf

S_r
S_θ components of S in the r, θ, z directions, lbf
S_z

S_r'
S_θ' components of S' in the r, θ, z directions, lbf
S_z'

Z force exerted by other fluid particles on P - in positive z direction, lbf

Z' force exerted by other fluid particles on P - in negative z direction, lbf

ρ static density of P, lbm/ft^3

ω angular velocity of accelerating reference frame about Z axis, rad/sec

Appendix D

DERIVATION OF LORENZ'S EQUATIONS FOR FORCES ON A FLUID PARTICLE WITH AXIAL SYMMETRY

We shall use the Lorenz axial symmetry assumption (reference 3, p. 990-991) to derive the forces which cause P to accelerate. We will derive these equations first for a compressor.

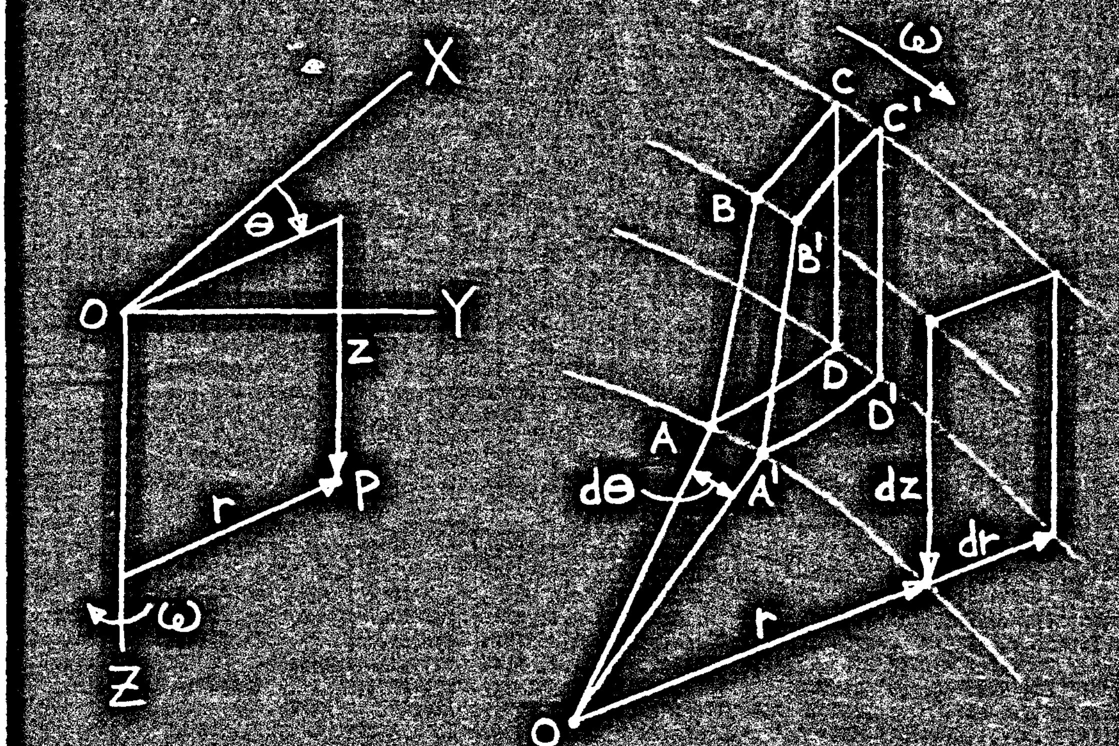

Figure 4

Cylindrical coordinates for a compressor

Figure 5

Adjacent compressor blades with axial symmetry

In Figure 5, ABCD and A'B'C'D' represent adjacent impeller blades an infinitesimal distance, $rd\theta$, apart. The blades are infinitely thin and there is an infinitesimal mass of fluid, P, between the blades. The blades exert forces S and S' on P, S from ABCD and S' from A'B'C'D'. We now assume P has zero viscosity, thus S and S' act normal to the blades. Since the blades, in general, are warped, S and S' will have components in the coordinate directions. We call these components S_r, S_θ, S_z, S_r', S_θ', and S_z'. The fluid outside of the blades also exerts forces on P at the open edges ABB'A', DCC'D', BCC'B', and ADD'A'. We call these fluid forces R, R', Z, Z', respectively.

We now define:

$$F_r \equiv \frac{S_r - S_r'}{P}$$

$$F_\theta \equiv \frac{S_\theta - S_\theta'}{P}$$

$$F_z \equiv \frac{S_z - S_z'}{P}$$

F_r, F_θ, and F_z are called the "distributed body forces per unit mass" in the coordinate directions. We can now write the Lorenz equations:

$$PF_r + R - R' \equiv \frac{P}{g_o} a_r \qquad (58a)$$

$$P F_\theta = \frac{P}{g_o} a_\theta \tag{58b}$$

$$P F_z + Z - Z' = \frac{P}{g_o} a_z \tag{58c}$$

From Figure 5, as P approaches zero,

$$P = \varphi \, dr \, r d\theta dz \tag{59a}$$

$$R = p_r \, r d\theta dz \tag{59b}$$

$$R' = (p_r + \frac{\partial p_r}{\partial r} dr) \, r d\theta dz \tag{59c}$$

$$Z = p_z \, dr \, r d\theta \tag{59d}$$

$$Z' = (p_z + \frac{\partial p_z}{\partial z} dz) \, dr \, r d\theta \tag{59e}$$

Since we have assumed that P has zero viscosity, as P approaches zero, $p_r = p_z = p$ (hydrostatic state of stress).

Combining (58) and (59), we have, after cancellation,

$$\varphi F_r - \frac{\partial p}{\partial r} = \frac{\varphi}{g_o} a_r \tag{60a}$$

$$F_\theta = \frac{a_\theta}{g_o} \tag{60b}$$

$$\varphi F_z - \frac{\partial p}{\partial z} = \frac{\varphi}{g_o} a_z \tag{60c}$$

The equations for a turbine are different only in sign. Our coordinate system is as follows:

We see that ω, θ, and z are reversed while r remains the same as before.

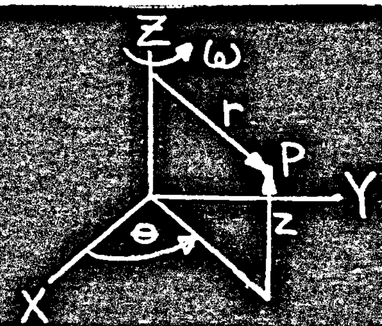

Figure 6

Cylindrical coordinates for a turbine

Our blades now look like this:

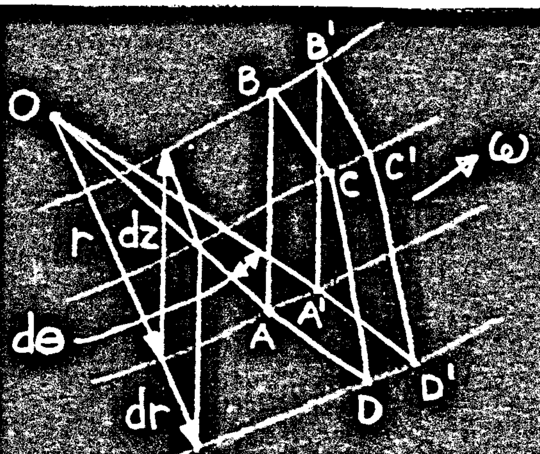

Figure 7

Adjacent turbine blades with axial symmetry

Our definitions of R, R', F_r, F_θ, and F_z are unchanged. We change the direction of Z and Z'. Z now acts on surface ADD'A' and Z' now acts on surface BCC'B'. The Lorenz equations for a turbine are then identical with those for a compressor (equations (60)).

Appendix E

D	indicates substantial differentiation while following a particle of fixed identity
F_r F_θ F_z	distributed body forces per unit mass in the r, θ, z directions, lbf/lbm
g_o	universal constant relating force and mass, 32.174 lbm ft/sec^2 lbf
p	static pressure, lbf/ft^2
r θ z	scalar cylindrical coordinates of a particle P moving in an accelerating reference frame
R_c	radius of curvature of the relative streamline along which P moves when P is at the point r, θ, z; ft
s n	scalar streamline coordinates of P when P is forced to move in the meridional plane
t_A	time as measured in the accelerating reference frame, sec
W_r W_θ W_z	scalar components of W in the r, θ, z directions, ft/sec
W_m	scalar component of W in the meridional plane, ft/sec (for impellers with axial symmetry and straight radial blades, $W_m \equiv W$)

α angle between Z axis and positive s direction (Figure 8), rad

ρ static density of P, lbm/ft^3

ω angular velocity of impeller about Z axis, rad/sec

∂ indicates partial differentiation while holding all other variables constant

Appendix E

LORENZ EQUATIONS FOR IMPELLERS WITH STRAIGHT RADIAL BLADES

Combining (60) in Appendix D and (57) in Appendix C, we have:

$$\varphi F_r - \frac{\partial p}{\partial r} = \frac{\varphi}{g_o} \Big(W_r \frac{\partial W_r}{\partial r} + \frac{W_\theta}{r} \frac{\partial W_r}{\partial \theta} + W_z \frac{\partial W_r}{\partial z}$$

$$+ \frac{\partial W_r}{\partial t_A} - \frac{W_\theta^{\,2}}{r} - \omega^2 r - 2\,\omega W_\theta\Big) \qquad (61a)$$

$$F_\theta = \frac{1}{g_o} \Big(W_r \frac{\partial W_\theta}{\partial r} + \frac{W_\theta}{r} \frac{\partial W_\theta}{\partial \theta} + W_z \frac{\partial W_\theta}{\partial z}$$

$$+ \frac{\partial W_\theta}{\partial t_A} + \frac{W_\theta W_r}{r} + 2\,\omega W_r\Big) \qquad (61b)$$

$$\varphi F_z - \frac{\partial p}{\partial z} = \frac{\varphi}{g_o} \Big(W_r \frac{\partial W_z}{\partial r} + \frac{W_\theta}{r} \frac{\partial W_z}{\partial \theta} + W_z \frac{\partial W_z}{\partial z}$$

$$+ \frac{\partial W_z}{\partial t_A}\Big) \qquad (61c)$$

By our assumption of axial symmetry, all partial derivatives with respect to θ are zero. By our assumptions of zero viscosity and straight radial blades, $F_r = F_z = W_\theta = 0$. Equations (61) become:

$$- \frac{\partial p}{\partial r} = \frac{\varphi}{g_o} \Big[\Big(W_r \frac{\partial W_r}{\partial r} + W_z \frac{\partial W_r}{\partial z} + \frac{\partial W_r}{\partial t_A}\Big) - \omega^2 r\Big] \qquad (62a)$$

$$g_o F_\theta = 2\,\omega W_r \tag{62b}$$

$$-\frac{\partial p}{\partial z} = \frac{\varphi}{g_o}\left(W_r \frac{\partial W_z}{\partial r} + W_z \frac{\partial W_z}{\partial z} + \frac{\partial W_z}{\partial t_A}\right) \tag{62c}$$

With straight, radial blades, the particle P is forced to move in the meridional (axial-radial) plane and it is convenient to follow its motion in this plane in terms of streamline coordinates, s and n, as shown in Figure 8.

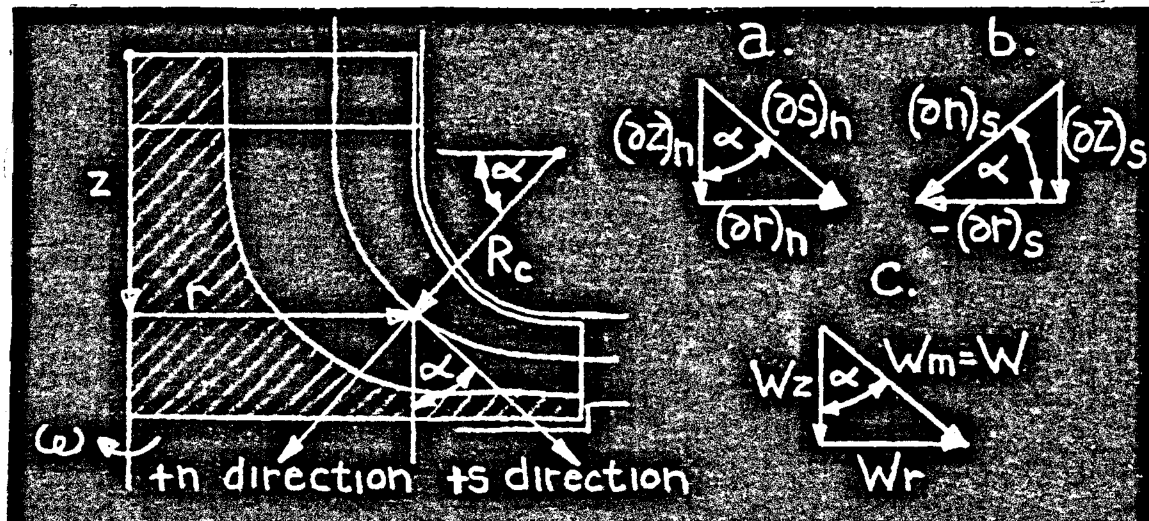

Figure 8
Streamline coordinates in the meridional plane for a compressor impeller

Figure 9
Relations between velocities and distances

We notice that the parentheses terms in (62a) and (62c) are the substantial derivatives of W_r and W_z, respectively (Appendix A, equation (15)). That is, since $\frac{\partial}{\partial \theta} = 0$,

$$\frac{DW_r}{Dt_A} = W_r \frac{\partial W_r}{\partial r} + W_z \frac{\partial W_r}{\partial z} + \frac{\partial W_r}{\partial t_A} \tag{63a}$$

$$\frac{DW_z}{Dt_A} = W_r \frac{\partial W_z}{\partial r} + W_z \frac{\partial W_z}{\partial z} + \frac{\partial W_z}{\partial t_A} \tag{63b}$$

We now assume that the flow relative to the rotating impeller does not vary with time ("steady" flow), thus

$$\frac{\partial W_r}{\partial t_A} \equiv \frac{\partial W_z}{\partial t_A} \equiv 0 \tag{64}$$

From Figure 9c,

$$W_r = W \sin\alpha \tag{65a}$$

$$W_z = W \cos\alpha \tag{65b}$$

Taking the substantial derivative of (65):

$$\frac{DW_r}{Dt_A} = W \cos\alpha \frac{D\alpha}{Dt_A} + \frac{DW}{Dt_A} \sin\alpha \tag{66a}$$

$$\frac{DW_z}{Dt_A} = -W \sin\alpha \frac{D\alpha}{Dt_A} + \frac{DW}{Dt_A} \cos\alpha \tag{66b}$$

From Figure 8,

$$R_c D\alpha = Ds \tag{67}$$

By definition of a streamline in steady flow,

$$\frac{Ds}{Dt_A} = W \tag{68a}$$

$$\frac{Dn}{Dt_A} = 0 \tag{68b}$$

Taking the substantial derivative of W,

$$\frac{DW}{Dt_A} = \frac{\partial W}{\partial s} \frac{Ds}{Dt_A} + \frac{\partial W}{\partial n} \frac{Dn}{Dt_A} \tag{69}$$

Combining (67) and (68a):

$$\frac{D\alpha}{Dt_A} = \frac{W}{R_c} \tag{70}$$

Combining (66), (68b), (69), and (70):

$$\frac{DW_r}{Dt_A} = \frac{W^2}{R_c} \cos\alpha + W \frac{\partial W}{\partial s} \sin\alpha \tag{71a}$$

$$\frac{DW_z}{Dt_A} = - \frac{W^2}{R_c} \sin\alpha + W \frac{\partial W}{\partial s} \cos\alpha \tag{71b}$$

Combining (62), (63), and (71):

$$- \frac{\partial p}{\partial r} = \frac{\varphi}{g_o} \left[\frac{W^2}{R_c} \cos\alpha + W \frac{\partial W}{\partial s} \sin\alpha - \omega^2 r\right] \tag{72a}$$

$$g_o F_\theta = 2 \omega W_r \tag{72b}$$

$$- \frac{\partial p}{\partial z} = \frac{\varphi}{g_o} \left[- \frac{W^2}{R_c} \sin\alpha + W \frac{\partial W}{\partial s} \cos\alpha\right] \tag{72c}$$

We now find $\frac{\partial p}{\partial s}$ and $\frac{\partial p}{\partial n}$.

$$\frac{\partial p}{\partial s} = \frac{\partial p}{\partial r} \frac{\partial r}{\partial s} + \frac{\partial p}{\partial z} \frac{\partial z}{\partial s} \tag{73a}$$

$$\frac{\partial p}{\partial n} = \frac{\partial p}{\partial r} \frac{\partial r}{\partial n} + \frac{\partial p}{\partial z} \frac{\partial z}{\partial n} \tag{73b}$$

From Figures 9a and 9b,

$$\frac{\partial r}{\partial s} = \sin\alpha \tag{74a}$$

$$\frac{\partial z}{\partial s} = \cos\alpha \tag{74b}$$

$$\frac{\partial r}{\partial n} = -\cos\alpha \tag{74c}$$

$$\frac{\partial z}{\partial n} = \sin\alpha \tag{74d}$$

Combining (72), (73), and (74):

$$\frac{\partial p}{\partial s} = -\frac{\varphi}{g_o}\left(\frac{W^2}{R_c}\sin\alpha\cos\alpha + W\frac{\partial W}{\partial s}\sin^2\alpha\right.$$

$$\left.-\omega^2 r\sin\alpha - \frac{W^2}{R_c}\sin\alpha\cos\alpha + W\frac{\partial W}{\partial s}\cos^2\alpha\right) =$$

$$-\frac{\varphi}{g_o}\left(W\frac{\partial W}{\partial s} - \omega^2 r\sin\alpha\right) \tag{75a}$$

$$\frac{\partial p}{\partial n} = -\frac{\varphi}{g_o}\left(-\frac{W^2}{R_c}\cos^2\alpha - W\frac{\partial W}{\partial s}\sin\alpha\cos\alpha\right.$$

$$\left.+\omega^2 r\cos\alpha - \frac{W^2}{R_c}\sin^2\alpha + W\frac{\partial W}{\partial s}\sin\alpha\cos\alpha\right) =$$

$$-\frac{\varphi}{g_o}\left(-\frac{W^2}{R_c} + \omega^2 r\cos\alpha\right) \tag{75b}$$

Combining (74) and (75):

$$\frac{\partial p}{\partial s} = -\frac{\varphi}{g_o}\left(W\frac{\partial W}{\partial s} - \omega^2 r \frac{\partial r}{\partial s}\right) \tag{76a}$$

$$\frac{\partial p}{\partial n} = -\frac{\varphi}{g_o}\left(-\frac{W^2}{R_c} - \omega^2 r \frac{\partial r}{\partial n}\right) \tag{76b}$$

Equations (76) are identical for a centripetal turbine if the s and n directions are as shown in Figure 9d.

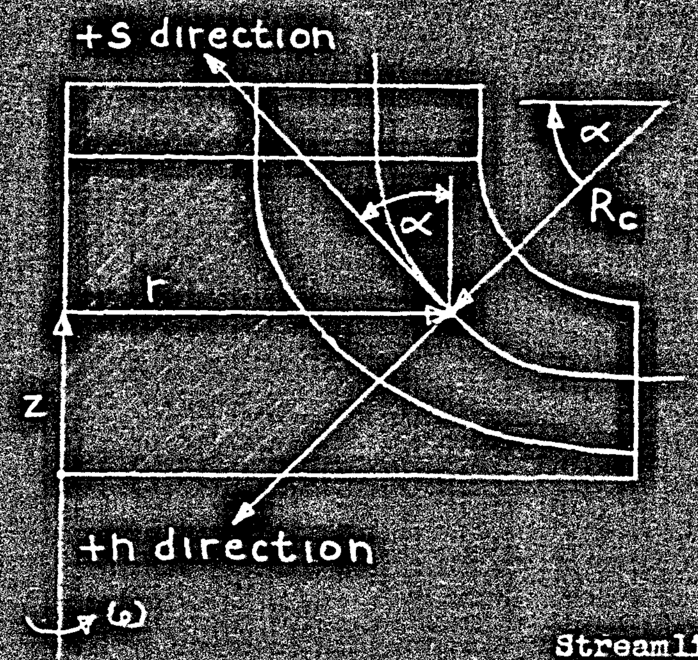

Figure 9d

Streamline coordinates for a centripetal turbine

Appendix F

C_p specific heat at constant pressure, BTU/lbm R

C_v specific heat at constant volume, BTU/lbm R

g_o universal constant relating force and mass, 32.174 lbm ft/sec^2 lbf

H_A Bernoulli constant for flow along a relative streamline, ft^2/sec^2

H_I Bernoulli constant for flow along an inertial (absolute) streamline, ft^2/sec^2

h static enthalpy, BTU/lbm

h_{oA} stagnation enthalpy defined by equation (110), BTU/lbm

h_{oI} stagnation enthalpy defined by equation (110a), BTU/lbm

J universal constant relating work and heat, 778.2 ft lbf/BTU

k ratio of specific heats, C_p/C_v

p static pressure, lbf/ft^2

R gas constant, ft lbf/lbm R

R_c radius of curvature of the relative streamline, ft

r radius from Z axis, ft

s
n streamline coordinates for two-dimensional flow in the meridional plane

T static temperature, R

u intrinsic energy, BTU/lbm

V	absolute velocity, ft/sec
W	relative velocity, ft/sec
ρ	static density, lbm/ft^3
ω	angular velocity of impeller about Z axis, rad/sec

Appendix F

CHANGE IN RELATIVE VELOCITY NORMAL TO A STREAMLINE

We have shown in Appendix E that the Lorenz equations for impellers with straight, radial blades are:

$$\frac{\partial p}{\partial s} = - \frac{\varphi}{g_o} \left(W \frac{\partial W}{\partial s} - \omega^2 r \frac{\partial r}{\partial s}\right) \qquad (77a)$$

$$\frac{\partial p}{\partial n} = - \frac{\varphi}{g_o} \left(- \frac{W^2}{R_c} - \omega^2 r \frac{\partial r}{\partial n}\right) \qquad (77b)$$

If we temporarily confine our attention to changes <u>along</u> a particular relative streamline, (77a) becomes:

$$\frac{dp}{ds} = - \frac{\varphi}{g_o} \left(W \frac{dW}{ds} - \omega^2 r \frac{dr}{ds}\right) \qquad (77c)$$

Multiplying (77c) by ds and integrating,

$$-g_o \int \frac{dp}{\varphi} - \frac{W^2}{2} + \frac{\omega^2 r^2}{2} = \text{constant of integration} \equiv H_A \qquad (78)$$

We see that H_A (usually called the Bernoulli constant of the streamline) is invariable along the streamline but may vary from streamline to streamline. We now investigate changes in H_A <u>normal</u> to a particular streamline. In this case, (77b) becomes:

$$\frac{dp}{dn} = - \frac{\varphi}{g_o} \left(- \frac{W^2}{R_c} - \omega^2 r \frac{dr}{dn}\right) \qquad (77d)$$

If we differentiate (78) with respect to n (at constant s), we have:

$$-g_o \frac{d}{dn} \int \frac{dp}{\varphi} - W \frac{dW}{dn} + \omega^2 r \frac{dr}{dn} = \frac{dH_A}{dn} \qquad (79)$$

But $-g_o \frac{d}{dn} \int \frac{dp}{\varphi} = - \frac{g_o}{\varphi} \frac{dp}{dn}$, so (79) may be written:

$$- \frac{g_o}{\varphi} \frac{dp}{dn} - W \frac{dW}{dn} + \omega^2 r \frac{dr}{dn} = \frac{dH_A}{dn} \qquad (79a)$$

Rewriting (77d):

$$- \frac{g_o}{\varphi} \frac{dp}{dn} + \frac{W^2}{R_c} + \omega^2 r \frac{dr}{dn} = 0 \qquad (77d)$$

Subtracting (77d) from (79a), we see that:

$$-W \frac{dW}{dn} - \frac{W^2}{R_c} = \frac{dH_A}{dn} \qquad (80)$$

Now, if H_A, the constant of integration in equation (78), is identical for <u>all</u> relative streamlines, it will not vary in <u>any</u> direction and:

$$\frac{dH_A}{dn} = 0 \qquad (81)$$

If (81) is true, then (80) becomes:

$$\frac{dW}{dn} = - \frac{W}{R_c} \qquad (82)$$

Equation (82) gives the rate of change of the relative velocity in the normal direction, under the condition of (81). We now investigate condition (81). If the fluid flowing through the impeller originated in a large reservoir (such as the atmosphere) where $\frac{dp}{dn} \equiv \frac{dp}{ds}$, we see from equations (77c) and (77d) that $\frac{dW}{ds} \equiv \frac{dW}{dn} = -\frac{W}{R_c}$, which is equation (82). Thus, in a large reservoir, equation (81) holds.

According to Kelvin's theorem (reference 9, p. 280), equation (81) will hold in <u>any</u> region in which three conditions are met:

1. Frictionless flow
2. Conservative body forces only
3. Density of the fluid depends only on the pressure

Condition 1 has already been specified in deriving the Lorenz equations (Appendix D); condition 2 is satisfied by gravity and centrifugal force fields; and condition 3 is satisfied, for air and other perfect gases, by the isentropic relation:

$$p\varphi^{-k} = \text{constant} \tag{83}$$

We now specify that the flow through our compressor and turbine impellers originates in the atmosphere and also that the three conditions of Kelvin's theorem are always satisfied. Any flow which satisfies Kelvin's theorem is called "irrotational", and equations (81) and (82) may be used in all irrotational flows.

Equation (81) holds for <u>relative</u> flows only. In an <u>inertial</u> reference frame, the absolute velocity (V) is the velocity "relative" to the frame, thus (81) holds, under the conditions of Kelvin's theorem. (81) does <u>not</u> hold for the relative velocity (W) in an <u>inertial</u> frame. Thus, under the conditions of Kelvin's theorem,

$$\left.\begin{array}{l} \dfrac{dH_I}{dn} = 0 \\[2ex] \dfrac{dH_A}{dn} \neq 0 \end{array}\right\} \text{ in an inertial frame} \qquad (84a)$$

$$\left.\begin{array}{l} \dfrac{dH_A}{dn} = 0 \\[2ex] \dfrac{dH_I}{dn} \neq 0 \end{array}\right\} \text{ in an accelerating frame} \qquad (84b)$$

where, using (83),

$$H_I \equiv -g_o \int \frac{dp}{\varphi} - \frac{V^2}{2} = -g_o \left(\frac{k}{k-1}\right) \frac{p}{\varphi} - \frac{V^2}{2} \qquad (85a)$$

$$H_A \equiv -g_o \int \frac{dp}{\varphi} - \frac{W^2}{2} + \frac{\omega^2 r^2}{2}$$

$$= -g_o \left(\frac{k}{k-1}\right) \frac{p}{\varphi} - \frac{W^2}{2} + \frac{\omega^2 r^2}{2} \qquad (85b)$$

H_I and H_A are related to the stagnation enthalpy (110a) and (110) in Appendix G. To show this relationship, we make use of the perfect gas relations:

By definition, for any substance,

$$h \equiv u + \frac{p}{J\varphi} \qquad (86a)$$

For all perfect gases,

$$u = C_v \, T \qquad (86b)$$

$$k \equiv \frac{C_p}{C_v} \qquad (86c)$$

$$C_p - C_v = \frac{R}{J} \qquad (86d)$$

$$\frac{JC_v}{R} = \frac{1}{k-1} \qquad (86e)$$

$$p = \varphi R \, T \qquad (86f)$$

$$h = c_p \, T \qquad (86g)$$

From (110) and (110a),

$$h_{OA} \equiv h + \frac{W^2}{2g_o J} - \frac{\omega^2 r^2}{2g_o J} \qquad (110\ )$$

$$h_{OI} \equiv h + \frac{V^2}{2g_o J} \qquad (110a)$$

Combining (110), (110a), (86a), (86b), (86e), and (86f),

$$-g_o J h_{OA} = -g_o \left(\frac{k}{k-1}\right) \frac{p}{\varphi} - \frac{W^2}{2} + \frac{\omega^2 r^2}{2} \qquad (87a)$$

$$-g_o J h_{OI} = -g_o \left(\frac{k}{k-1}\right) \frac{p}{\varphi} - \frac{V^2}{2} \qquad (87b)$$

Thus, from (85) and (87),

$$H_I \equiv -g_o J h_{OI}$$

$$H_A \equiv -g_o J h_{OA}$$

We see that (84) may be written:

$$\left.\begin{aligned} \frac{dh_{OI}}{dn} &= 0 \\ \frac{dh_{OA}}{dn} &\neq 0 \end{aligned}\right\} \text{ in an inertial frame} \qquad (84c)$$

$$\left.\begin{aligned} \frac{dh_{OA}}{dn} &= 0 \\ \frac{dh_{OI}}{dn} &\neq 0 \end{aligned}\right\} \text{ in an accelerating frame} \qquad (84d)$$

Appendix G

CS	a control surface, fixed in a specified reference frame, through which systems flow
$\mathcal{V}$	a control volume (the space enclosed by a control surface)
$d\mathcal{V}$	an infinitesimal volume element of a control volume, ft^3
dA	an infinitesimal area element of a control surface, ft^2
dA_{in}	an infinitesimal area element of a control surface through which a system enters the control volume, ft^2
dA_{out}	an infinitesimal area element of a control surface through which a system leaves the control volume, ft^2
c_p	specific heat at constant pressure, BTU/lbm R
D	denotes substantial differentiation while following the motion of a system of fixed identity
E	total internal energy of a system, BTU
e	internal energy of a system, BTU/lbm
e_{in}	internal energy of a system just before the system enters a control volume, BTU/lbm
e_{out}	internal energy of a system just before the system leaves a control volume, BTU/lbm
g_o	universal constant relating force and mass, 32.174 lbm ft/sec^2 lbf

h	static enthalpy of a system, BTU/lbm
h_{OA}	stagnation enthalpy of a system, defined by equation (110), BTU/lbm
$h_{OA\ in}$	stagnation enthalpy of a system just before the system enters a control volume which is fixed in an accelerating reference frame, BTU/lbm
$h_{OA\ out}$	stagnation enthalpy of a system just before the system leaves a control volume which is fixed in an accelerating reference frame, BTU/lbm
h_{OI}	stagnation enthalpy of a system, defined by equation (110a), BTU/lbm
$h_{OI\ in}$	stagnation enthalpy of a system just before the system enters a control volume which is fixed in an inertial reference frame, BTU/lbm
$h_{OI\ out}$	stagnation enthalpy of a system just before the system leaves a control volume which is fixed in an inertial reference frame, BTU/lbm
J	universal constant relating work and heat, 778.2 ft lbf/BTU
M	total mass of a system, lbm
m	time rate of mass flow of a system, lbm/sec
m_{in}	mass flow of a system just before the system enters a control volume, lbm/sec
m_{out}	mass flow of a system just before the system leaves a control volume, lbm/sec

P_1, P_2	systems
p	static pressure, lbf/ft^2
p_{in}	static pressure acting on a system just before the system enters a control volume, lbf/ft^2
p_{out}	static pressure exerted by a system just before the system leaves a control volume, lbf/ft^2
Q	heat flowing into a control volume, BTU
r	radius from Z axis to system, ft
r_{in}	radius from Z axis to system just before the system enters a control volume, ft
r_{out}	radius from Z axis to system just before the system leaves a control volume, ft
T	static temperature, R
T_{OI}	stagnation temperature, defined by equation (113a), R
t	time as measured in a particular reference frame, sec
u	intrinsic energy of a system, BTU/lbm
u_{in}	intrinsic energy of a system just before the system enters a control volume, BTU/lbm
u_{out}	intrinsic energy of a system just before the system leaves a control volume, BTU/lbm
V	absolute velocity, ft/sec
W	relative velocity, ft/sec
W	work flowing into a control volume, ft lbf
$W_{friction}$	work flowing out of a control volume because of friction on the control surface, ft lbf

W_n component of relative velocity of a system which is normal to a control surface, ft/sec

$W_{n\ in}$ component of relative velocity of a system which is normal to a control surface just before the system enters a control volume, ft/sec

$W_{n\ out}$ component of relative velocity of a system which is normal to a control surface just before the system leaves a control volume, ft/sec

W_p net work flowing into a control volume due to static pressure (normal stresses) on the control surface, ft lbf

W_s net work flowing into a control volume due to shearing stresses on the control surface, ft lbf

W_{shaft} work flowing into a control volume due to a rotating shaft piercing the control surface, ft lbf

X any extensive property of a system

x the value of X per unit mass

ρ static density of a system, lbm/ft^3

ρ_{in} static density of a system just before the system enters a control volume, lbm/ft^3

ρ_{out} static density of a system just before the system leaves a control volume, lbm/ft^3

ω angular velocity of accelerating reference frame about the Z axis, rad/sec

Appendix G

CONTROL SURFACE ANALYSIS IN AN ACCELERATING REFERENCE FRAME

We here derive general equations relating the time rate of change of those extensive properties of a system which are expressed per unit mass, such as specific mass, specific energy, specific momentum, etc. as the system flows through an imaginary closed surface which is fixed in an accelerating reference frame. We call this imaginary surface the "control surface".

We define the following:

CS ≡ an imaginary "control surface" which is fixed in an arbitrarily accelerating reference frame.

$\mathcal{V}$ ≡ the invariable volume contained within CS

P_1 ≡ a system, that is, a collection of matter of fixed identity. By definition, the total mass of a system is constant (nuclear reactions excluded).

P_2 ≡ a system different from P_1

X ≡ any extensive property of a system (see reference 9, p. 24 for a discussion of "properties")

M ≡ the total mass of a system (constant, by definition)

x ≡ the value of X per unit mass. By definition, $x \equiv \frac{X}{M}$.

Consider the flow of 2 systems, P_1 and P_2, through a CS. Figures 10 and 11 show the positions of P_1 and P_2 at time t_1 and time t_2.

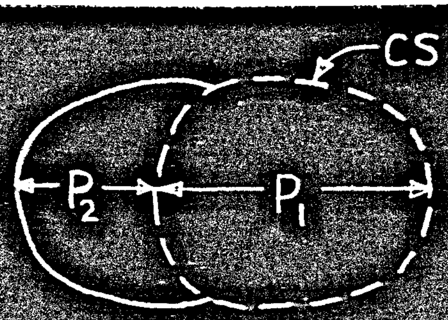

Figure 10
Position of Systems P_1 and P_2 at time t_1

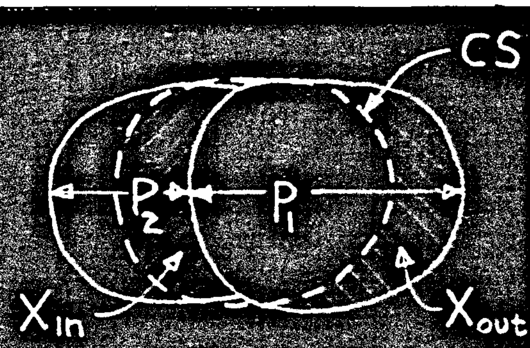

Figure 11
Position of Systems P_1 and P_2 at time t_2

At time t_1, system P_1 lies entirely within the CS and system P_2 is entirely outside the CS. At time t_2, system P_1 has partially moved out of the CS and system P_2 has partially entered the CS. X_{out} is the total amount of X of system P_1 which has passed through the CS. X_{in} is the total amount of X of system P_2 which has also passed through the CS. We now define:

$X_{t1} \equiv$ the total amount of X of <u>both</u> systems which is <u>inside</u> the CS at time t_1.

$X_{t2} \equiv$ the total amount of X of <u>both</u> systems which is <u>inside</u> the CS at time t_2.

$X_{P1} \equiv$ the total amount of X of <u>system P_1 only</u> at <u>any</u> given time .

From Figures 10 and 11,

$$X_{t1} = X_{P1t1} \tag{88a}$$

$$X_{t2} = X_{in} + X_{P1t2} - X_{out} \tag{88b}$$

Subtracting (88a) from (88b):

$$X_{t2} - X_{t1} = X_{P1t2} - X_{P1t1} + X_{in} - X_{out}$$

$$X_{P1t2} - X_{P1t1} = X_{t2} - X_{t1} + X_{out} - X_{in} \qquad (88c)$$

Expressing (88c) in words, the change in the total value of X of system P_1 during the time interval $t_2 - t_1$ equals the accumulation of X within the CS during this time interval plus the flow of X outward through the CS minus the flow of X inward through the CS, during this time interval.

To find the time rate of change of X_{P1}, we divide (88c) by $t_2 - t_1$ (which we define as Dt):

$$\frac{X_{P1t2} - X_{P1t1}}{t_2 - t_1} = \frac{DX}{Dt} = \left(\frac{X_{t2} - X_{t1}}{Dt}\right)$$

$$+ \frac{X_{out}}{Dt} - \frac{X_{in}}{Dt} \qquad (89)$$

The term $\left(\frac{X_{t2} - X_{t1}}{Dt}\right)$ in (89) represents the time rate of accumulation of X within the CS, that is, throughout the control volume, $\mathcal{V}$. Since $\mathcal{V}$ is <u>fixed</u> in our accelerating reference frame, we see that $\left(\frac{X_{t2} - X_{t1}}{Dt}\right)$ is independent of the movement of the systems and is a function of time only. Thus, we write:

$$\left(\frac{X_{t2} - X_{t1}}{Dt}\right) \equiv \left[\frac{(Mx)_{t2} - (Mx)_{t1}}{\partial t}\right] = \int_{\mathcal{V}} \frac{\partial}{\partial t} (\varphi x) d\mathcal{V} \quad (90)$$

where φ is the density of the mass instantaneously within the control volume, and $d\mathcal{V}$ is a control volume element. We now find integral forms for the other two terms in (89).

$$\frac{X}{Dt} \equiv \frac{Mx}{Dt} \equiv \frac{M}{Dt}\, x \equiv mx = \int_{CS} x\, \varphi W_n \, dA \tag{91}$$

In (91), $m \equiv \frac{M}{Dt}$ is the mass rate of flow through the control surface, φ is the density of the mass as it passes through the CS, W_n is the component of the relative velocity $\bar{W}$ which is normal to the CS, and dA is a CS area element. Combining (89), (90), and (91):

$$\frac{DX}{Dt} = \int_{\mathcal{V}} \frac{\partial}{\partial t}(\varphi\, x) d\mathcal{V} + \int_{CS} (x\, \varphi\, W_n \, dA)_{out} - \int_{CS} (x\, \varphi\, W_n \, dA)_{in} \tag{92}$$

If the flow is "steady", that is, if no extensive property accumulates within the control surface with time, the term $\left(\frac{X_{t2} - X_{t1}}{Dt}\right)$ in equation (90) is zero since $X_{t2} = X_{t1}$. Thus, equation (92) becomes:

$$\frac{DX}{Dt} = \int_{CS} (x\, \varphi\, W_n \, dA)_{out} - \int_{CS} (x\, \varphi\, W_n \, dA)_{in} \tag{92a}$$

If, in addition, the flow is one dimensional, that is, if the following four conditions are met:

1. φ_{out} and $W_{n\ out}$ are <u>constant</u> over <u>all</u> the "out" CS area elements,

2. φ_{in} and $W_{n\ in}$ are <u>constant</u> over <u>all</u> the "in" CS area elements,

3. $x_{out} = \frac{1}{A_{out}} \int_{CS} (x\ dA)_{out}$, that is, x_{out} is the mean value of all the x's over the "out" CS,

4. $x_{in} = \frac{1}{A_{in}} \int_{CS} (x\ dA)_{in}$, that is, x_{in} is the mean value of all the x's over the "in" CS, equation (92a) becomes:

$$\frac{DX}{Dt} = (x\,\varphi\,W_n\,A)_{out} - (x\,\varphi\,W_n\,A)_{in} \qquad (92b)$$

<u>Conservation of mass (Continuity)</u>

We now use (92) and (92b) to express the law of conservation of mass in terms of a control surface analysis. Let $X \equiv M$, the total mass of a system. For problems not involving nuclear reactions, M is constant. Also, $x \equiv \frac{X}{M} = 1$. Equations(92) and (92b) become:

$$0 = \int_{\mathcal{V}} \frac{\partial}{\partial t}(\varphi)\,d\mathcal{V} + \int_{CS} (\varphi\,W_n\,dA)_{out} - \int_{CS} (\varphi\,W_n\,dA)_{in} \qquad (93a)$$

$$0 = (\varphi\,W_n\,A)_{out} - (\varphi\,W_n\,A)_{in} \qquad (93b)$$

But, in (93b), for one-dimensional flow,

$$m \equiv \varphi\,W_n\,A \qquad (94)$$

Thus, from (93b) and (94),

$$m_{out} = m_{in} = \text{constant} = \varphi\, W_n\, A \qquad (95)$$

(95) is the steady, one-dimensional continuity equation. Applying (95) to (92b),

$$\frac{DX}{Dt} = m\,(x_{out} - x_{in}) \qquad (96)$$

(96) is the steady, one-dimensional equation for the time rate of change of <u>any</u> extensive property of a system.

<u>Conservation of Energy (First Law of Thermodynamics)</u>

As a system flows through space and time, the first law of thermodynamics states that (barring nuclear reactions) its total energy content remains constant. We conveniently separate total energy into three catagories: internal energy, heat, and work. Of these, only internal energy is a <u>property</u> of the system since heat and work are dependent on the past history of the system. The conservation of energy equation may be expressed as follows (reference 9, p. 28, with a change in sign convention and using substantial derivatives):

$$\frac{DE}{Dt} = \frac{Q}{Dt} + \frac{W}{J\,Dt} \qquad (97)$$

where E is the total internal energy of a system (BTU) which is instantaneously within a fixed control volume, Q is the heat (BTU) <u>flowing into</u> the control volume by reason of a higher temperature outside the control volume than inside, W is the work flowing into the control volume (ft lbf), and J is heat-work conversion factor (778.2 ft lbf per BTU). Work may be done by surface forces, such as pressure and shear; by body forces, such as gravity and centrifugal force; and by line forces, such as capillarity. We neglect line forces here. Also, "work" done by conservative body forces is not really work as we have defined it. These forces do "work" which is independent of the past history of the system and thus must be classified in the energy catagory. The work term in (97) will then consist of work done by pressure and shear forces on the control surface.

$$W = W_p + W_s \tag{98}$$

$$W_p = \int_{CS} \text{pressure force x distance moved} = \int_{CS} (p\ dA)(W_n\ Dt)$$

$$\frac{W_p}{Dt} = \int_{CS} (\frac{p}{\rho}\ \rho W_n\ dA)_{in} - \int_{CS} (\frac{p}{\rho}\ \rho\ W_n\ dA)_{out} \tag{99}$$

In (99), $(\frac{p}{\rho})_{in}$ is the work flowing into the CS per unit mass as the surroundings push fluid in through the CS. $(\frac{p}{\rho})_{out}$ is the work flowing out of the CS per unit mass as the surroundings are pushed aside by fluid leaving the CS.

$$W_s = W_{shaft} - W_{friction} \tag{100}$$

W_{shaft} is the work flowing into the CS by means of a rotating shaft which pierces the CS. $W_{friction}$ is the work flowing out of the CS because of friction on the CS.

Combining (97), (98), (99), and (100):

$$\frac{DE}{Dt} = \frac{Q}{Dt} + \frac{1}{J}\int_{CS}\left(\frac{p}{\varphi}\varphi W_n\, dA\right)_{in} - \frac{1}{J}\int_{CS}\left(\frac{p}{\varphi}\varphi W_n\, dA\right)_{out}$$

$$+ \frac{W_{shaft}}{J\,Dt} - \frac{W_{friction}}{J\,Dt} \qquad (101)$$

But, from (92),

$$\frac{DX}{Dt} \equiv \frac{DE}{Dt} = \int_{\mathcal{V}} \frac{\partial}{\partial t}(\varphi e)\, d\mathcal{V} + \int_{CS}(e\,\varphi\, W_n\, dA)_{out}$$

$$- \int_{CS}(e\,\varphi\, W_n\, dA)_{in} \qquad (102)$$

where e is the internal energy per unit mass of the matter instantaneously within the control volume or of the matter which passes outward or inward through the CS. Combining (101) and (102),

$$\frac{Q}{Dt} + \frac{W_{shaft}}{J\,Dt} - \frac{W_{friction}}{J\,Dt} = \int_{\mathcal{V}} \frac{\partial}{\partial t}(\varphi e)\, d\mathcal{V}$$

$$+ \int_{CS}\left[\left(\frac{p}{\varphi J} + e\right)\varphi W_n\, dA\right]_{out} - \int_{CS}\left[\left(\frac{p}{\varphi J} + e\right)\varphi W_n\, dA\right]_{in} \quad (103)$$

(103) is the general form of the "energy" equation. For steady, one-dimensional flow, we use (96):

$$\frac{Q}{Dt} + \frac{W_{shaft}}{J\ Dt} - \frac{W_{friction}}{J\ Dt} = m\ [(\frac{p}{\varphi J} + e)_{out}$$

$$- (\frac{p}{\varphi J} + e)_{in}] \qquad (104)$$

We now specify that our system is a pure substance (reference 10, p. 18). Air is a pure substance as long as it is all vapor (or all liquid). It is a matter of experience that the internal energy of a pure substance at rest and not acted upon by conservative body forces is a definite value which depends only on the state of the substance. We call this special property "intrinsic energy", u. When a system is in motion with velocity $\overline{W}$, Newton's law of motion says that its internal energy is:

$$e = u + \frac{W^2}{2g_o J} \qquad (105)$$

if no body forces act upon the system. The only body force which is of appreciable magnitude for our purposes is the centrifugal field caused by the rotation of our reference frame about the Z inertial axis (see Figure 1, Appendix A). This field produces a body force equal to $-\frac{\omega^2 r^2}{2g_o J}$ where ω is the angular velocity of the rotating reference frame about the Z axis and r is the shortest distance from the Z axis to the system. The negative sign is used since the system has <u>used up</u> energy in going from zero radius to radius r in the centrifugal field. Equation (105) becomes:

$$e = u + \frac{W^2}{2g_o J} - \frac{\omega^2 r^2}{2g_o J} \qquad (106)$$

Thus, (104) becomes (noting that m Dt = M):

$$\frac{Q}{M} + \frac{W_{shaft}}{JM} - \frac{W_{friction}}{JM} = \left(\frac{p}{\varphi J} + u + \frac{W^2}{2g_oJ} - \frac{\omega^2 r^2}{2g_oJ}\right)_{out}$$

$$- \left(\frac{p}{\varphi J} + u + \frac{W^2}{2g_oJ} - \frac{\omega^2 r^2}{2g_oJ}\right)_{in} \qquad (107)$$

Now, if we specify that there is just one shaft piercing the CS and this shaft is rotating with angular velocity ω about the Z axis, W_{shaft} in (107) is zero. This is true because the CS and the shaft are both rotating at the same speed and there is no <u>relative</u> motion. We also assume that the heat transfer into (or out of) the CS is negligible compared with the other terms. Under these conditions, (107) becomes:

$$- \frac{W_{friction}}{JM} = \left(\frac{p}{\varphi J} + u + \frac{W^2}{2g_oJ} - \frac{\omega^2 r^2}{2g_oJ}\right)_{out}$$

$$- \left(\frac{p}{\varphi J} + u + \frac{W^2}{2g_oJ} - \frac{\omega^2 r^2}{2g_oJ}\right)_{in} \qquad (108)$$

If we define:

$$h \equiv \frac{p}{\varphi J} + u \qquad (86a)$$

$$h_{OA} \equiv h + \frac{W^2}{2g_oJ} - \frac{\omega^2 r^2}{2g_oJ} \qquad (110)$$

(108) becomes:

$$- \frac{W_{friction}}{JM} = h_{OA\ out} - h_{OA\ in} \qquad (111)$$

If we <u>neglect</u> the <u>work</u> done by friction, (111) becomes:

$$h_{0A\ out} = h_{0A\ in} \tag{112}$$

(112) is the energy equation for steady, one-dimensional flow of a non-viscous pure substance through a control surface fixed in a reference frame which <u>rotates</u> with angular velocity ω about the Z axis.

If the reference frame in (107) is an <u>inertial</u> frame, (107) becomes:

$$\frac{Q}{M} + \frac{W_{shaft}}{JM} - \frac{W_{friction}}{JM} = \left(\frac{p}{\rho J} + u + \frac{V^2}{2g_oJ}\right)_{out} - \left(\frac{p}{\rho J} + u + \frac{V^2}{2g_oJ}\right)_{in} \tag{107a}$$

If we now define:

$$h \equiv \frac{p}{\rho J} + u \tag{86a}$$

$$h_{0I} \equiv h + \frac{V^2}{2g_oJ} \tag{110a}$$

(107a) becomes, assuming negligible heat transfer,

$$\frac{W_{shaft}}{JM} - \frac{W_{friction}}{JM} = h_{0I\ out} - h_{0I\ in} \tag{107b}$$

If we neglect the work done by friction,

$$\frac{W_{shaft}}{JM} = h_{oI\,out} - h_{oI\,in} \qquad (107c)$$

(107c) is the energy equation for steady, one-dimensional flow of a non-viscous pure substance through a control surface fixed in an inertial reference frame.

We may express h_{OI} in terms of T and V by using (86g) and (110a):

$$h_{OI} = c_p\ T + \frac{V^2}{2g_oJ} \equiv c_p\ T_{OI} \qquad (113)$$

$$T_{OI} \equiv T + \frac{V^2}{2g_oJ\ c_p} \qquad (113a)$$

Appendix H

D	indicates substantial differentiation while following the motion of a system of fixed identity
g_o	universal constant relating force and mass, 32.174 lbm ft/sec^2 lbf
M	total mass of a system, lbm
m	time rate of mass flow of a system, lbm/sec
P	a system
P_{shaft}	power developed by a rotating shaft, ft lbf/sec
r	radial distance from Z axis to system, ft
r_{in}	radial distance from Z axis to a system just before the system enters a control volume, ft
r_{out}	radial distance from Z axis to a system just before the system leaves a control volume, ft
$T_{friction}$	unbalanced torque exerted by a system (lying within a control volume) because of friction on the control surface, ft lbf
T_{shaft}	unbalanced torque exerted on a system (lying within a control volume) by a rotating shaft which pierces the control surface symmetrically about the Z axis, ft lbf
T_z	unbalanced torque acting about the Z axis, ft lbf
t	time, sec

V_θ — that component of the absolute velocity of a system which lies in a plane perpendicular to the Z axis and is normal to r, ft/sec

$V_{\theta\ in}$ — the value of V_θ just before a system enters a control volume, ft/sec

$V_{\theta\ out}$ — the value of V_θ just before a system leaves a control volume, ft/sec

W_{shaft} — work flowing into a control volume due to a rotating shaft which pierces the control surface symmetrically about the Z axis, ft/lbf

X — total angular momentum of a system about the Z axis, defined by equation (114), lbm ft^2/sec

x — unit angular momentum of a system about the Z axis, defined by equation (115), ft^2/sec

ω — angular velocity of the rotating shaft which pierces the control surface symmetrically about the Z axis, rad/sec

Appendix H

EULERS PUMP AND TURBINE EQUATION

Euler's equation relates the shaft work required to produce a given change in angular momentum (moment of momentum) of a system. We specify that our system instantaneously occupies a control volume which is fixed in an inertial reference frame.

If the system, as it flows in the inertial reference frame, has a component of velocity which will produce a torque about some given axis (the "Z" axis), we say that the system has angular momentum about the Z axis. We use (96), Appendix G, to express the time rate of change of angular momentum of the system as it flows through a fixed control surface. Figure 12 shows a system P which has a component of velocity, V_θ, about the Z axis. r is the shortest distance from the Z axis to P.

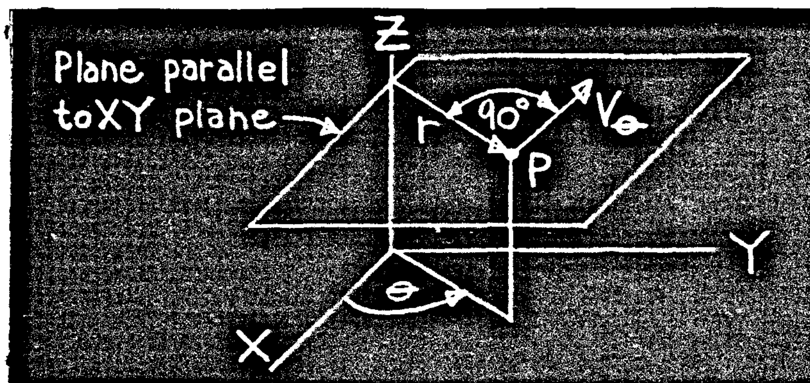

Figure 12

Definition of V_θ

We define:

$$X \equiv \text{angular momentum about the Z axis} \equiv Mr\,V_\theta \quad (114)$$

$$x \equiv \text{angular momentum per unit mass} \equiv r\,V_\theta \quad (115)$$

From (96), (114), and (115),

$$\frac{D(Mr\ V_\theta)}{Dt} = m\ [(r\ V_\theta)_{out} - (r\ V_\theta)_{in}] \qquad (116)$$

From Newton's law of motion, the sum of the unbalanced torques acting on the system about the Z axis equals the time rate of change of the angular momentum about the Z axis.

$$g_o \sum T_Z = \frac{D(Mr\ V_\theta)}{Dt} \qquad (117)$$

Combining (116) and (117),

$$g_o \sum T_Z = m\ [(r\ V_\theta)_{out} - (r\ V_\theta)_{in}] \qquad (118)$$

We shall specify the following:

1. A CS concentric with the Z axis, and symmetrical about the Z axis.

2. If there are electrical or magnetic fields or capillary forces present, their effect on the system is negligible. Electrical and magnetic fields, even if very strong, will not affect the flow of air, unless the air were ionized. Capillary forces are present only in control surfaces of very small size.

Specification 1 means that pressure forces and gravity forces have no unbalanced torque about the Z axis, regardless of the inclination of the Z axis. Specifications 1 and 2 together mean that only shear forces may have an unbalanced torque about the Z axis. The forces mentioned are the only forces of importance in an inertial reference frame.

For convenience, we separate the unbalanced shear torques into two groups:

$$\sum T_Z = T_{shaft} - T_{friction} \tag{119}$$

T_{shaft} is the torque exerted on the system by a shaft which pierces the CS and is symmetrical about the Z axis (positive for a compressor, negative for a turbine). $T_{friction}$ is the torque exerted by the system on the <u>boundries</u> of the CS (always negative). Friction within the CS does not affect the analysis.

If the shaft rotates with constant angular velocity ω about the Z axis,

$$T_{shaft} = \frac{P_{shaft}}{\omega} = \frac{m\, W_{shaft}}{M\,\omega} \tag{120}$$

Combining (118), (119), and (120),

$$g_o\, [(\frac{m\, W_{shaft}}{M\,\omega}) - T_{friction}] = m\, [(r\, V_\theta)_{out} - (r\, V_\theta)_{in}]$$

$$\frac{W_{shaft}}{M} - \frac{T_{friction}\,\omega}{m} = \frac{\omega}{g_o}\, [(r\, V_\theta)_{out} - (r\, V_\theta)_{in}] \tag{121}$$

(121) is Euler's pump and turbine equation for steady, one-dimensional flow through a fixed CS in an inertial reference frame.

Appendix J

A	net flow area normal to the mean streamline, ft^2
c	local speed of sound, defined by equation (124), ft/sec
c_o	reference velocity (local speed of sound corresponding to stagnation temperature, equation (129)), ft/sec
g_o	universal constant relating force and mass, 32.174 lbm ft/sec^2 lbf
K	constant in equation (143), 1/sec
k	ratio of specific heats
M_A	Mach number as measured in an accelerating reference frame, defined by equation (123)
M_I	Mach number as measured in an inertial reference frame, defined by equation (122)
m	time rate of mass flow along the mean streamline, lbm/sec
p	static pressure, lbf/ft^2
Q	symbol used in equation (155)
R	gas constant, ft lbf/lbm R
r	radial distance from the Z axis, ft
s	distance along the mean streamline (Figures 8 and 9d), ft
T	static temperature, R
T_o	stagnation temperature, R
V	absolute velocity, ft/sec
W	relative velocity, ft/sec

x	symbol used in equation (153)
ρ	static density, lbm/ft^3
ω	angular velocity of accelerating reference frame about Z axis, rad/sec
sub s	at constant entropy
sub 1.1	on the mean relative streamline at the impeller inlet

Appendix J

ONE-DIMENSIONAL ISENTROPIC FLOW OF A PERFECT GAS ALONG A RELATIVE STREAMLINE IN A COMPRESSOR OR TURBINE IMPELLER WITH STRAIGHT RADIAL BLADES AND AXIAL SYMMETRY

In this appendix, we express the governing physical laws of isentropic flow in an impeller in differential form. We will then have "influence coefficients" (reference 9, p. 227) which express the effects of area and radius changes on fluid properties such as static pressure and static temperature along a relative streamline.

We now define:

$$M_I \equiv \frac{V}{c} \equiv \text{absolute Mach number} \qquad (122)$$

$$M_A \equiv \frac{W}{c} \equiv \text{relative Mach number} \qquad (123)$$

$$c^2 \equiv g_o \left(\frac{\partial p}{\partial \varphi}\right)_s \equiv \text{local speed of sound} \qquad (124)$$

We may transform (124) by using (83), the isentropic relation for a perfect gas, and (86f), the perfect gas pressure-density-temperature relationship.

$$p = \text{constant} \times \varphi^k \qquad (83)$$

$$p = \varphi R T \qquad (86f)$$

Taking the logarithmic differential of (83),

$$\left(\frac{\partial p}{p}\right)_s = k \left(\frac{\partial \rho}{\rho}\right)_s$$

$$\left(\frac{\partial p}{\partial \rho}\right)_s = k \frac{p}{\rho} \qquad (126)$$

Combining (126) and (86f),

$$\left(\frac{\partial p}{\partial \rho}\right)_s = k\, R\, T \qquad (127)$$

Combining (127) and (124),

$$c^2 = g_o k\, R\, T \qquad (128)$$

Also,

$$c_o^{\,2} \equiv g_o k\, R\, T_o \qquad (129)$$

From Appendix E, equation (76a),

$$\frac{\partial p}{\partial s} = - \frac{\rho}{g_o} \left(W \frac{\partial W}{\partial s} - \omega^2 r \frac{\partial r}{\partial s}\right) \qquad (76a)$$

For changes along a particular relative streamline,

$$dp = - \frac{\rho}{g_o} \left(W^2 \frac{dW}{W} - \omega^2 r^2 \frac{dr}{r}\right) \qquad (76c)$$

Noting that, from (123) and (128),

$$M_A \equiv \frac{W}{c} = \frac{W}{\sqrt{g_o k\, R\, T}} \qquad (130)$$

From (86f) and (130),

$$\frac{\varphi}{g_o} W^2 = \frac{kp}{g_o k R T} W^2 = kp\, M_A{}^2 \tag{131}$$

We may now write (76c) in the differential form:

$$\frac{dp}{p} = -k\, M_A{}^2 \frac{dW}{W} + k \frac{\omega^2 r^2}{c^2} \frac{dr}{r} \tag{132}$$

We have, from Appendix G, the continuity equation for one-dimensional flow:

$$m = \varphi A W = \text{constant} \tag{95}$$

Writing (95) in differential form (by differentiating the natural logarithm):

$$\frac{d\varphi}{\varphi} + \frac{dA}{A} + \frac{dW}{W} = 0 \tag{133}$$

Similarly, (86f), (83), and (130) may be written:

$$\frac{dp}{p} = \frac{d\varphi}{\varphi} + \frac{dT}{T} \tag{134}$$

$$\frac{dp}{p} = k \frac{d\varphi}{\varphi} \tag{135}$$

$$\frac{dM_A{}^2}{M_A{}^2} = 2 \frac{dW}{W} - \frac{dT}{T} \tag{136}$$

We now have 5 simultaneous equations (132 to 136) in 7 unknowns; $\frac{dp}{p}$, $\frac{dW}{W}$, $\frac{\omega^2 r^2}{c^2} \frac{dr}{r}$, $\frac{d\varphi}{\varphi}$, $\frac{dA}{A}$, $\frac{dT}{T}$, and $\frac{dM_A^2}{M_A^2}$. We are free to choose any 2 of these unknowns as independent and express each of the remaining 5 unknowns in terms of these 2. For our purposes, we choose $\frac{dA}{A}$ and $\frac{\omega^2 r^2}{c^2} \frac{dr}{r}$ as the 2 independent variables. We then have, using (132), (135), and (133):

$$\frac{dp}{p} = -k\, M_A{}^2 \frac{dW}{W} + k \frac{\omega^2 r^2}{c^2} \frac{dr}{r} = k \frac{d\varphi}{\varphi} = k\left(-\frac{dA}{A} - \frac{dW}{W}\right)$$

Rearranging,

$$\frac{dW}{W} = -\frac{1}{1-M_A{}^2} \frac{dA}{A} - \frac{1}{1-M_A{}^2} \frac{\omega^2 r^2}{c^2} \frac{dr}{r} \tag{137}$$

Using (132) and (137),

$$\frac{dp}{p} = \frac{kM_A{}^2}{1-M_A{}^2} \frac{dA}{A} + \frac{k}{1-M_A{}^2} \frac{\omega^2 r^2}{c^2} \frac{dr}{r} \tag{138}$$

Using (135) and (138),

$$\frac{d\varphi}{\varphi} = \frac{M_A{}^2}{1-M_A{}^2} \frac{dA}{A} + \frac{1}{1-M_A{}^2} \frac{\omega^2 r^2}{c^2} \frac{dr}{r} \tag{139}$$

Using (134), (138), and (139),

$$\frac{dT}{T} = \frac{M_A{}^2(k-1)}{1-M_A{}^2} \frac{dA}{A} + \frac{k-1}{1-M_A{}^2} \frac{\omega^2 r^2}{c^2} \frac{dr}{r} \tag{140}$$

From (128),

$$\frac{dc^2}{c^2} = \frac{dT}{T} \tag{141}$$

Using (136), (137), and (140),

$$\frac{dM_A{}^2}{M_A{}^2} = -\frac{2 + M_A{}^2(k-1)}{1-M_A{}^2}\ \frac{dA}{A} - \frac{k+1}{1-M_A{}^2}\ \frac{\omega^2\ r^2}{c^2}\ \frac{dr}{r} \tag{142}$$

These formulas are summarized in Table 1.

TABLE 1

INFLUENCE COEFFICIENTS FOR ONE-DIMENSIONAL ISENTROPIC FLOW OF A PERFECT GAS ALONG A RELATIVE STREAMLINE IN A COMPRESSOR OR TURBINE IMPELLER WITH STRAIGHT RADIAL BLADES AND AXIAL SYMMETRY

	$\frac{dA}{A}$	$\frac{\omega^2 r^2}{c^2} \frac{dr}{r}$
$\frac{dM_A^2}{M_A^2}$	$-\frac{2 + M_A^2(k-1)}{1-M_A^2}$	$-\frac{k+1}{1-M_A^2}$
$\frac{dW}{W}$	$-\frac{1}{1-M_A^2}$	$-\frac{1}{1-M_A^2}$
$\frac{dp}{p}$	$\frac{kM_A^2}{1-M_A^2}$	$\frac{k}{1-M_A^2}$
$\frac{d\varphi}{\varphi}$	$\frac{M_A^2}{1-M_A^2}$	$\frac{1}{1-M_A^2}$
$\frac{dT}{T} = \frac{dc^2}{c^2}$	$\frac{M_A^2(k-1)}{1-M_A^2}$	$\frac{k-1}{1-M_A^2}$

All of the above was taken, by permission, from unpublished notes of Professor Ascher H. Shapiro.

From Table 1, we list the following rules for one-dimensional flow, within the specified assumptions:

1. Area increase and radius increase have the same qualitative effect on all listed properties and conversely.

2. Due to the factor $1-M_A^2$ in the denominator, all listed properties undergo opposite effects as M_A passes through unity. For example, radius (or area) increase decreases M_A in subsonic flows and increases M_A in supersonic flows.

3. Increase of area or radius always drives M_A away from unity. Thus, for a centrifugal compressor with subsonic entry, the increase in radius makes it very difficult to reach Mach number unity (due to the factor r^2) while the opposite is true for centripetal turbines with subsonic entry. We see that choking (Mach number reaching unity) will normally occur in the inducer of a compressor and in the exducer of a turbine (with subsonic entry).

Area Variation Along a Relative Streamline for a Linear Variation in Relative Velocity with Radius

We now derive, in closed form, the necessary area change required to maintain a prescribed linear variation of relative velocity with radius. This prescribed velocity variation has the form:

$$W = W_{1.1} + K\,(r - r_{1.1}) \tag{143}$$

where K is a prescribed constant having the dimension sec^{-1} and station 1.1 is at the impeller inlet.

From Table 1,

$$\frac{dW}{W} = -\frac{1}{1-M_A{}^2}\,\frac{dA}{A} - \frac{1}{1-M_A{}^2}\,\frac{\omega^2 r^2}{c^2}\,\frac{dr}{r}$$

Thus,

$$\frac{dA}{A} = -\,(1-M_A{}^2)\,\frac{dW}{W} - \frac{\omega^2 r^2}{c^2}\,\frac{dr}{r} \tag{144}$$

From Table 1,

$$\frac{dc^2}{c^2} = \frac{M_A{}^2(k-1)}{1-M_A{}^2} \frac{dA}{A} + \frac{k-1}{1-M_A{}^2} \frac{\omega^2 r^2}{c^2} \frac{dr}{r} \qquad (145)$$

Combining (145) and (144),

$$dc^2 = - c^2 M_A{}^2(k-1) \frac{dW}{W} + (k-1) \omega^2 r\, dr \qquad (146)$$

Noting that

$$c^2 M_A{}^2 = W^2 \qquad (123)$$

(146) becomes

$$dc^2 = -(k-1)\, WdW + (k-1) \omega^2 r\, dr \qquad (146a)$$

Before integrating (146a), we must select <u>one</u> particular relative streamline as being a sort of average or "mean" streamline which represents the flow through the entire impeller channel (see Figure 14 in Appendix L).

Integrating (146a) from the impeller inlet to any station downstream on the "mean" relative streamline,

$$c^2 = c_{1.1}{}^2 - \frac{k-1}{2} (W^2 - W_{1.1}{}^2) + \frac{k-1}{2} \omega^2 (r^2 - r_{1.1}{}^2) \qquad (147)$$

Introducing (147) into (144),

$$\frac{dA}{A} = -(1-M_A{}^2) \frac{dW}{W} - \frac{\omega^2 r^2}{c_{1.1}{}^2 - \frac{k-1}{2} (W^2 - W_{1.1}{}^2) + \frac{k-1}{2} \omega^2 (r^2 - r_{1.1}{}^2)} \frac{dr}{r}$$

(148)

From (143),

$$W^2 = W_{1.1}{}^2 + 2W_{1.1}\,K(r - r_{1.1}) + K^2\,(r - r_{1.1})^2 \tag{149}$$

Introducing (123) and (149) into (148),

$$\frac{dA}{A} + \frac{dW}{W} = \frac{2(WdW - \omega^2\,r\,dr)}{2c^2}$$

where (150)

$$2c^2 = 2c_{1.1}{}^2 - (k-1)[2W_{1.1}\,K(r - r_{1.1}) + K^2(r - r_{1.1})^2]$$
$$+ (k-1)\omega^2\,(r^2 - r_{1.1}{}^2)$$

From (143),

$$dW = K\,dr \tag{151}$$

Inserting (151) and (143) into (150),

$$\frac{dA}{A} + \frac{dW}{W} = \frac{2W_{1.1}\,K\,dr + 2K^2(r - r_{1.1})\,dr - 2\,\omega^2\,r\,dr}{2c^2} \tag{152}$$

We now observe that

$$\left.\begin{aligned} d(2c^2) \equiv dx = -(k-1)(2W_{1.1}\,K\,dr) - 2(k-1)K^2\,(r - r_{1.1}) \\ dr + 2\,(k-1)\,\omega^2 r\,dr \end{aligned}\right\} \tag{153}$$

(152) is of the form

$$\frac{dA}{A} + \frac{dW}{W} = -\frac{1}{k-1}\,\frac{dx}{x} \tag{154}$$

Integrating (154),

$$\ln \frac{A}{A_{1.1}} + \ln \frac{W}{W_{1.1}} = \ln \left(\frac{A}{A_{1.1}} \ \frac{W}{W_{1.1}}\right) = -\frac{1}{k-1} \ln \frac{x}{x_{1.1}}$$

$$\frac{A}{A_{1.1}} = \frac{W_{1.1}}{W} \ (Q)^{-\frac{1}{k-1}}$$

where

$$Q \equiv \left(\frac{2c_{1.1}^{\ 2} - (k-1)K^2(r^2 - r_{1.1}^{\ 2})[\frac{2}{K} \frac{W_1}{(r-r_{1.1})} + 1] + (k-1)\omega^2 r_{1.1}^{\ 2}[(\frac{r}{r_{1.1}})^2 - 1]}{2c_{1.1}^{\ 2}}\right)$$

$$\frac{A}{A_{1.1}} = \frac{W_{1.1}}{W_{1.1} + K(r-r_{1.1})} \left(1 - \frac{k-1}{2} \ \frac{K^2(r^2 - r_{1.1}^{\ 2})}{c_{1.1}^{\ 2}}\right.$$

$$\left.[\frac{2}{K} \frac{W_1}{(r-r_{1.1})} + 1] + \frac{k-1}{2} \ \frac{\omega^2 \ r_{1.1}^{\ 2}}{c_{1.1}^{\ 2}} \ [(\frac{r}{r_{1.1}})^2 - 1]\right)^{-\frac{1}{k-1}} \tag{155}$$

(155) gives the required area variation with radius for one-dimensional isentropic flow with a linear variation in relative velocity.

If $K \equiv 0$, that is, if $W = W_{1.1}$ = constant, (155) becomes

$$\frac{A}{A_{1.1}} = \left(1 + \frac{k-1}{2} \ \frac{\omega^2 \ r_{1.1}^{\ 2}}{c_{1.1}^{\ 2}} \ [(\frac{r}{r_{1.1}})^2 - 1]\right)^{-\frac{1}{k-1}} \tag{156}$$

In order to illustrate the effects of important parameters, we rearrange (155) and introduce (123).

$$\frac{A}{A_{1.1}} = \frac{1}{1 + \frac{Kr_{1.1}}{W_{1.1}}(\frac{r}{r_{1.1}} - 1)} \left\{ 1 - \frac{k-1}{2} \frac{Kr_{1.1}}{W_{1.1}} M_{1.1A}{}^{2}(\frac{r}{r_{1.1}} - 1) \right.$$

$$\left. [2 + \frac{Kr_{1.1}}{W_{1.1}}(\frac{r}{r_{1.1}} - 1)] + \frac{k-1}{2} \; \frac{\omega^2 \, r_{1.1}{}^2}{c_{1.1}{}^2} \, [(\frac{r}{r_{1.1}})^2 - 1] \right\}^{-\frac{1}{k-1}}$$

(155a)

Important parameters are seen to be:

$$\frac{Kr_{1.1}}{W_{1.1}} \; , \; \frac{r}{r_{1.1}} \; , \; M_{1.1A}, \text{ and } \; \frac{\omega^2 \, r_{1.1}{}^2}{c_{1.1}{}^2}$$

Appendix K

c local speed of sound, ft/sec

g_o universal constant relating force and mass, 32.174 lbm ft/sec^2 lbf

k ratio of specific heats

M_A Mach number as measured in an accelerating reference frame

n distance normal to the mean streamline (Figures 8 and 9d), ft

p static pressure, lbf/ft^2

R_c local radius of curvature of the mean streamline (Figures 8 and 9d), ft

r radial distance from the Z axis, ft

T static temperature, R

W relative velocity along the mean streamline, ft/sec

ρ static density, lbm/ft^3

ω angular velocity of accelerating reference frame (impeller) about Z axis, rad/sec

Appendix K

CHANGE IN FLUID PROPERTIES NORMAL TO THE MEAN RELATIVE STREAMLINE

We parallel the development of Appendix J. The governing physical laws for isentropic changes in fluid properties normal to the mean streamline are as follows:

From Appendix F, equations (77d) and (82):

$$dp = \frac{\varphi}{g_o} W^2 \frac{dn}{R_c} + \frac{\varphi}{g_o} \omega^2 r^2 \frac{dr}{r} \qquad (77d)$$

$$\frac{dW}{W} = - \frac{dn}{R_c} \qquad (82)$$

We have shown previously (Appendix J, (131) and (123)):

$$\frac{\varphi}{g_o} W^2 = kp\, M_A^2 \qquad (131)$$

$$c^2 = \frac{W^2}{M_A^2} \qquad (123)$$

Introducing (82), (131), and (123) into (77d),

$$\frac{dp}{p} = -k\, M_A^2 \frac{dW}{W} + k \frac{\omega^2 r^2}{c^2} \frac{dr}{r} \qquad (132)$$

Thus, we see that for isentropic and irrotational flow, the differential pressure change normal to a streamline is identical to the change along a streamline.

Equations (134), (135), (136), and (141) are valid in <u>any</u> direction:

$$\frac{dp}{p} = \frac{d\varphi}{\varphi} + \frac{dT}{T} \tag{134}$$

$$\frac{dp}{p} = k\,\frac{d\varphi}{\varphi} \tag{135}$$

$$\frac{dM_A{}^2}{M_A{}^2} = 2\,\frac{dW}{W} - \frac{dT}{T} \tag{136}$$

$$\frac{dc^2}{c^2} = \frac{dT}{T} \tag{141}$$

We now have 6 simultaneous equations [(82), (132), (134), (135), (136), and (141)] in 8 unknowns; $\frac{dW}{W}$, $\frac{dn}{R_c}$, $\frac{dp}{p}$, $\frac{\omega^2 r^2}{c^2}\ \frac{dr}{r}$, $\frac{d\varphi}{\varphi}$, $\frac{dT}{T}$, $\frac{dM_A{}^2}{M_A{}^2}$, and $\frac{dc^2}{c^2}$. As before, we are free to choose any 2 as independent and express the remaining 6 as functions of these 2. Here we choose $\frac{dn}{R_c}$ and $\frac{\omega^2 r^2}{c^2}\ \frac{dr}{r}$ as the independent variables. We then have,

$$\frac{dW}{W} = -\frac{dn}{R_c} \tag{82}$$

$$\frac{dp}{p} = k\,M_A{}^2\,\frac{dn}{R_c} + k\,\frac{\omega^2 r^2}{c^2}\ \frac{dr}{r} \tag{157}$$

$$\frac{d\varphi}{\varphi} = M_A{}^2\,\frac{dn}{R_c} + \frac{\omega^2 r^2}{c^2}\ \frac{dr}{r} \tag{158}$$

$$\frac{dT}{T} = M_A{}^2(k-1)\,\frac{dn}{R_c} + (k-1)\,\frac{\omega^2 r^2}{c^2}\ \frac{dr}{r} \tag{159}$$

$$\frac{dc^2}{c^2} = M_A{}^2(k-1)\,\frac{dn}{R_c} + (k-1)\,\frac{\omega^2 r^2}{c^2}\,\frac{dr}{r} \tag{160}$$

$$\frac{dM_A{}^2}{M_A{}^2} = -[2 + M_A{}^2(k-1)]\,\frac{dn}{R_c} - (k-1)\,\frac{\omega^2 r^2}{c^2}\,\frac{dr}{r} \tag{161}$$

These formulas are summarized in Table 2.

TABLE 2

INFLUENCE COEFFICIENTS FOR ONE-DIMENSIONAL ISENTROPIC CHANGES IN FLUID PROPERTIES OF A PERFECT GAS NORMAL TO A RELATIVE STREAMLINE IN A COMPRESSOR OR TURBINE IMPELLER WITH STRAIGHT RADIAL BLADES AND AXIAL SYMMETRY

	$\frac{dn}{R_c}$	$\frac{\omega^2 r^2}{c^2}\ \frac{dr}{r}$
$\frac{dM_A{}^2}{M_A{}^2}$	$-[2 + M_A{}^2(k-1)]$	$-(k-1)$
$\frac{dW}{W}$	-1	0
$\frac{dp}{p}$	$kM_A{}^2$	k
$\frac{d\varphi}{\varphi}$	$M_A{}^2$	1
$\frac{dT}{T} = \frac{dc^2}{c^2}$	$M_A{}^2(k-1)$	$(k-1)$

From Table 2 we list the rules for changes in properties normal to a streamline:

1. Increase in distance from the center of curvature and radius increase have the same qualitative effect on all listed properties (except relative velocity) and conversely.

2. Relative velocity decreases as distance from the center of curvature increases and conversely, but relative velocity is unaffected by changes in radius.

3. Passage of M_A through unity has no effect on the direction of change of all listed properties.

4. For changes in radius only (constant area), all listed properties are unaffected by Mach number. Thus, for simple radius change, compressibility of the gas has no effect on changes normal to a streamline.

Appendix L

F_θ	distributed body force in the θ direction, lbf/lbm
g_o	universal constant relating force and mass, 32.174 lbm ft/sec^2 lbf
h	static enthalpy, BTU/lbm
h_o	stagnation enthalpy, BTU/lbm
J	universal constant relating work and heat, 778.2 ft lbf/BTU
K	constant defined by equation (167), BTU/lbm
M	total mass of a system instantaneously within a control volume, lbm
p	static pressure, lbf/ft^2
r	radial distance from Z axis, ft
s	entropy, BTU/lbm R
T	static temperature, R
V	absolute velocity, ft/sec
$V_{\theta\ in}$	component of absolute velocity of a system in the θ direction just before the system enters a control volume, ft/sec
$V_{\theta\ out}$	component of absolute velocity of a system in the θ direction just before the system leaves a control volume, ft/sec
W	relative velocity, ft/sec
W_r, W_z	components of relative velocity in the r and z directions, ft/sec

W_{shaft}	work flowing into a control volume due to a rotating shaft which pierces the control surface symmetrically about the Z axis, ft lbf
ρ	static density, lbm/ft^3
ω	angular velocity of accelerating reference frame (same as angular velocity of impeller), rad/sec
sub I	in an inertial reference frame
sub 1	at the inducer inlet
sub 1.1	at the impeller inlet

Appendix L

PROPERTIES AT THE IMPELLER INLET

To determine the fluid properties at the impeller inlet (inducer outlet), we write the governing physical laws for fluid flow at the impeller inlet (station 1.1).

1. Relation between properties of a pure substance

$$T ds = dh - \frac{1}{J\varphi} dp \qquad (162)$$

2. Equations of motion in an axisymmetric rotating reference frame (equations (62a), (62b), (62c), and (64) from Appendix E)

$$-\frac{\partial p}{\partial r} = \frac{\varphi}{g_o}\left(W_r \frac{\partial W_r}{\partial r} + W_z \frac{\partial W_r}{\partial z} - \omega^2 r\right) \qquad (163)$$

$$g_o F_\theta = 2\,\omega\, W_r \qquad (62b)$$

$$-\frac{\partial p}{\partial z} = \frac{\varphi}{g_o}\left(W_r \frac{\partial W_z}{\partial r} + W_z \frac{\partial W_z}{\partial z}\right) \qquad (164)$$

3. Euler's equation in an inertial reference frame (equation (121) from Appendix H, and neglecting friction)

$$\frac{W_{shaft}}{M} = \left(\frac{\omega^2 r^2}{g_o}\right)_I \qquad (165)$$

where $V_{\theta\ in} \equiv 0$ and $V_{\theta\ out} \equiv \omega r$; r is any radius at the impeller inlet. We see from (165) that the shaft work is not uniform at the impeller inlet but varies as the square of the inlet radius.

4. Energy equation in an inertial reference frame (equation (107b) from Appendix G, and neglecting friction)

$$\frac{W_{shaft}}{M} = J\left[\left(h_{1.1} + \frac{V_{1.1}^2}{2g_o J}\right) - \left(h_1 + \frac{V_1^2}{2g_o J}\right)\right]_I \qquad (166)$$

We previously assumed that the inducer inlet flow was irrotational (Appendix F), thus from (84c) and (110a),

$$h_{OI} \equiv h_1 + \frac{V_1^2}{2g_o J} = \text{constant at any radius} \equiv K \qquad (167)$$

Combining (166) and (167)

$$\frac{W_{shaft}}{M} = J\left(h_{1.1} + \frac{V_{1.1}^2}{2g_o J} - K\right) \qquad (168)$$

We now use these 4 equations to determine the variation of relative velocity with radius at the impeller inlet.

From (162),

$$\frac{\partial h}{\partial r} = T\,\frac{\partial s}{\partial r} + \frac{1}{J\rho}\,\frac{\partial p}{\partial r} \qquad (169)$$

For frictionless, adiabatic, and irrotational flow,

$$\frac{\partial s}{\partial r} = 0 \text{ (the entropy is constant in any direction)}$$

(169) becomes,

$$\frac{\partial h}{\partial r} = \frac{1}{J\rho}\,\frac{\partial p}{\partial r} \qquad (170)$$

If we <u>assume</u> that W_r at the impeller inlet is zero, (163) becomes:

$$\frac{\partial p}{\partial r} = \frac{\rho}{g_o}\,\omega^2 r \qquad (163a)$$

Combining (170) and (163a),

$$\frac{\partial h}{\partial r} = \frac{1}{Jg_o} \omega^2 r \tag{171}$$

Combining (165) and (168),

$$\frac{\omega^2 r^2}{Jg_o} = h + \frac{V^2}{2g_o J} - K \tag{172}$$

But, at the impeller inlet, from (175a), Appendix M,

$$V^2 = \omega^2 r^2 + W^2 \tag{175a}$$

(172) becomes:

$$\frac{\omega^2 r^2}{2g_o J} = h + \frac{W^2}{2g_o J} - K \tag{173}$$

Differentiating (173) in the r direction,

$$\frac{\omega^2}{2g_o J} (2r) = \frac{\partial h}{\partial r} + \frac{1}{2g_o J} \left(2W \frac{\partial W}{\partial r}\right) \tag{174}$$

Combining (174) and (171),

$$\frac{\omega^2 r}{g_o J} = \frac{\omega^2 r}{g_o J} + \frac{W}{g_o J} \frac{\partial W}{\partial r}$$

Thus, since $W \neq 0$,

$$\frac{\partial W}{\partial r} = 0$$

This means that W is constant radially at the impeller inlet, if the assumed conditions are true.

This result checks with equation (82) in Appendix K.

$$\frac{dW}{W} = -\frac{dn}{R_c} \tag{82}$$

If W_r and W_θ are zero at the impeller inlet, the fluid is flowing parallel to the Z axis and the curvature of the relative streamlines is zero (R_c is infinite). Under this condition, (82) becomes

$$\frac{dW}{W} = \frac{dW_z}{W_z} = 0$$

which integrates to

$$W = W_z = \text{constant radially.}$$

Appendix M

A	area normal to the mean streamline, ft^2
A_g	gross area normal to the mean streamline (not including area taken up by blades), ft^2
A_{gc}	that part of A_g which lies between the casing and the mean streamline, ft^2
A_{gh}	that part of A_g which lies between the hub and the mean streamline, ft^2
A_{net}	net area normal to the mean streamline (including area taken up by blades), ft^2
CS	inertial control surface used to calculate impeller tip speed (Figure 13)
c	local speed of sound, ft/sec
c_o	local speed of sound corresponding to local stagnation temperature, ft/sec
C_p	specific heat at constant pressure, BTU/lbm R
C_v	specific heat at constant volume, BTU/lbm R
$D\bar{s}$	an infinitesimal distance travelled along the mean streamline by a particle of fixed identity (Figure 19), ft
$D\bar{r}$	the component of $D\bar{s}$ in the positive r direction, ft
$D\bar{z}$	the component of $D\bar{s}$ in the positive Z direction, ft
$D\bar{\alpha}$	the infinitesimal change in $\bar{\alpha}$ corresponding to $D\bar{s}$, rad
dn	an infinitesimal distance measured normal to the mean streamline, positive when away from the center of curvature of the mean streamline, ft

dW the infinitesimal velocity change normal to the mean streamline corresponding to dn, ft/sec

f_s slip factor (ratio of actual tangential component of absolute velocity at impeller outlet to impeller tip speed)

g_o universal constant relating force and mass, 32.174 lbm ft/sec^2 lbf

h_o enthalpy corresponding to stagnation temperature, BTU/lbm

J universal constant relating work and heat, 778.2 ft lbf/BTU

k ratio of specific heats, C_p/C_v

M total mass of a system, lbm

$\bar{M}$ molecular mass of fluid flowing through impeller, lbm/mole

M_A Mach number measured in an accelerating reference frame (defined by equation (123))

M_I Mach number measured in an inertial reference frame (defined by equation (122))

m time rate of mass flow through impeller, lbm/sec

m_o reference mass flow defined by equation (181), lbm/sec

n distance measured normal to the mean streamline, positive when away from the center of curvature of the mean streamline, ft

$\bar{n}$ distance from center of curvature of mean streamline to mean streamline (Figure 19), ft

n_c distance from center of curvature of mean streamline to casing (Figure 19 and 24), ft

n_c' actual radius of curvature of casing (Figure 24), ft

n_h distance from center of curvature of mean streamline to hub (Figures 19 and 24), ft

n_h' actual radius of curvature of hub (Figure 24), ft

$\bar{O}$ center of curvature of mean streamline (Figures 19 and 24)

O_c center of curvature of casing (Figure 24)

O_h center of curvature of hub (Figure 24)

p static pressure, lbf/ft^2

p_o isentropic stagnation pressure, lbf/ft^2

R gas constant for particular fluid flowing through impeller, ft lbf/lbm R

$\bar{R}$ universal gas constant, 1545.32 ft lbf/mole R

R_c local radius of curvature of any specified relative streamline, ft

$\bar{R}_c$ local radius of curvature of mean streamline, ft ($\bar{R}_c \equiv \bar{n}$)

r radius from Z axis, ft

$\bar{r}$ radius from Z axis to mean streamline, ft

r_c radius from Z axis to casing, ft

r_h radius from Z axis to hub, ft

r_h' imaginary hub radius defined by equation (180), ft

T static temperature, R

T_o	adiabatic stagnation temperature, R
$T_{friction}$	unbalanced torque exerted by a system (lying within a control volume) because of friction on the control surface, ft lbf
t	blade thickness, ft
V	absolute velocity of fluid, ft/sec
V_θ	tangential component of V, ft/sec
W	relative velocity of fluid, ft/sec
$\bar{W}$	relative velocity along the mean streamline, ft/sec
W_c	relative velocity along the casing, ft/sec
W_h	relative velocity along the hub, ft/sec
$W_{friction}$	work flowing out of a control volume because of friction on the control surface, ft lbf
W_{shaft}	work flowing into a control volume due to a rotating shaft which pierces the control surface symmetrically about the Z axis, ft/lbf
Z	number of blades
$\bar{\alpha}$	angle between tangent to mean streamline and Z axis (Figure 19), rad
$\Delta \cot \bar{\alpha}$	a finite increment in $\cot \bar{\alpha}$, defined by equation (205)
$\Delta \bar{r}$	a finite increment in $\bar{r}$, defined by equation (206), ft
ρ	static density of fluid, lbm/ft^3
ρ_o	fluid density corresponding to stagnation temperature and pressure, lbm/ft^3

ω angular velocity of rotating shaft and impeller, rad/sec

sub 1 at the inducer inlet

sub 1.1 at the impeller inlet

sub 2 at the impeller outlet

sub I quantity measured in an inertial (non-accelerating) reference frame

Appendix M

NUMERICAL EXAMPLE - COMPRESSOR IMPELLER

Universal constants

$$g_o = 32.174$$

$$J = 778.2$$

$$\bar{R} = 1545.32$$

Properties of air (assumed constant)

$$\bar{M} = 28.970$$

$$R = \frac{\bar{R}}{\bar{M}} = 53.342$$

$$k = 1.4000$$

$$c_p = \frac{k}{k-1} \frac{R}{J} = .2399$$

$$c_v = \frac{c_p}{k} = .1713$$

Performance parameters

$$T_{o1} = 550$$

$$p_{o1} = 14.7 \text{ PSIA}$$

$$\frac{p_{o2}}{p_{o1}} = 6$$

$$m = 10$$

where station 1 and station 2 are shown in Figure 13.

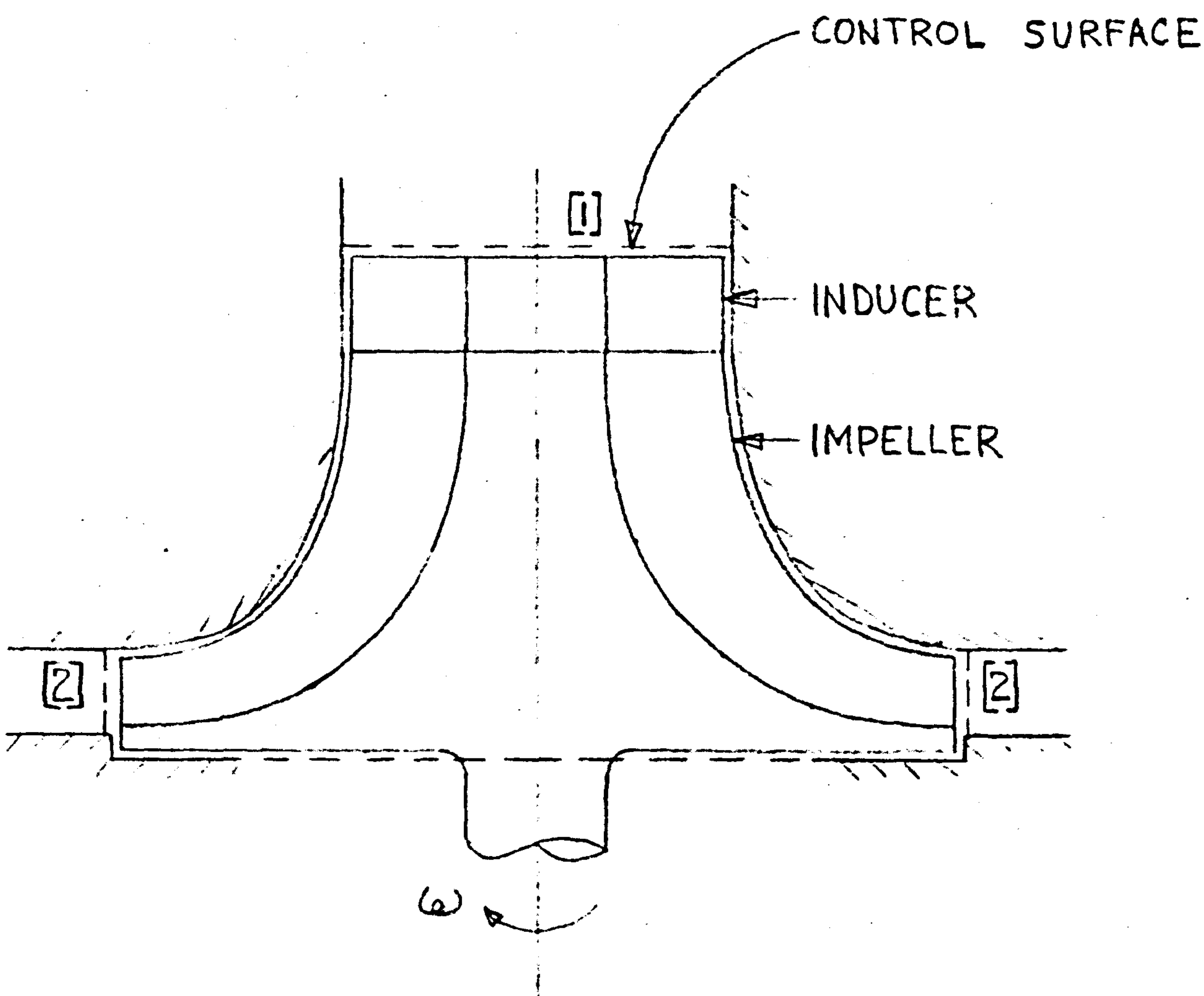

Figure 13

Compressor Inertial Control Surface

Calculation of ωr_2

From (121), Appendix H,

$$\frac{W_{shaft}}{M} - \frac{T_{friction}\,\omega}{m} = \frac{\omega}{g_o}\left[(r\,V_\theta)_2 - (r\,V_\theta)_1 \right]_I \qquad (121)$$

From (107b), Appendix G,

$$\frac{W_{shaft}}{M} - \frac{W_{friction}}{M} = J(h_{o2} - h_{o1})_I \qquad (107b)$$

We choose our fixed inertial control surface as shown in Figure 13. The only parts of the CS which are not at fixed walls are the inlet and exit areas, [1] and [2]. If we assume that the flow at [1] and [2] is one dimensional, the friction work term in (107b) is zero since there is no motion at the fixed walls and no force component parallel to the CS at [1] and [2]. This conclusion is true even if the fluid were viscous.

In (121), for a viscous fluid, $T_{friction}$ will not be zero, even though the CS boundries are fixed walls. By our assumption of a frictionless (non-viscous) fluid, however, this term is assumed to be zero.

Combining (107b) and (121), and noting that $V_{\theta 1} \equiv 0$, $V_{\theta 2} \equiv f_s \omega r_2$ where $f_s \equiv$ slip factor,

$$\frac{f_s \omega^2 r_2^2}{g_o} = J(h_{o2} - h_{o1})_I = J\ c_p\ (T_{o2} - T_{o1})_I$$

$$\omega r_2 = \sqrt{\frac{g_o J c_p}{f_s}\ (T_{o2} - T_{o1})}$$

$$T_{o2} = T_{o1}\ (\frac{p_{o2}}{p_{o1}})^{\frac{k-1}{k}} = 550\,(6)^{.286} = 930$$

$$T_{o2} - T_{o1} = 380$$

Assuming $f_s = .913$,

$$\omega r_2 = 1582$$

<u>Calculation of inducer and impeller casing radius</u>, r_c

We now select the casing radius which will pass the <u>maximum</u> mass flow at a specified <u>maximum relative Mach number</u>, $M_{1A\ max}$. Figure 14 shows the hub, mean, and casing radii and the mean streamline. The mean radius and streamline are discussed later. The velocity triangles at inducer inlet and outlet are given in Figure 15, which is a cylindrical section A-A through the inducer (see Figure 14).

From Figure 15,

$$W_1^2 = V_1^2 + \omega^2\ r_1^2 \qquad (175)$$

$$V_{1.1}^2 = W_{1.1}^2 + \omega^2\ r_{1.1}^2 \qquad (175a)$$

$$V_{\theta 1} = 0$$

$$V_{\theta 1.1} = \omega r_{1.1}$$

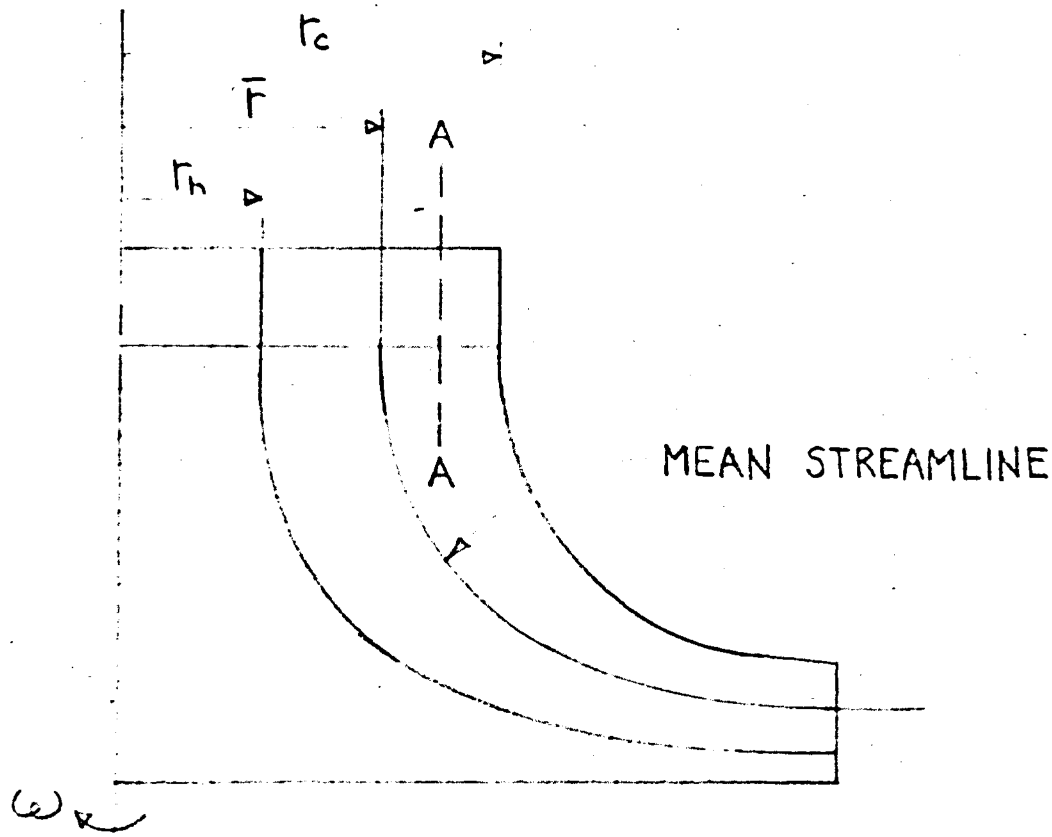

Figure 14

Definition of hub, mean, and casing radii
and mean streamline

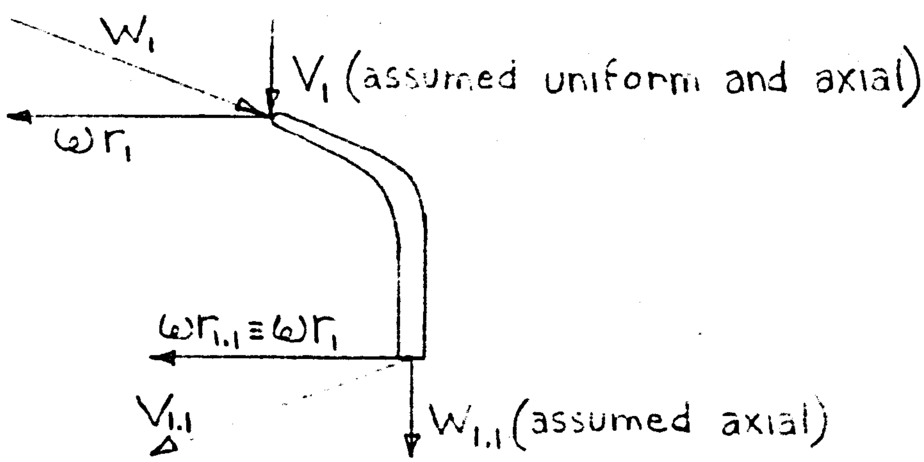

Figure 15

Velocity triangles at inducer
inlet and outlet

For adiabatic flow, we define:

$$T_o \equiv T(1 + \frac{k-1}{2} M_I^2) \tag{176}$$

Combining (129), (128), and (176),

$$c_{o1}^2 = [c^2(1 + \frac{k-1}{2} M_I^2)]_1 \tag{177}$$

Combining (175), (122), and (123),

$$(M_A^2 c^2)_1 = (M_I^2 c^2)_1 + \omega^2 r_1^2 \tag{178}$$

Combining (178) and (177),

$$\left[\frac{M_A^2 c_o^2}{1+\frac{k-1}{2} M_I^2}\right]_1 = \left[\frac{M_I^2 c_o^2}{1+\frac{k-1}{2} M_I^2}\right]_1 + \omega^2 r_1^2$$

$$\left[\frac{M_A^2 - M_I^2}{1+\frac{k-1}{2} M_I^2}\right]_1^{\frac{1}{2}} = \frac{\omega r_2}{c_{o1}} \frac{r_1}{r_2} \tag{179}$$

(179) is a dimensionless "tip speed parameter", which expresses the dimensionless impeller tip speed as a function of Mach numbers and radius ratio. Focusing our attention on the inducer casing radius where M_{1A} is a maximum, we derive a mass flow parameter which will allow us to select an inducer casing radius, at a given M_{1A}, which will pass the maximum mass flow. We define the following:

$$m = \varphi_1 V_1 \pi (r_c^2 - r_h'^2) \tag{180}$$

where m is the actual design mass flow through the machine, r_c is the inducer casing radius, and r_h' is the imaginary hub radius which will give the net flow area normal to V_1 (the flow area which includes the blockage of the inducer blades). The actual hub radius, r_h, must be smaller than r_h' and will be calculated later. Also,

$$m_o = \varphi_{o1} c_{o1} \pi r_2^2 \tag{181}$$

where m_o is an imaginary reference mass flow--the mass flow which would flow through an area equal to πr_2^2 if the fluid density and velocity were φ_{o1} and c_{o1}. We now combine (180) and (181) in dimensionless form:

$$\frac{m}{m_o} = \frac{\varphi_1 V_1 (r_c^2 - r_h'^2)}{\varphi_{o1} c_{o1} r_2^2} = \frac{\varphi_1 (M_I c)_1}{\varphi_{o1} [c(1+\frac{k-1}{2} M_I^2)]_1} \left(\frac{r_c^2}{r_2^2} - \frac{r_h'^2}{r_2^2}\right)$$

$$\frac{\frac{m}{m_o}}{(\frac{r_c}{r_2})^2 - (\frac{r_h'}{r_2})^2} = \left[\frac{M_I}{(1+\frac{k-1}{2} M_I^2)}\right]_1 \frac{p_1}{p_{o1}} \frac{T_{o1}}{T_1} \tag{182}$$

But,

$$\frac{p_1}{p_{o1}} = \left(\frac{T_1}{T_{o1}}\right)^{\frac{k}{k-1}}$$

$$\frac{T_1}{T_{o1}} = \frac{c_1^{\ 2}}{c_{o1}^{\ 2}} = \left[\frac{1}{1+\frac{k-1}{2} M_I^{\ 2}}\right]_1$$

Thus,

$$\frac{p_1}{p_{o1}} \frac{T_{o1}}{T_1} = \left[\frac{1}{1+\frac{k-1}{2} M_I^{\ 2}}\right]_1^{\frac{k}{k-1}} \left(1+\frac{k-1}{2} M_I^{\ 2}\right)_1$$

$$= \left(1+\frac{k-1}{2} M_I^{\ 2}\right)_1^{-\frac{1}{k-1}} \qquad (183)$$

Combining (182) and (183),

$$\frac{\frac{m}{m_o}}{\left(\frac{r_c}{r_2}\right)^2 - \left(\frac{r_h'}{r_2}\right)^2} = M_{II} \left(1+\frac{k-1}{2} M_I^{\ 2}\right)_1^{-\frac{k+1}{2(k-1)}} \qquad (184)$$

Using (184) and (179), we may plot curves of

$$\frac{\frac{m}{m_o}}{\left(\frac{r_c}{r_2}\right)^2 - \left(\frac{r_h'}{r_2}\right)^2} \quad \text{vs.} \quad \frac{\omega r_2}{c_{o1}} \quad \frac{r_c}{r_2}$$ for any assigned maximum value

of M_{1A}. For this design, we are using $M_{1A} = 0.900$ and this curve is plotted in Figure 16, for $k = 1.4$, by taking corresponding values of M_{1I} in (184) and (179). The calculations are given on the next page.

(1)	(2)	(3)	(4)	(5)	(6)	(7)
M_I	$1+\frac{k-1}{2}M_I^2$	$\left[1+\frac{k-1}{2}M_I^2\right]^{-\frac{k+1}{2(k-1)}}$	$\dfrac{\frac{m}{m_o}}{\left[\frac{r_c}{r_2}\right]^2-\left[\frac{r_h'}{r_2}\right]^2}$	$M_A^2-M_I^2$	$\dfrac{M_A^2-M_I^2}{1+\frac{k-1}{2}M_I^2}$	$\frac{\omega r_2}{C_{01}}\ \frac{r_1}{r_2}$
	$=1+.2\times(1)^2$	$=\dfrac{1}{(2)^3}$	$=(1)\times(3)$	$=.810-(1)^2$	$=\dfrac{(5)}{(2)}$	$=(6)^{\frac{1}{2}}$
0.1	1.0020	0.995	0.0995	0.800	0.798	0.892
.2	1.0080	.976	.1952	.770	.764	.873
.3	1.0180	.948	.2844	.720	.707	.840
.4	1.0320	.910	.3640	.650	.630	.793
.5	1.0500	.864	.4320	.560	.533	.730
.6	1.0720	.812	.4872	.450	.419	.647
.7	1.0980	.755	.5285	.320	.291	.539
.8	1.1280	.697	.5576	.170	.151	.388
.85	1.1446	.668	.5680	.087	.076	.276
.9	1.1620	.639	.5751	0	0	0

Column [4] is plotted against column [7] on the following page

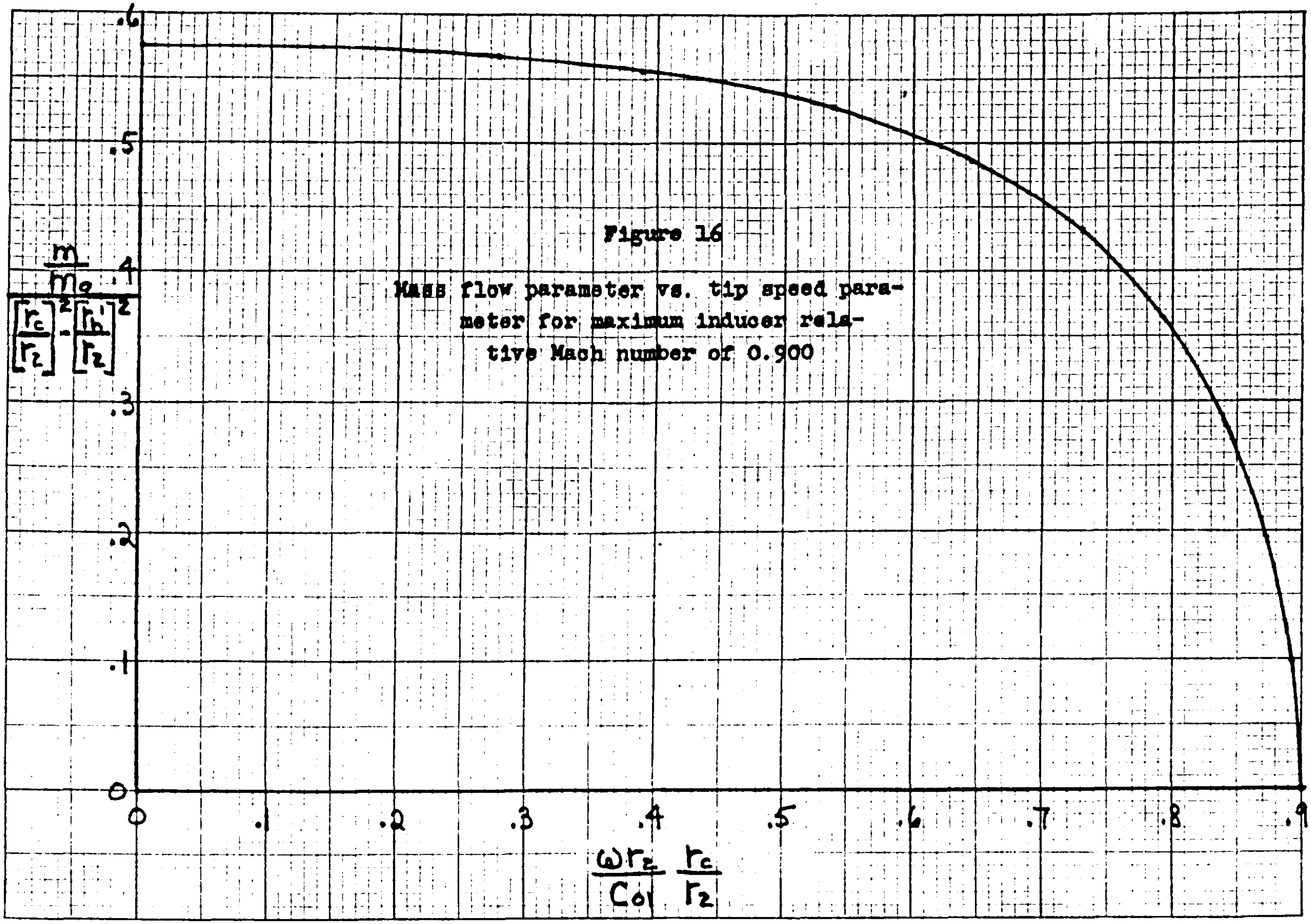

Figure 16

Mass flow parameter vs. tip speed parameter for maximum inducer relative Mach number of 0.900

Now, if we assume a value for $\frac{r_h'}{r_2}$, and knowing ωr_2 and c_{o1}, we can plot a curve of $\frac{m}{m_o}$ vs. $\frac{r_c}{r_2}$. This is done by assuming values of $\frac{r_c}{r_2}$ and, from Figure 16, reading off the corresponding values of $\frac{m}{m_o} / (\frac{r_c}{r_2})^2 - (\frac{r_h'}{r_2})^2$. The values of $\frac{m}{m_o}$ are calculated and plotted against $\frac{r_c}{r_2}$. Figure 17 is this curve for an assumed $\frac{r_h'}{r_2}$ ratio of 0.25.

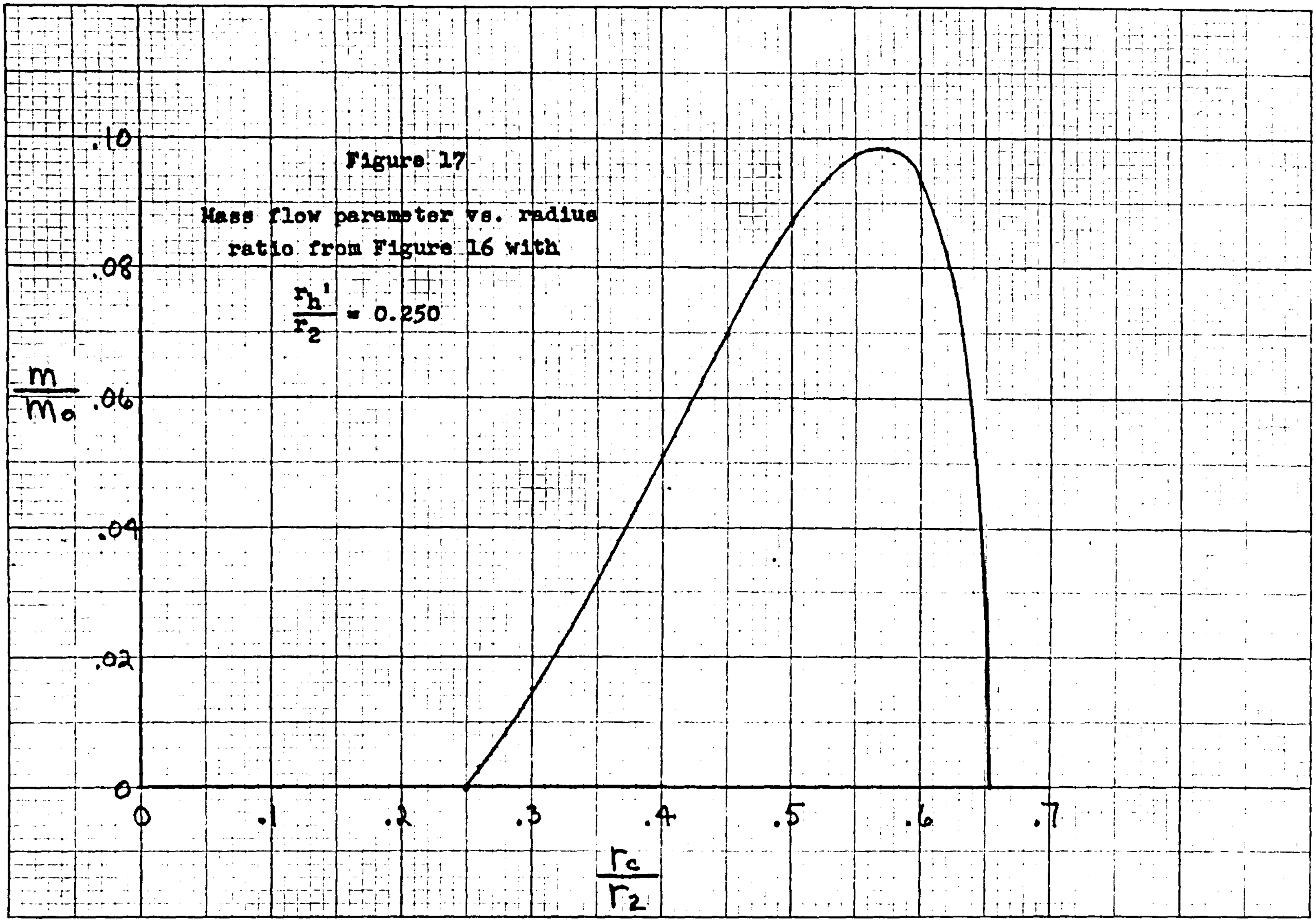

Figure 17

Mass flow parameter vs. radius ratio from Figure 16 with

$\frac{r_h'}{r_2} = 0.250$

From Figure 17, a radius ratio of 0.55 is selected and $\frac{m}{m_o}$ = .0975 is read from the curve.

$$m_o = \frac{10}{.0975} = 102.57$$

$$\rho_{o_1} = \frac{p_{o1}}{R\ T_{o1}} = .0722$$

$$c_{o1} = \sqrt{g_o k\ R\ T_{o1}} = 1149.6$$

$$r_2^{\ 2} = \frac{m_o}{\rho_{o1}\ c_{o1}\ \pi} = .3935$$

$$r_2 = .627$$

$$r_h{}' = 0.25\ r_2 = .1568$$

$$r_c = 0.55\ r_2 = .345$$

The above analysis was adapted from reference 12.

<u>Angular velocity and actual hub radius</u>

$$\omega = \frac{\omega r_2}{r_2} = 2523$$

$$A_{1\ net} = \pi\,(r_c^{\,2} - r_h'^{\,2}) = .296$$

We now assume values for:

$Z_1 \equiv$ number of inducer (and impeller) blades = 23

$t_1 \equiv$ blade thickness at inlet (in a plane normal to V_1) = .005

Then,

$r_h \equiv$ actual hub radius =

$$\frac{Z_1 t_1}{2\pi} + \sqrt{r_c^{\,2} - \frac{r_c Z_1 t_1}{\pi} + \left(\frac{Z_1 t_1}{2\pi}\right)^2 - \left(\frac{A_{1\ net}}{\pi}\right)}$$

$$r_h = .130$$

<u>Properties at inducer inlet</u>

We assume:

$$\varphi_1 = .07$$

Using this assumed density, we can calculate:

$$V_1 = \frac{m}{\rho_1 A_{1\,net}} = 482$$

$$T_1 = T_{o1} - \frac{V_1^2}{2g_o J\, c_p} = 530.7$$

$$p_1 = p_{o1} \left(\frac{T_1}{T_{o1}}\right)^{\frac{k}{k-1}} = 12.98 \quad \text{PSIA}$$

$$\rho_1 = \frac{144\, p_1}{R\, T_1} = .0660 \neq .07$$

Second trial:

$$\rho_1 = .0650$$

Then:

$$V_1 = 520$$

$$T_1 = 527.5$$

$$p_1 = 12.68 \quad \text{PSIA}$$

$$\rho_1 = .0650 \quad \text{O.K.}$$

$$c_1 = \sqrt{g_o k\, R\, T_1} = 1124$$

$$M_{II} = \frac{V_1}{c_1} = .462$$

Properties at impeller inlet

We now calculate the value of W at the impeller inlet. We have shown in Appendix L that W is constant from hub to casing at the impeller inlet *if* W_r is zero at the impeller inlet. By continuity, assuming no change in inducer flow area in planes normal to the Z axis,

$$A_{1\ net} = A_{1.1\ net}$$

$$\rho_1 V_1 = \rho_{1.1} W_{1.1} \text{ (from (95) and Figure 15)}$$

$$33.80 = \rho_{1.1} W_{1.1} \qquad (185)$$

From (165) and (166),

$$\frac{\omega^2 r_{1.1}^{\ 2}}{g_o} = J(h_{o1.1} - h_{o1})_I = J\ c_p\ (T_{o1.1} - T_{o1})_I \qquad (186)$$

Since T_{o1} is constant radially, (186) shows that $T_{o1.1}$ varies as the square of $r_{1.1}$. From (186),

$$T_{o1.1} = T_{o1} + \frac{\omega^2 r_{1.1}^{\ 2}}{g_o J\ c_p} \qquad (187)$$

Using the isentropic relation,

$$p_{o1.1} = p_{o1} \left(\frac{T_{o1.1}}{T_{o1}}\right)^{\frac{k}{k-1}}$$

And (187), we can write:

$$p_{o1.1} = p_{o1} \left(1 + \frac{\omega^2 r_{1.1}^{\;2}}{g_o J \; c_p T_{o1}}\right)^{\frac{k}{k-1}} \tag{188}$$

From (113) and (175),

$$T_{1.1} + \frac{W_{1.1}^{\;2}}{2g_o J \; c_p} - \frac{\omega^2 r_{1.1}^{\;2}}{2g_o J \; c_p} = T_{o1}$$

$$T_{1.1} = T_{o1} - \frac{W_{1.1}^{\;2}}{2g_o J \; c_p} + \frac{\omega^2 r_{1.1}^{\;2}}{2g_o J \; c_p} \tag{189}$$

Also,

$$p_{1.1} = p_{o1.1} \left(\frac{T_{1.1}}{T_{o1.1}}\right)^{\frac{k}{k-1}} \tag{190}$$

$$\rho_{1.1} = \frac{p_{1.1}}{R \; T_{1.1}} \tag{86f}$$

Combining (86f), (190), (188), and (189),

$$\rho_{1.1} = \frac{p_{o1}}{R(T_{o1})^{k/k-1}(2g_o J \; c_p)^{1/k-1}} (2g_o J \; c_p \; T_{o1} - W_{1.1}^{\;2} + \omega^2 r_{1.1}^{\;2})^{\frac{1}{k-1}} \tag{191}$$

To use the one-dimensional approach, as we have done up to now, we must use an average density at the impeller inlet. We define this average density as:

$$\bar{\varphi}_{1.1} \equiv \frac{\int_{r_h}^{r_c} \varphi_{1.1} \, dr}{r_c - r_h} = \frac{m}{A_{1.1\,net} W_{1.1}} \qquad (192)$$

The integral in (192) is evaluated by Simpson's rule after an assumed value of $W_{1.1}$ is inserted in (191). After $\bar{\varphi}_{1.1}$ is calculated, the assumed value of $W_{1.1}$ is checked by using (185). After several trials, we find:

$$\bar{\varphi}_{1.1} = .0778$$

$$W_{1.1} = 435 \qquad (193)$$

Detailed calculations: In (191), we use

$p_{o1} = 2116$

$R = 53.342$

$T_{o1} = 550$

$g_o = 32.174$

$J = 778.2$

$k = 1.4000$

$\omega = 2523$

$$\varphi_{1.1} = 6.410 \times 10^{-19} \left(6.611 \times 10^{6} - W_{1.1}^{2} + 6.365 \times 10^{6}\, r_{1.1}^{2}\right)^{2.500}$$

First trial: Assume $W_{1.1} = 450$

station	r	φ
0	.130	.0695
1	.184	.0724
2	.238	.0765
3	.292	.0817
4	.346	.0882

Simpson's Rule:

$$\int_{r_h}^{r_c} \varphi_{1.1}\, dr \cong \frac{\Delta r}{3} \left(\varphi_o + 4\varphi_1 + 2\varphi_2 + 4\varphi_3 + \varphi_4\right)$$

$$= \frac{.054}{3} (.0695 + .2896 + .1530 + .3268 + .0882) = .01670$$

$$\bar{\varphi}_{1.1} = \frac{.01670}{.346 - .130} = .0773$$

$$W_{1.1} = \frac{33.80}{.0773} = 437 \neq 450$$

Second trial: Assume $W_{1.1} = 425$

station	r	φ
0	.130	.0701
1	.184	.0730
2	.238	.0771
3	.292	.0825
4	.346	.0889

$$\int_{r_h}^{r_c} \varphi_{1.1}\, dr \cong \frac{.054}{3} \; (.0701 + .2920 + .1542$$

$$+ .3300 + .0889) = .01683$$

$$\Phi_{1.1} = \frac{.01683}{.346 - .130} = .0779$$

$$W_{1.1} = \frac{33.80}{.0779} = 434 \neq 425$$

Plotting these results, we have:

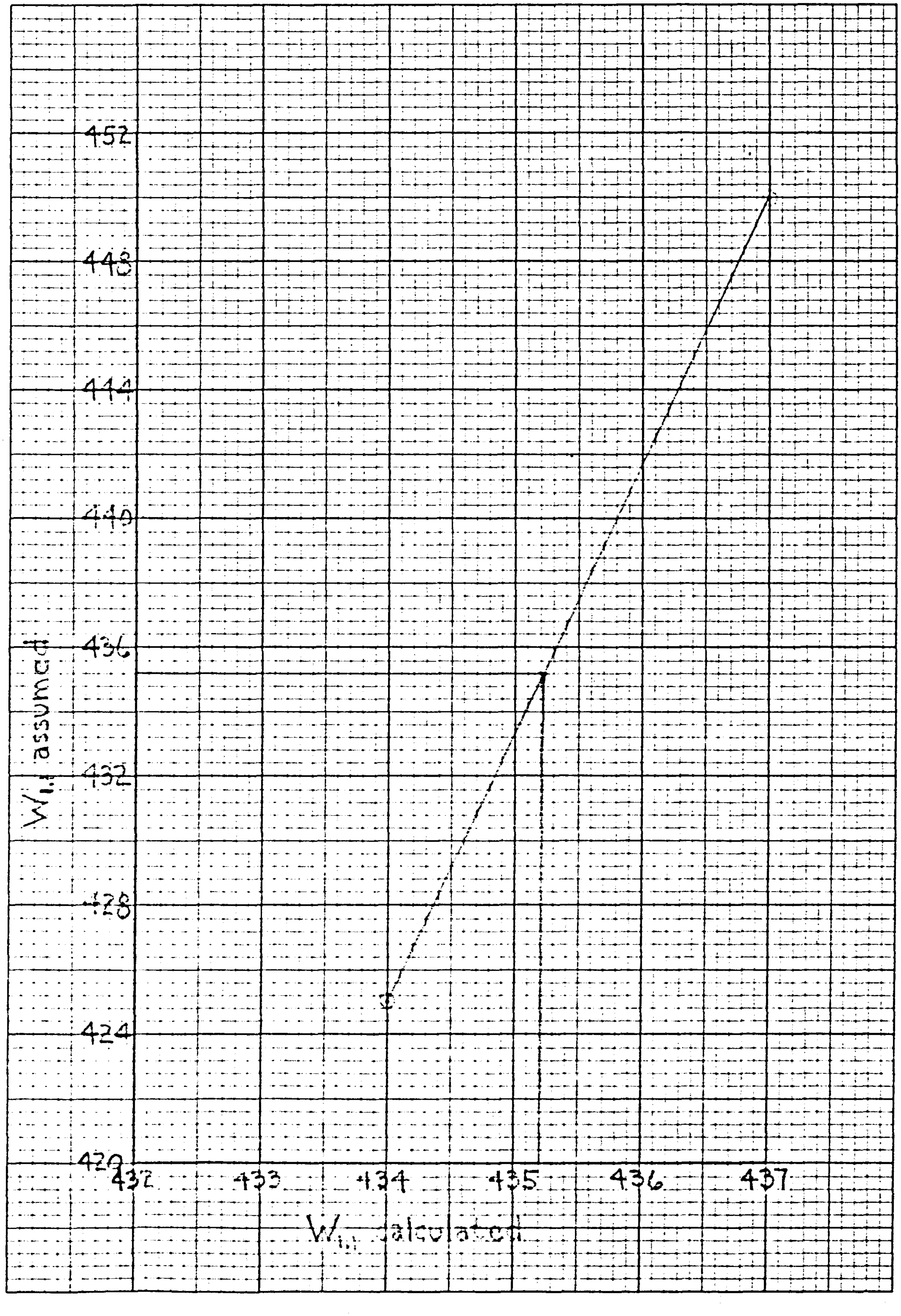
452
448
444
440
436
432
428
424
420
432
433
434
435
436
437
assumed
calculated

The intersection occurs at $W_{1.1} = 435.20$. Using $W_{1.1} = 435$ in (185), we find

$$\bar{\varphi}_{1.1} = \frac{33.80}{435} = .0778$$

Inserting $\bar{\varphi}_{1.1} = .0778$ and $W_{1.1} = 435$ into (191), we find that $\bar{r}_{1.1} = .2487$. We will use this radius as the "mean" radius of the flow at the impeller inlet (see Figure 14).

$$\bar{r}_{1.1} \equiv .2487 \qquad (194)$$

Using (194), we now calculate the following: From (189) and (193),

$$\bar{T}_{1.1} = 550 - 15.75 + 32.75 = 567.0 \qquad (195)$$

From (188),

$$\bar{P}_{o1.1} = 14.7 \left(1 + \frac{3.94 \times 10^5}{3.305 \times 10^6}\right)^{3.50} = 21.80 \text{ PSIA} \qquad (196)$$

From (187),

$$T_{o1.1} = 550 + \frac{3.94 \times 10^5}{6.01 \times 10^3} = 615.5 \qquad (197)$$

From (190), (196), (195), and (197),

$$\bar{p}_{1.1} = 21.80 \left(\frac{567.0}{615.5}\right)^{3.50} = 16.30 \text{ PSIA}$$

This value is checked by computing:

$$\bar{p}_{1.1} = (\bar{\rho} R \bar{T})_{1.1} = 2350 \text{ PSFA} = 16.30 \text{ PSIA} \quad \text{O.K.}$$

In summary, at the impeller inlet,

$$\bar{r} = .2487$$

$$\bar{W} = 435$$

$$\bar{T} = 567$$

$$\bar{p} = 16.30 \text{ PSIA}$$

$$\bar{\rho} = .0778$$

$$\bar{c} = \sqrt{g_o k R \bar{T}} = 1168$$

$$M_A = \frac{\bar{W}}{\bar{c}} = .372$$

$$A_{net} = .296$$

$$r_h = .130$$

$$r_c = .345$$

$$A_{gross} \equiv \pi (r_c^2 - r_h^2) = .321$$

$$\omega = 2523$$

Area variation along the mean streamline

Having found the mean properties at the impeller inlet, we now assume that changes in area, velocity, etc. along the mean streamline represent average or "mean" changes throughout the entire impeller. This assumption permits us to develop a straight-forward design method and is in accord with our previous one-dimensional treatment of Euler's equation and the energy equation.

We now select a particular variation of relative velocity along the mean streamline. From boundry layer considerations (reference 19, page 34), we know that any deceleration of the main flow, with its corresponding rise in pressure, increases the danger of boundry layer separation and subsequent mixing losses. Pressure increases due to the centrifugal force field do not affect separation as the pressure increase acts on main flow and boundry layer alike. It is desirable to avoid deceleration of the main flow whenever possible, so we shall design the impeller channel to have constant relative velocity along the mean streamline. It would be even more desirable to have the flow accelerate along the mean streamline. However, if we realize that some sort of non-rotating diffuser will be used after the impeller, and the flow must decelerate in the diffuser to achieve a pressure rise, we must compromise in our choice of velocity distribution in the impeller. This argument does not apply at all for turbine impellers. The falling pressure in the direction of flow means we can safely decelerate in turbine impeller and have the flow leave the impeller at a low velocity.

There is an additional reason for choosing a constant velocity along the mean streamline. We can show that for constant velocity and subsonic entering Mach number ($\overline{M}_{A1.1} = .372$ for this design) the Mach number at any radius greater than $\overline{r}_{1.1}$ must be <u>less</u> than $\overline{M}_{A1.1}$. Thus, in a compressor impeller with constant mean velocity and subsonic initial relative Mach number, shock waves and choking <u>cannot</u> occur. We show this by using equations (123) and (147) from Appendix J.

$$\overline{c}^2 \, \overline{M}_A{}^2 \equiv \overline{W}^2 \qquad (123)$$

$$\overline{c}^2 = \overline{c}_{1.1}{}^2 - \frac{k-1}{2} (\overline{W} - \overline{W}_{1.1}{}^2) + \frac{k-1}{2}\omega^2(\overline{r}^2 - \overline{r}_{1.1}{}^2) \qquad (147)$$

Combining (123) and (147), and noting that

$$\overline{W} = \overline{W}_{1.1} = \text{constant}$$

we have

$$\overline{M}_A{}^2 = \frac{\overline{W}^2}{\overline{c}_{1.1}{}^2 + \frac{k-1}{2}\omega^2 (\overline{r}^2 - \overline{r}_{1.1}{}^2)}$$

Since $\overline{r}$ is always greater than or equal to $\overline{r}_{1.1}$, $\overline{M}_A{}^2$ is always less than or equal to $\overline{M}_{A1.1}{}^2$ and, for $\overline{M}_{A1.1} = .372$, shock waves and choking cannot occur.

To compute the flow area for constant relative velocity, we use equation (156) from Appendix J.

$$\frac{A}{A_{1.1}} = [1 + \frac{k-1}{2} \frac{\omega^2 r_{1.1}^2}{c_{1.1}^2} [(\frac{r}{r_{1.1}})^2 - 1]]^{-\frac{1}{k-1}} \qquad (156)$$

$A_{1.1} \equiv A_{gross} = .321$

$k = 1.4$

$\omega = 2523$

$r_{1.1} \equiv \bar{r}_{1.1} = .2487$

$c_{1.1} \equiv \bar{c}_{1.1} = 1168$

Detailed calculations of (156) are given in Table 3 and the curve of $\frac{A}{A_{1.1}}$ vs. $\frac{\bar{r}}{\bar{r}_{1.1}}$ is plotted in Figure 18.

TABLE 3

① STATION ALONG MEAN STREAMLINE	② $\bar{r}$	③ $\frac{\bar{r}}{\bar{r}_{1.1}} = \frac{②}{.2487}$	④ $\frac{A}{A_{1.1}} = \left\{1 + \frac{\kappa-1}{2}\left(\frac{\omega \bar{r}_{1.1}}{\bar{c}_{1.1}}\right)^2 \left[\left(\frac{\bar{r}}{\bar{r}_{1.1}}\right)^2 - 1\right]\right\}^{-2.5} = \left\{1 + 0.057720\left[③^2 - 1\right]\right\}^{-2.5}$	⑤ $A_\gamma = .3210 \frac{A}{A_{1.1}}$
1.1	.2487	1.0000	1.0000	.3210
1.2	.2676	1.0760	.9776	.3138
1.3	.2865	1.1520	.9543	.3063
1.4	.3054	1.2280	.9303	.2986
1.5	.3244	1.3044	.9055	.2907
1.6	.3433	1.3804	.8803	.2826
1.7	.3622	1.4564	.8549	.2744
1.8	.3811	1.5324	.8292	.2662
1.9	.4000	1.6084	.8032	.2578
1.10	.4189	1.6844	.7773	.2495
1.11	.4378	1.7604	.7512	.2411
1.12	.4568	1.8368	.7254	.2329
1.13	.4757	1.9127	.6999	.2247
1.14	.4946	1.9887	.6745	.2165
1.15	.5135	2.0647	.6496	.2085
1.16	.5324	2.1407	.6250	.2006
1.17	.5513	2.2167	.6010	.1929
1.18	.5703	2.2931	.5773	.1853
1.19	.5892	2.3691	.5543	.1779
1.20	.6081	2.4451	.5317	.1707
2	.6270	2.5211	.5100	.1637

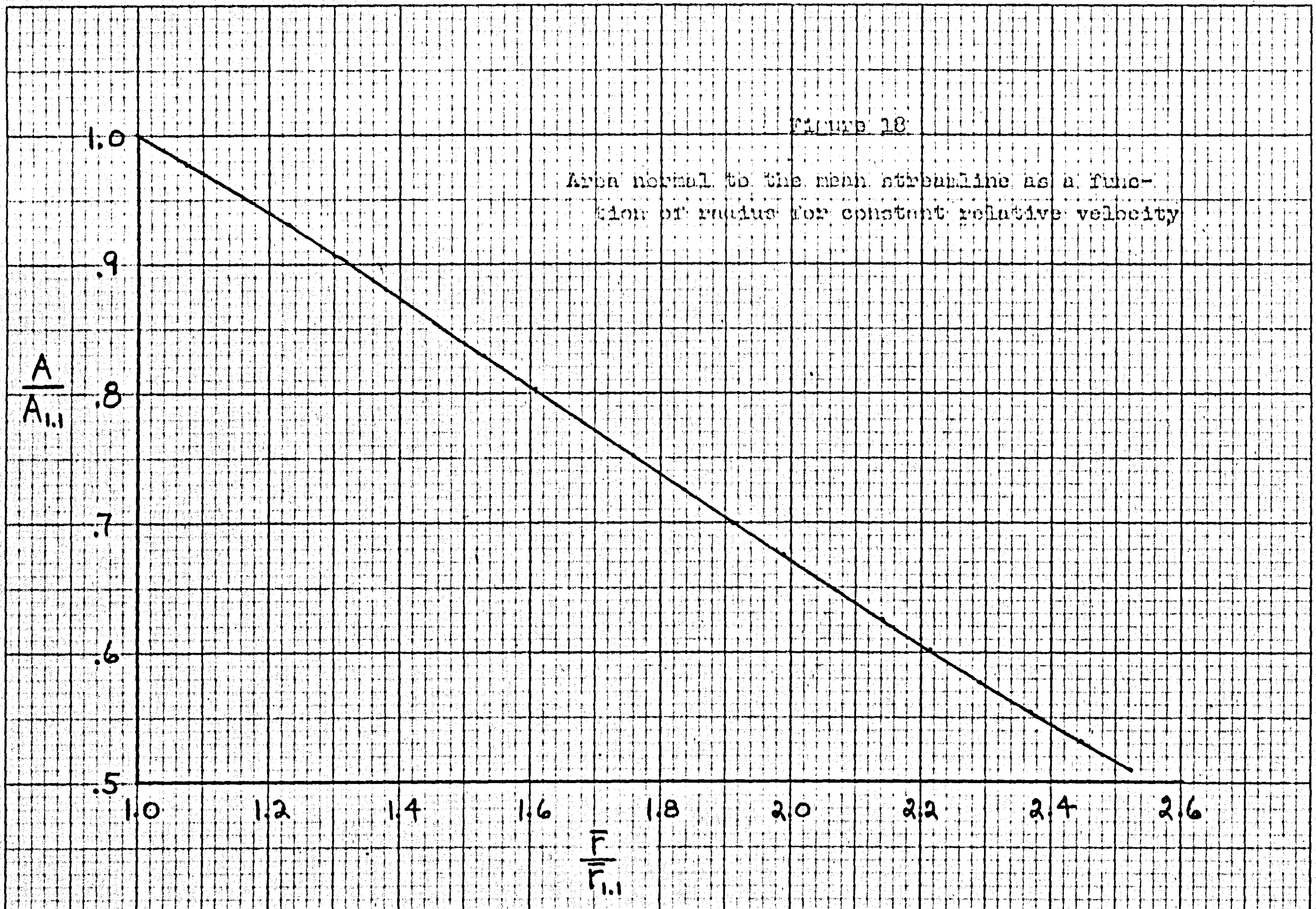

Figure 18

Area normal to the mean streamline as a function of radius for constant relative velocity

Figure 18 gives the required area at any radius to have $\bar{W} = 435 =$ constant along the mean streamline.

Selecting the mean streamline

We must now select a particular mean streamline from the infinite number which could satisfy Figure 18. The choice depends on the axial depth which is available for the impeller, the desired discharge angle (the angle α at the impeller tip - Figure 8), and experience as to what shape of mean streamline yields high efficiency.

Let us assume that we have no experience with "mean streamlines" but are familiar with the basic laws of fluid mechanics. We know that any deceleration of velocity results in a pressure rise with attendant danger of boundry layer separation. Thus we are guided in a choice of mean streamline by the velocity distributions along the hub and casing. These distributions should result in gradual, rather than rapid, decelerations. After the impeller channel has been completely designed, we may use the equations developed in Appendix K to calculate the velocities along the hub and casing. Unfortunately, it has been found impossible to choose a mean streamline by initially specifying desirable velocity distributions along the hub and casing. If these distributions are specified initially, the resulting hub and casing shapes would not satisfy our basic one-dimensional approach. The mean streamline, which would be determined by these specified distributions, would not, in general, lie approximately midway between the hub and casing.

The method of selecting the mean streamline used in this thesis consists in specifying the values of $\overline{\alpha}$ and $\overline{R}_c$ at all radii (Figure 19) and using these values to calculate the hub and casing velocity distributions. We must then refer to boundry layer theory, or to our own experience, as to the desirability of these distributions.

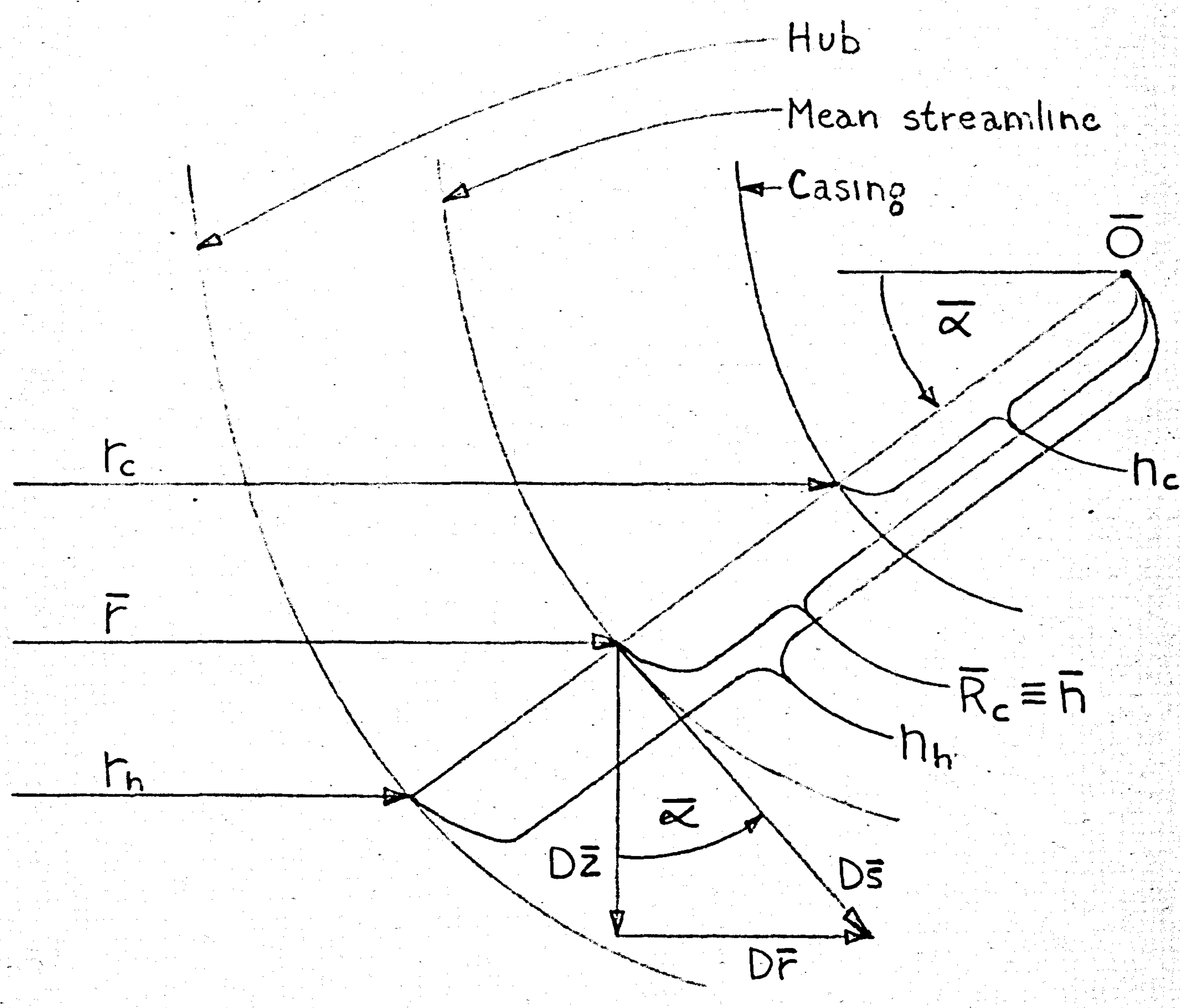

Figure 19

Definition of terms used in the design method

We now derive an approximate equation for $\overline{R}_c$, the radius of curvature of the mean streamline.

From Figure 19,

$$D\overline{s}^2 = D\overline{r}^2 + D\overline{z}^2 \tag{198}$$

$$\frac{D\overline{s}}{D\overline{r}} = [1 + (D\overline{z}/D\overline{r})^2]^{0.5} \tag{199}$$

$$\overline{R}_c = D\overline{s}/D\overline{\alpha} \tag{67}$$

$$\cot \overline{\alpha} = D\overline{z}/D\overline{r} \tag{200a}$$

$$\overline{\alpha} = \text{arc cot } D\overline{z}/D\overline{r} \tag{200b}$$

We now obtain an equation for $\overline{R}_c$ in terms of $\cot \overline{\alpha}$. Differentiating (200b) in the r direction,

$$\frac{D\overline{\alpha}}{D\overline{r}} = -\frac{D^2\overline{z}/D\overline{r}^2}{1 + (D\overline{z}/D\overline{r})^2} \tag{201}$$

From (67), (199), and (201),

$$\bar{R}_c = \frac{D\bar{s}/D\bar{r}}{D\bar{\alpha}/D\bar{r}} = - \frac{[1 + (D\bar{z}/D\bar{r})^2]^{1.5}}{D^2\bar{z}/D\bar{r}^2} \tag{202}$$

From (202) and (200a)

$$\bar{R}_c = - \frac{[1 + \cot^2 \bar{\alpha}\ ]^{1.5}}{\frac{D}{D\bar{r}} \cot \bar{\alpha}} \tag{203}$$

(203) may be approximated for small $\Delta \bar{r}$, as follows:

$$\bar{R}_c \cong - \frac{[1 + \cot^2 \bar{\alpha}\ ]^{1.5}}{\Delta \cot \bar{\alpha} / \Delta \bar{r}} \tag{204}$$

We now define:

$$\Delta \cot \bar{\alpha} \equiv \cot \bar{\alpha}_{r+1} - \cot \bar{\alpha}_r \tag{205}$$

$$\Delta \bar{r} \equiv \bar{r}_{r+1} - \bar{r}_r \tag{206}$$

where sub r is a station (radius) on the mean streamline and sub r+1 is the next station in the direction of flow.

Combining (204) and (205),

$$\bar{R}_c \cong \Delta \bar{r} \frac{[1 + \cot^2 \bar{\alpha}_r]^{1.5}}{\cot \bar{\alpha}_r - \cot \bar{\alpha}_{r+1}} \tag{207}$$

(207) contains all the information needed to determine the mean streamline. The procedure consists in specifying values of $\bar{\alpha}$ at all $\bar{r}$. $\bar{R}_c$ is then calculated from (207). To <u>illustrate the method</u>, we <u>arbitrarily</u> specify a <u>linear</u> variation of $\bar{\alpha}$ with radius, as shown by the curve labeled "linear" in Figure 20.

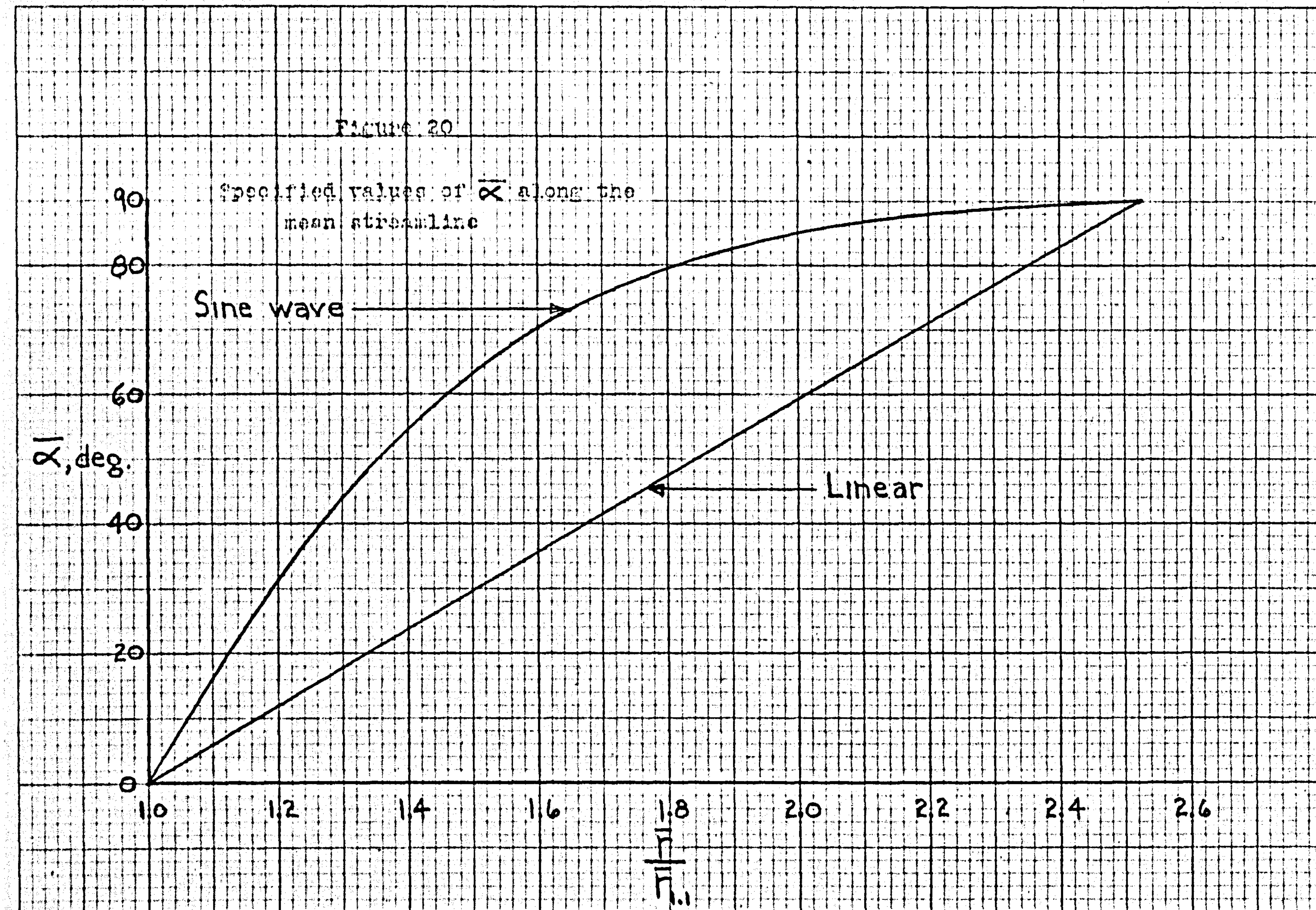

Figure 20
Specified values of $\overline{\alpha}$ along the mean streamline
$\overline{\alpha}$, deg.
Sine wave
Linear
0
20
40
60
80
90
1.0
1.2
1.4
1.6
1.8
2.0
2.2
2.4
2.6
$\frac{\overline{r}}{\overline{r}_{.1}}$

Using values of $\overline{\alpha}$ from Figure 20, $\overline{R}_c$ is calculated as shown in Table 4.

TABLE 4

① STATION ALONG MEAN STREAMLINE	② $\bar{\alpha}$ (SPECIFIED)	③ $\cot\bar{\alpha}$	④ $[1+\cot^2\bar{\alpha}]^{1.5} = [1+③^2]^{1.5}$	⑤ $\cot\bar{\alpha}_r - \cot\bar{\alpha}_{r+1}$	⑥ $\Delta\bar{F}$ (FROM TABLE 3)	⑦ $\bar{R}_c \cong ⑥ \times \frac{④}{⑤}$
1.1	0°	∞	∞	∞	.0189	∞
1.2	4.5	12.7062	2070.5	5.5908	.0189	6.9994
1.3	9.0	7.1154	370.97	2.9501	.0189	2.3766
1.4	13.5	4.1653	78.606	1.0876	.0190	1.3732
1.5	18.0	3.0777	33.888	.6635	.0189	.9653
1.6	22.5	2.4142	17.843	.4516	.0189	.7466
1.7	27.0	1.9626	10.687	.3307	.0189	.6108
1.8	31.5	1.6319	7.0109	.2555	.0189	.5186
1.9	36.0	1.3764	4.9245	.2056	.0189	.4527
1.10	40.5	1.1708	3.6504	.1708	.0189	.4039
1.11	45.0	1.0000	2.8284	.1459	.0190	.3683
1.12	49.5	.8541	2.2745	.1276	.0189	.3369
1.13	54.0	.7265	1.8884	.1137	.0189	.3139
1.14	58.5	.6128	1.6132	.1035	.0189	.2952
1.15	63.0	.5095	1.4137	.0953	.0189	.2804
1.16	67.5	.4142	1.2681	.0893	.0189	.2684
1.17	72.0	.3249	1.1625	.0848	.0190	.2605
1.18	76.5	.2401	1.0876	.0817	.0189	.2516
1.19	81.0	.1584	1.0379	.0797	.0189	.2461
1.20	85.5	.0787	1.0093	.0787	.0189	.2424
2	90.0	0	1.0000	—	—	—

The mean streamline is now completely determined as we know its angle with the Z axis ($\overline{\alpha}$) and its radius of curvature at all stations. We may layout the mean streamline as follows:

1. Draw, to a <u>large</u> scale (4 times or larger), all the radii from column 2 of Table 3.

2. At 4 or 5 points on each radius, draw a short streak which has the correct $\overline{R}_c$ and $\overline{\alpha}$ for that radius, from columns 2 and 7 of Table 4.

3. Using a French curve, draw a smooth curve which has the correct angle and radius of curvature at all stations. This is the mean streamline.

Figure 21 is the layout (half size) of the design of Table 4.

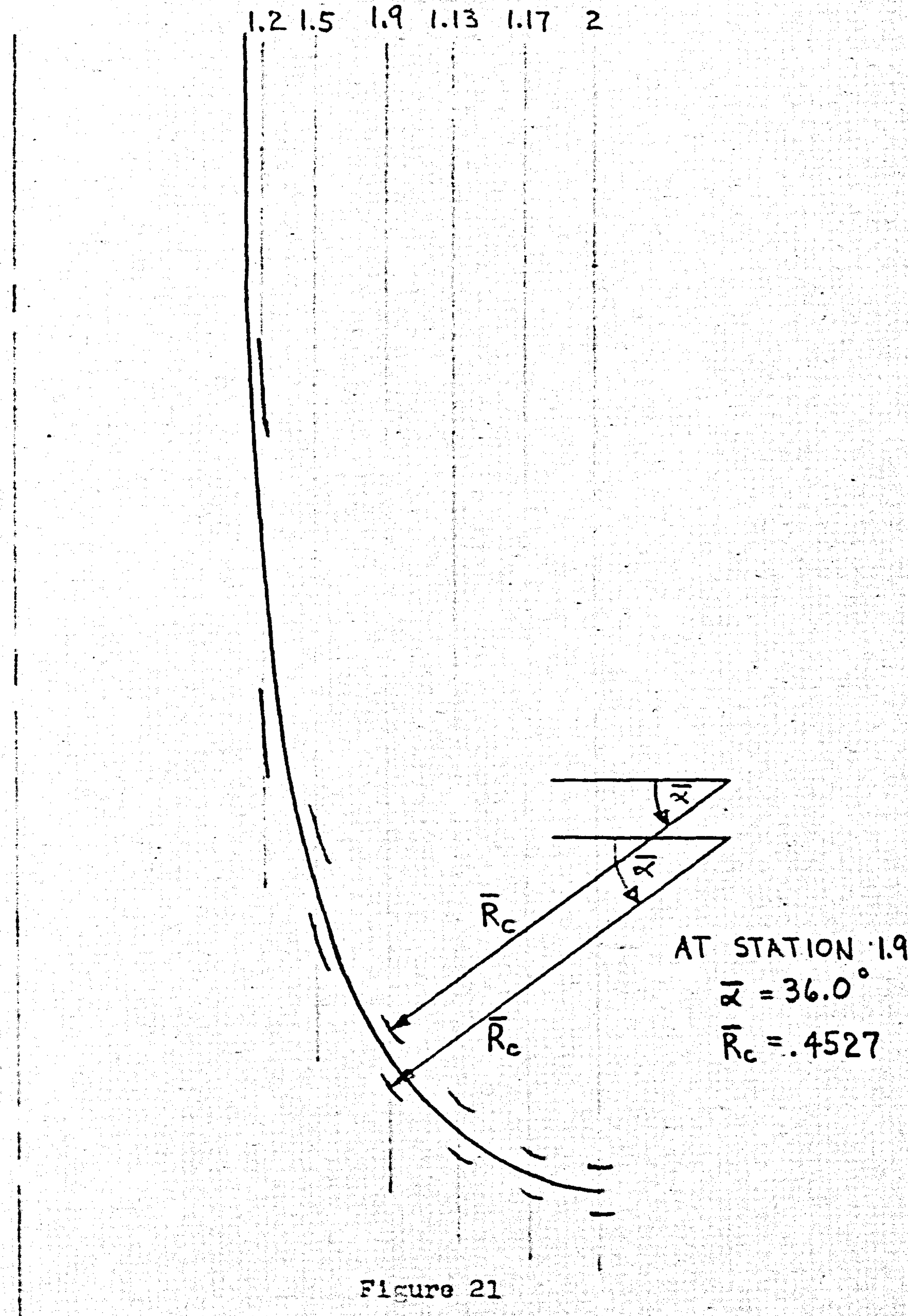

Figure 21
Layout of mean streamline (Table 4)

Hub and casing layout

To determine the hub and casing, we use the geometric relations given in Figure 19.

A_{gc} ≡ surface area of a truncated cone between the mean streamline and the casing

$$A_{gc} = \frac{\pi}{\cos \overline{\alpha}} (r_c^{\,2} - \overline{r}^2) \qquad (0 < \cos\overline{\alpha} \leqq 1) \qquad (208)$$

A_{gh} ≡ surface area of a truncated cone between the mean streamline and the hub

$$A_{gh} = \frac{\pi}{\cos \overline{\alpha}} (\overline{r}^2 - r_h^{\,2}) \qquad (0 < \cos\overline{\alpha} \leqq 1) \qquad (209)$$

In order to obtain physically acceptable hub and casing shapes, it is necessary to specify A_{gc} and A_{gh} as a function of $\overline{r}$. We know A_{gc} and A_{gh} at station 1.1.

$$A_{gc1.1} = \pi\ (.345^2 - .2487^2) = .1799$$

$$A_{gh1.1} = \pi\ (.2487^2 - .130^2) = .1411$$

We specify that, at station 2, the mean streamline is midway between hub and casing.

$$A_{gc2} \equiv A_{gh2} = \frac{A_{g2}}{2} = .08185$$

We now plot curves of A_{gc} and A_{gh} as a function of $\frac{\overline{r}}{\overline{r}_{1.1}}$, taking care that $A_{gc} + A_{gh} = A_g$ in Table 3.

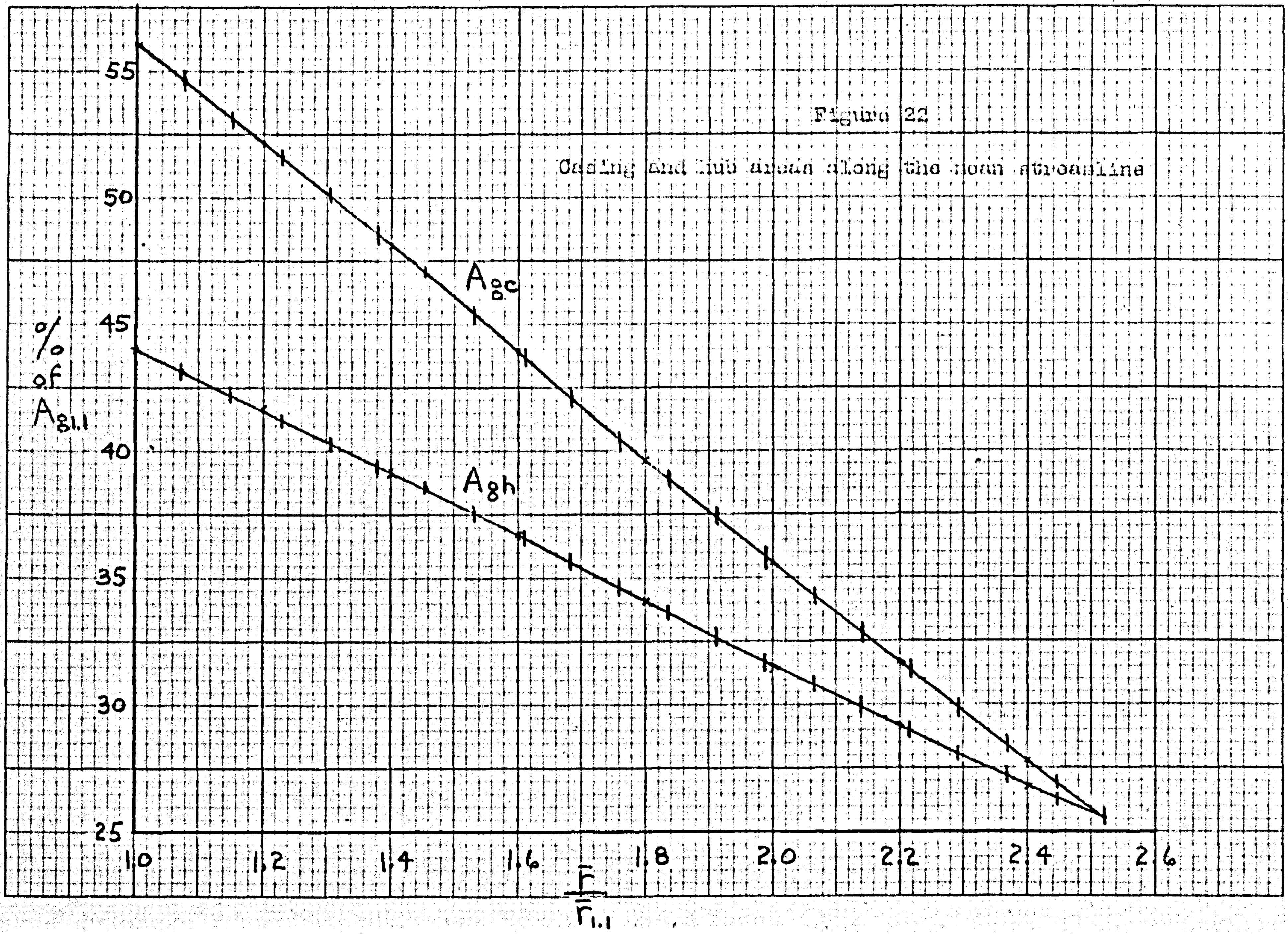

Figure 22

Casing and hub areas along the mean streamline

Using Figure 22, (208) and (209), we calculate r_c and r_h. From (208) and (209),

$$r_c = [\bar{r}^2 + \frac{A_{gc} \cos \overline{\alpha}}{\pi}]^{0.5} \tag{208a}$$

$$r_h = [\bar{r}^2 - \frac{A_{gh} \cos \overline{\alpha}}{\pi}]^{0.5} \tag{209a}$$

Table 5 presents the detailed calculations.

TABLE 5

① STATION ALONG MEAN STREAMLINE	② A_{gc} FROM FIG. 22	③ A_{gh} FROM FIG. 22	④ $\cos\bar{\alpha}$ FROM TABLE 4	⑤ $\bar{r}$ FROM TABLE 3	⑥ r_c $\left[⑤^2 + \frac{②\times④}{\pi}\right]^{\frac{1}{2}}$	⑦ r_h $\left[⑤^2 - \frac{③\times④}{\pi}\right]^{\frac{1}{2}}$
1.1	.1799	.1411	1.0000	.2487	.3452	.1304
1.2	.1755	.1383	.9969	.2676	.3568	.1664
1.3	.1708	.1355	.9877	.2865	.3685	.1987
1.4	.1666	.1320	.9724	.3054	.3806	.2259
1.5	.1612	.1295	.9511	.3244	.3924	.2569
1.6	.1560	.1267	.9239	.3433	.4047	.2839
1.7	.1510	.1234	.8910	.3622	.4171	.3102
1.8	.1456	.1206	.8526	.3811	.4298	.3354
1.9	.1404	.1174	.8090	.4000	.4430	.3603
1.10	.1348	.1147	.7604	.4189	.4562	.3842
1.11	.1297	.1114	.7071	.4378	.4700	.4082
1.12	.1248	.1081	.6494	.4568	.4843	.4318
1.13	.1197	.1050	.5878	.4757	.4987	.4546
1.14	.1148	.1017	.5225	.4946	.5135	.4772
1.15	.1100	.0985	.4540	.5135	.5286	.4995
1.16	.1051	.0955	.3827	.5324	.5442	.5213
1.17	.1001	.0928	.3090	.5513	.5601	.5430
1.18	.0954	.0899	.2334	.5703	.5765	.5644
1.19	.0909	.0870	.1564	.5892	.5930	.5856
1.20	.0862	.0845	.0785	.6081	.6099	.6064
2	.0819	.0818	0	.6270	.6270	.6270

On the layout of the mean streamline, Figure 21, we draw lines normal to the mean streamline using the values of $\bar{\alpha}$ from Table 4. The intersection of each normal line with the corresponding values of r_c and r_h from Table 5 locates a series of points on the hub and casing. A smooth curve drawn through the points determines the hub and casing completely. Figure 23 is the complete impeller layout (half size).

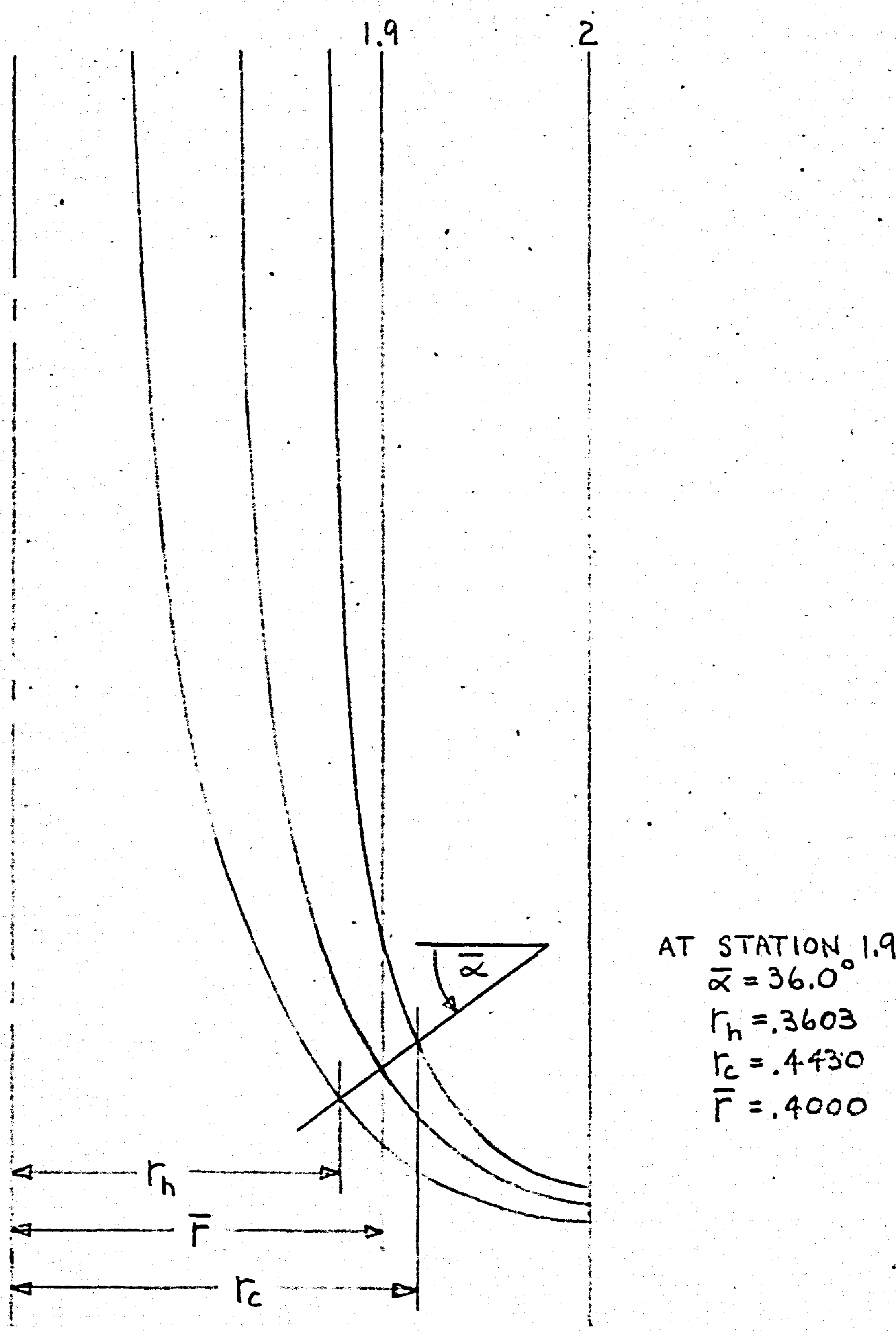

Figure 23
Hub and casing layout - r from Table 3, $\bar{\alpha}$ from Table 4, r_c and r_h from Table 5

Velocity distribution along hub and casing

Having designed the impeller channel to satisfy the area curves of Figures 18 and 22, and the $\overline{\alpha} - \overline{R}_c$ relationship of Table 4, we now investigate the relative velocity distributions along the hub and casing. These distributions are a very important indication of the aerodynamic correctness of the design.

From Appendix K, Table 2, the incremental change in velocity normal to the mean streamline is given by

$$\frac{dW}{W} = -\frac{dn}{R_c} \tag{82}$$

In order to integrate (82), we must know how R_c varies with n, the distance outward from the mean streamline (see Figure 8). The layout of the impeller channel, Figure 23, gives us this information. A full-size view of a portion of Figure 23 is given in Figure 24.

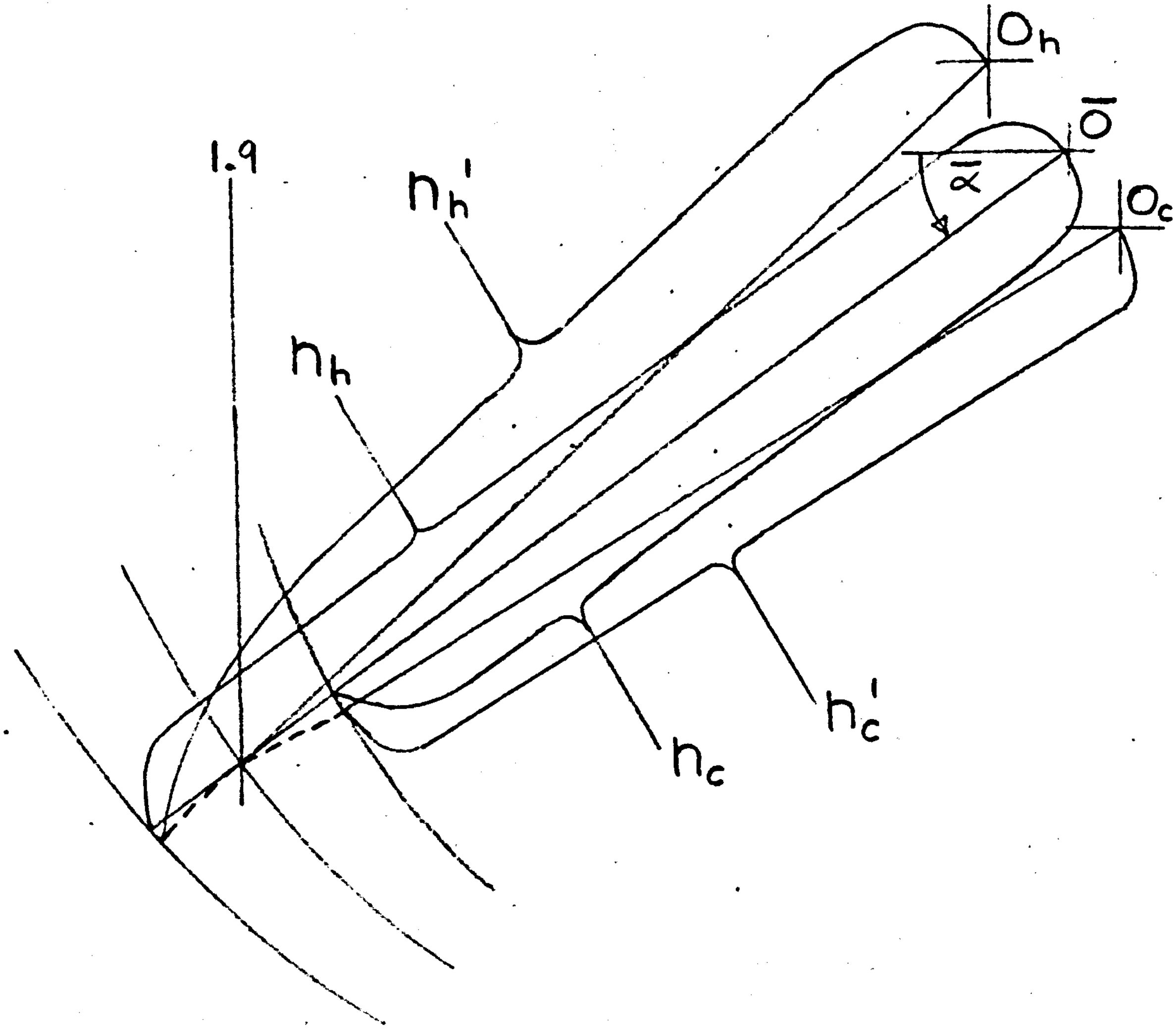

Figure 24

Impeller layout showing curvature of streamlines

From Figure 24, we see that normals to the hub, mean streamline, and casing at each station are, in general, curved lines lying downstream of the $\bar{\alpha}$ lines (the normal line for station 1.9 is shown dashed in Figure 24). The integration of (82) must be done along these curved lines. Figure 24 shows that the curvature of the streamlines <u>decreases</u> from casing to hub, that is, in the positive n direction. This means that W_c must be greater than W_h, except at the impeller inlet, where W_c equals W_h. Also, the radii of curvature of the casing and the hub from centers O_c and O_h are equal to the identical radii from $\bar{O}$. That is, n_c measured from $\bar{O}$ is equal to n_c' measured from O_c; n_h measured from $\bar{O}$ is equal to n_h' measured from O_h.

From these observations, we may write:

$$R_c \equiv n \tag{210}$$

that is, the radii of curvature of the casing, mean streamline, and the hub are identical to the values using $\bar{O}$ as the center of curvature for <u>all</u> streamlines. This fact allows us to integrate (82) directly.

Combining (82) and (210) and integrating from the mean streamline to the casing,

$$\int_{\overline{W}}^{W_c} \frac{dW}{W} = - \int_{\overline{n} \equiv \overline{R}_c}^{n_c} \frac{dn}{n}$$

$$\ln \frac{W_c}{\overline{W}} = - \ln \frac{n_c}{\overline{R}_c}$$

$$\frac{W_c}{\overline{W}} = \frac{\overline{R}_c}{n_c} \tag{211a}$$

Similarly, integrating from the mean streamline to the hub,

$$\int_{\overline{W}}^{W_h} \frac{dW}{W} = - \int_{\overline{n} \equiv \overline{R}_c}^{n_h} \frac{dn}{n}$$

$$\ln \frac{W_h}{\overline{W}} = - \ln \frac{n_h}{\overline{R}_c}$$

$$\frac{W_h}{\overline{W}} = \frac{\overline{R}_c}{n_h} \tag{211b}$$

The results of (211) show that W_c, $\overline{W}$, and W_h satisfy a potential vortex velocity distribution in the impeller channel (reference 9, page 271).

From Figure 19,

$$n_c = \overline{R}_c - \frac{(r_c - \overline{r})}{\cos \overline{\alpha}} \tag{212a}$$

$$n_h = \bar{R}_c + \frac{(\bar{r} - r_h)}{\cos \bar{\alpha}} \qquad (212b)$$

Combining (211) and (212),

$$\frac{W_c}{\bar{W}} = \frac{\bar{R}_c}{\bar{R}_c - \frac{(r_c - \bar{r})}{\cos \bar{\alpha}}} \qquad (213a)$$

$$\frac{W_h}{\bar{W}} = \frac{\bar{R}_c}{\bar{R}_c + \frac{(r - \bar{r}_h)}{\cos \bar{\alpha}}} \qquad (213b)$$

In solving (213) we use:

$\bar{R}_c$ and $\bar{\alpha}$ from Table 4

$\bar{r}$ from Table 3

r_c and r_h from Table 5

Figure 25 presents the results of these calculations as curves of $\frac{W}{\bar{W}_{1.1}}$ as a function of $\frac{\bar{r}}{\bar{r}_{1.1}}$.

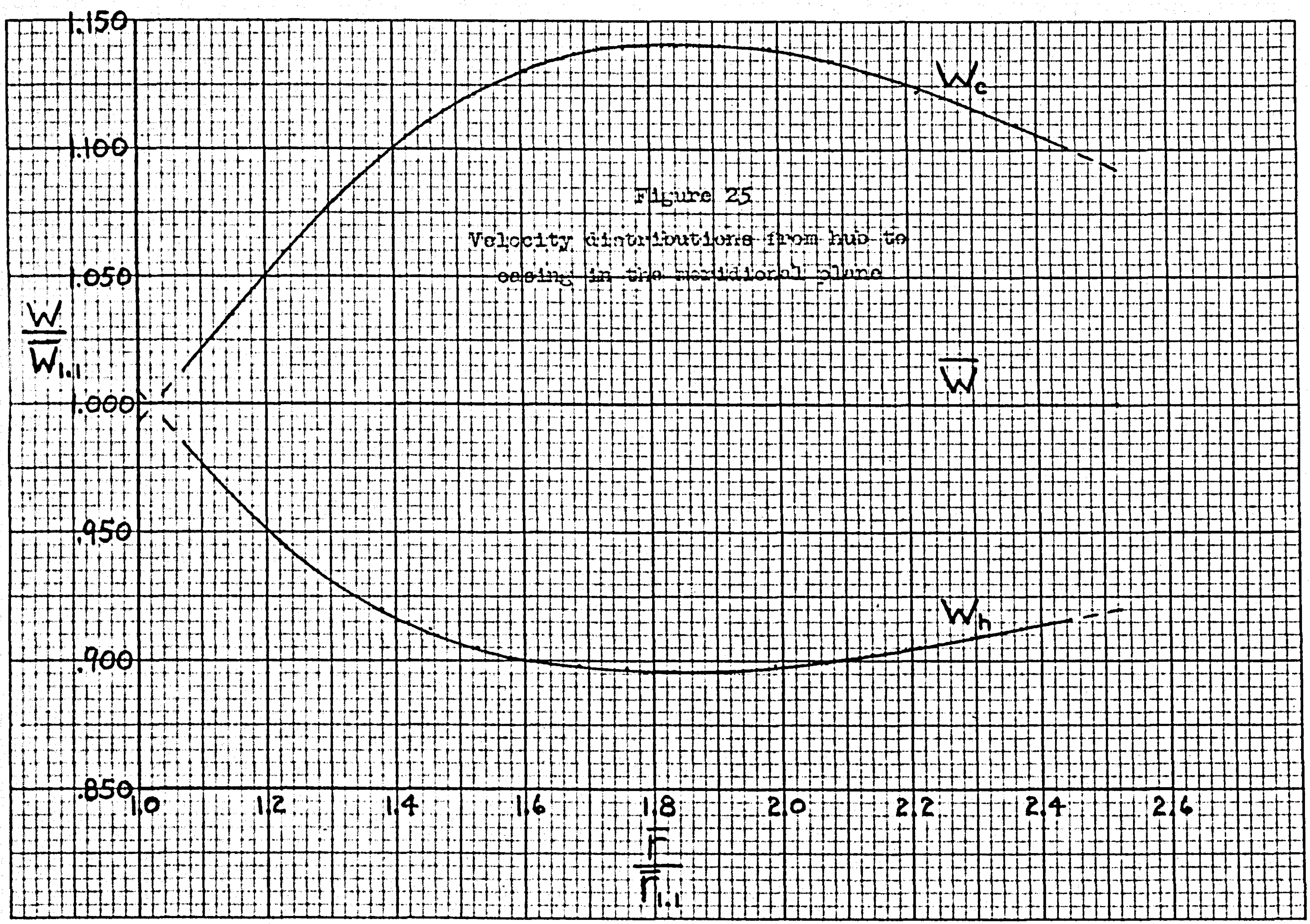

Figure 25

Velocity distributions from hub to casing in the meridional plane

We draw three important conclusions from Figure 25.

1. W_c and W_h are shown to be not quite equal to $\overline{W}$ at the impeller inlet. This discrepency from the previous assumption of constant relative velocity at the impeller inlet (Appendix L) is the result of using just 20 stations along the mean streamline. However, the error is less than one percent, which is certainly acceptable considering the extremely rapid change in cot $\overline{\alpha}$ at the impeller inlet (Table 4).

2. The decelerations of W_c and W_h are quite gradual and should be acceptable as regards boundry layer separation.

3. The large difference between W_c and W_h at the impeller outlet has no significance for frictionless flow. However, with a boundry layer present on the casing, the deceleration of W_c in the diffuser following the impeller may result in boundry layer separation. It would be better to design the impeller to have W_c, $\overline{W}$, and W_h equal at the outlet. This would require that $\overline{R}_c$ be infinite at the outlet.

In view of these conclusions, and the extremely great axial depth of the impeller (Figure 23), it would be advisable to specify a different distribution of $\overline{\alpha}$ with radius (Table 4) and to repeat the design. The curve labeled "sine wave" in Figure 20 would shorten the impeller axial depth considerably while the velocity distributions of Figure 25 would show more rapid decelerations and less difference at the outlet. The final design, as is always the case, must be a compromise between space and weight limitations and the need for highest possible efficiency.

Appendix N

A	area normal to the mean streamline, ft^2
$\bar{F}_\theta$	mean value of distributed body force per unit mass in the tangential direction, lbf/lbm
$\bar{F}_\theta'$	mean value of distributed body force per unit volume in the tangential direction, lbf/ft^3
g_o	universal constant relating force and mass, 32.174 lbm ft/sec^2 lbf
H_A	Bernoulli constant for flow along a relative streamline, ft^2/sec^2
k	ratio of specific heats, C_p/C_v
m	time rate of mass flow of a system, lbm/sec
n	streamline coordinate for two-dimensional flow in the meridional plane
p	static pressure on the surface of a blade, lbf/ft^2
$\bar{p}$	static pressure on the mean streamline, lbf/ft^2
p_p	static pressure on the pressure surface of a blade, lbf/ft^2
p_s	static pressure on the suction surface of a blade, lbf/ft^2
r	radius from Z axis, ft
$\bar{r}$	radius from Z axis to a point on the mean streamline, ft
t	thickness of impeller blades, ft
V	absolute velocity of fluid, ft/sec

V_m meridional component of V, ft/sec

V_θ tangential component of V, ft/sec

W relative velocity of fluid, ft/sec

$\bar{W}$ relative velocity along the mean streamline, ft/sec

$\bar{W}_r$ component of $\bar{W}$ in radial direction, ft/sec

W_c relative velocity along casing in meridional plane (Figure 28), ft/sec

W_h relative velocity along hub in meridional plane (Figure 28), ft/sec

W_p relative velocity on the pressure surface of a blade (Figure 28), ft/sec

W_s relative velocity on the suction surface of a blade (Figure 28), ft/sec

Z number of impeller blades

$\bar{\alpha}$ angle between tangent to mean streamline and Z axis (Figure 19), rad

p pressure difference between adjacent blade surfaces, lbf/ft^2

θ angular spacing between adjacent blade surfaces, rad

ρ static density, lbm/ft^3

$\bar{\rho}$ static density on the mean streamline, lbm/ft^3

ω angular velocity of impeller, rad/sec

sub 1.1 at the impeller inlet

sub 2 at the impeller outlet

Appendix N

RELATIVE VELOCITY ON THE BLADE SURFACES

In Appendix M, Figure 25, we have shown the velocity distribution from hub to casing in the meridional plane for the design of Figure 23. In this Appendix we consider the velocity distribution in the impeller channel in the direction normal to the meridional plane, that is, in the θ direction. We are particularly interested in the velocities on the blade surfaces. The velocity distributions on the blade surfaces give important information as to boundry layer behavior and blade loading.

From (85b), Appendix F, we have the equation for changes in fluid properties along a streamline, which we now take to lie on the surface of a blade.

$$-g_o \left(\frac{k}{k-1}\right) \frac{p}{\rho} - \frac{W^2}{2} + \frac{\omega^2 r^2}{2} = \text{constant} \equiv H_A \qquad (85b)$$

For irrotational flow, we have already shown that

$$\frac{dH_A}{dn} = 0 \qquad (84b)$$

Thus, H_A is constant in any direction and may be evaluated at any convenient location in the accelerating frame. We know the properties at the impeller inlet, station 1.1 on the mean streamline, from Appendix M.

$$H_A = -g_o \left(\frac{k}{k-1}\right) \frac{\bar{p}_{1.1}}{\bar{\varphi}_{1.1}} - \frac{\bar{W}_{1.1}^{\,2}}{2} + \frac{\omega^2 \, \bar{r}_{1.1}^{\,2}}{2} \tag{214}$$

Combining (85b) and (214),

$$g_o \left(\frac{k}{k-1}\right) \frac{\bar{p}_{1.1}}{\bar{\varphi}_{1.1}} \left[1 - \frac{p}{\bar{p}_{1.1}} \; \frac{\bar{\varphi}_{1.1}}{\varphi}\right] + \frac{\bar{W}_{1.1}^{\,2}}{2} \left[1 - \left(\frac{W}{\bar{W}_{1.1}}\right)^2\right]$$

$$+ \frac{\omega^2 \, \bar{r}_{1.1}^{\,2}}{2} \left[\left(\frac{r}{\bar{r}_{1.1}}\right)^2 - 1\right] = 0 \tag{215}$$

From (83),

$$\frac{\bar{\varphi}_{1.1}}{\varphi} = \left(\frac{\bar{p}_{1.1}}{p}\right)^{\frac{1}{k}} \tag{216}$$

Combining (215) and (216),

$$\left(\frac{W}{\bar{W}_{1.1}}\right)^2 = 1 + \frac{2}{\bar{W}_{1.1}^{\,2}} \left\{ g_o \left(\frac{k}{k-1}\right) \frac{\bar{p}_{1.1}}{\bar{\varphi}_{1.1}} \left[1 - \left(\frac{p}{\bar{p}_{1.1}}\right)^{\frac{k-1}{k}}\right]\right.$$

$$\left. + \frac{\omega^2 \, \bar{r}_{1.1}^{\,2}}{2} \left[\left(\frac{r}{\bar{r}_{1.1}}\right)^2 - 1\right] \right\} \tag{217}$$

We have, in (217), the blade surface velocity, W, at any radius, r, as a function of known properties at the impeller inlet and the blade surface pressure, p, at radius r.

We now derive an approximate equation for p as a function of known properties on the <u>mean streamline</u>. This means we shall compute the (approximate) blade surface velocity distributions approximately midway up on the blades, that is, in the θ direction from the mean streamline. These particular distributions may be taken to be the average distributions over the entire blade surfaces (from hub to casing). We proceed as follows: <u>Assume</u> that

$$p_p = \overline{p} + \frac{\Delta p}{2} \tag{218a}$$

$$p_s = \overline{p} - \frac{\Delta p}{2} \tag{218b}$$

where p_p is the pressure on the blade "pressure" surface (leading surface for a compressor), p_s is the pressure on the blade "suction" surface (trailing surface for a compressor), and Δp is the pressure difference in the θ direction between adjacent blades. In other words, we are assuming a linear pressure variation across the channel with $\overline{p}$ as the average value.

We may express Δp in terms of properties on the mean streamline by using (62b) from Appendix E.

$$g_o F_\theta = 2\,\omega W_r \tag{62b}$$

where F_θ is the average "distributed body force per unit mass" in the θ direction (Appendix D) and W_r is the radial component of the relative velocity on the mean streamline. We now define,

$$\overline{F}_\theta' \equiv \overline{\rho}\ \overline{F}_\theta \qquad (219)$$

where $\overline{F}_\theta'$ is the average distributed body force per unit <u>volume</u> in the θ direction and $\overline{\rho}$ is the density on the mean streamline. If we multiply (219) by $\overline{r}\,\Delta\theta$, the distance across the channel between adjacent blades, we obtain the average distributed body force per unit <u>area of blade surface</u>. This body force per unit area is <u>identical</u> to Δp, equation (218). That is,

$$\Delta p \equiv \overline{F}_\theta'\,\overline{r}\,\Delta\theta \qquad (220)$$

Combining (220), (219), and (62b),

$$\Delta p = \frac{2\,\omega\,\overline{W}_r\,\overline{\rho}\ \ \overline{r}\,\Delta\theta}{g_o} \qquad (221)$$

From (65a), Appendix E,

$$\overline{W}_r = \overline{W}\sin\overline{\alpha} \qquad (65a)$$

where $\overline{\alpha}$ is defined in Figure 19, Appendix M, and $\overline{W}$ is the velocity on the mean streamline.

Combining (218), (221), and (65a),

$$p_p = \overline{p} + \frac{\omega\overline{W}\,\overline{\rho}\,\overline{r}\,\Delta\theta\,\sin\overline{\alpha}}{g_o} \qquad (222a)$$

$$p_s = \bar{p} - \frac{\omega \bar{W} \bar{\varphi}\, \bar{r}\, \Delta\theta \sin\bar{\alpha}}{g_o} \qquad (222b)$$

By dividing through by $\bar{p}_{1.1}$, we put (222) in the form of (217)

$$\frac{p}{\bar{p}_{1.1}} = \frac{\bar{p}}{\bar{p}_{1.1}} \pm \frac{\omega \bar{W} \bar{\varphi}\, \bar{r}\, \Delta\theta \sin\bar{\alpha}}{g_o\, \bar{p}_{1.1}} \qquad (223)$$

where the plus sign is used for p_p and the minus sign for p_s. We may put (223) into a more convenient form as follows:

$$\frac{p}{\bar{p}_{1.1}} = \frac{\bar{p}}{\bar{p}_{1.1}} \pm \frac{\omega \bar{W}\, \bar{r}_{1.1}\, \bar{\varphi}_{1.1}}{g_o\, \bar{p}_{1.1}}\, \frac{\bar{r}}{\bar{r}_{1.1}}\, \frac{\bar{\varphi}}{\bar{\varphi}_{1.1}}\, \Delta\theta \sin\bar{\alpha} \qquad (223a)$$

$\dfrac{\bar{p}}{\bar{p}_{1.1}}$ and $\dfrac{\bar{\varphi}}{\bar{\varphi}_{1.1}}$ are easily computed. From (95), Appendix G,

$$m = \bar{\varphi}\ A\ \bar{W} = \text{constant} = \bar{\varphi}_{1.1}\, A_{1.1}\, W_{1.1} \qquad (95)$$

We see that, for $\bar{W} = \bar{W}_{1.1}$ = constant,

$$\bar{\varphi}\, A = \bar{\varphi}_{1.1}\, A_{1.1}$$

$$\frac{\bar{\varphi}}{\bar{\varphi}_{1.1}} = \frac{A_{1.1}}{A} \qquad (224)$$

$\dfrac{A_{1.1}}{A}$ is tabulated in Table 3 for the design of Appendix M. Also, from (83), Appendix F,

$$\bar{p}\ \bar{\varphi}^{-k} = \text{constant} = \bar{p}_{1.1}\ \bar{\varphi}_{1.1}^{-k} \qquad (83)$$

Thus,

$$\frac{\bar{p}}{\bar{p}_{1.1}} = \left(\frac{\bar{\varphi}_{1.1}}{\bar{\varphi}}\right)^{-k} = \left(\frac{\bar{\varphi}}{\bar{\varphi}_{1.1}}\right)^{k} = \left(\frac{A_{1.1}}{A}\right)^{k} \qquad (225)$$

Combining (223a), (224), and (225),

$$\frac{p}{\bar{p}_{1.1}} = \left(\frac{A_{1.1}}{A}\right)^{k} \pm \frac{\omega^{W}\ \bar{r}_{1.1}\ \bar{\varphi}_{1.1}}{g_o\ \bar{p}_{1.1}}\ \frac{\bar{r}}{\bar{r}_{1.1}}\ \frac{A_{1.1}}{A}\ \Delta\theta \sin\bar{\alpha}$$

$$\frac{p}{\bar{p}_{1.1}} = \frac{A_{1.1}}{A}\left[\left(\frac{A_{1.1}}{A}\right)^{k-1} \pm \frac{\omega^{W}\ \bar{r}_{1.1}\ \bar{\varphi}_{1.1}}{g_o\ \bar{p}_{1.1}}\ \frac{\bar{r}}{\bar{r}_{1.1}}\ \Delta\theta \sin\bar{\alpha}\right] \qquad (226)$$

We may estimate $\Delta\theta$ as follows: From Appendix M, Z = number of blades = 23 and t = blade thickness at inlet = .005. Since we do not have the values of blade thickness at all radii, we assume that t = .005 = constant throughout the impeller. Then,

$$\bar{r}\,\Delta\theta = \frac{2\pi\bar{r} - zt}{Z} = \frac{2\pi\bar{r}}{Z} - t$$

$$\Delta\theta = \frac{2\pi}{Z} - \frac{t}{\bar{r}} = .2732 - \frac{.005}{\bar{r}} = .2732 - \frac{.005/\bar{r}_{1.1}}{\bar{r}/\bar{r}_{1.1}} \qquad (227)$$

The general formula for the blade surface velocity, W, as a function of properties on the mean streamline, is obtained by combining (217) with (226) and (227).

$$\left(\frac{W}{\bar{W}_{1.1}}\right)^2 = 1 + \frac{2g_o}{\bar{W}_{1.1}^{\,2}}\left(\frac{k}{k-1}\right)\frac{\bar{p}_{1.1}}{\bar{\rho}_{1.1}}\left[1 - \left\{\frac{A_{1.1}}{A}\left[\left(\frac{A_{1.1}}{A}\right)^{k-1} \pm \frac{\omega \bar{W}\,\bar{r}_{1.1}\,\bar{\rho}_{1.1}}{g_o\,\bar{p}_{1.1}}\;\frac{\bar{r}}{\bar{r}_{1.1}}\left(\frac{2\pi}{Z} - \frac{t/\bar{r}_{1.1}}{\bar{r}/\bar{r}_{1.1}}\right)\sin\bar{\alpha}\right]\right\}^{\frac{k-1}{k}}\right]$$

$$+ \left(\frac{\omega\bar{r}_{1.1}}{\bar{W}_{1.1}}\right)^2\left[\left(\frac{\bar{r}}{\bar{r}_{1.1}}\right)^2 - 1\right] \qquad (228)$$

The solutions of (228) are presented in Figure 26 as curves of $\frac{W}{\bar{W}_{1.1}}$ as a function of $\frac{\bar{r}}{\bar{r}_{1.1}}$, using $\frac{\bar{r}}{\bar{r}_{1.1}}$ and $\frac{A_{1.1}}{A}$ from Table 3 and the following station 1.1 values:

$$\bar{W}_{1.1} = \bar{W} = 435$$

$$\bar{p}_{1.1} = 2350$$

$$\bar{\rho}_{1.1} = .0778$$

$$\bar{r}_{1.1} = .2487$$

Also,

$$\omega = 2523$$

$$Z = 23$$

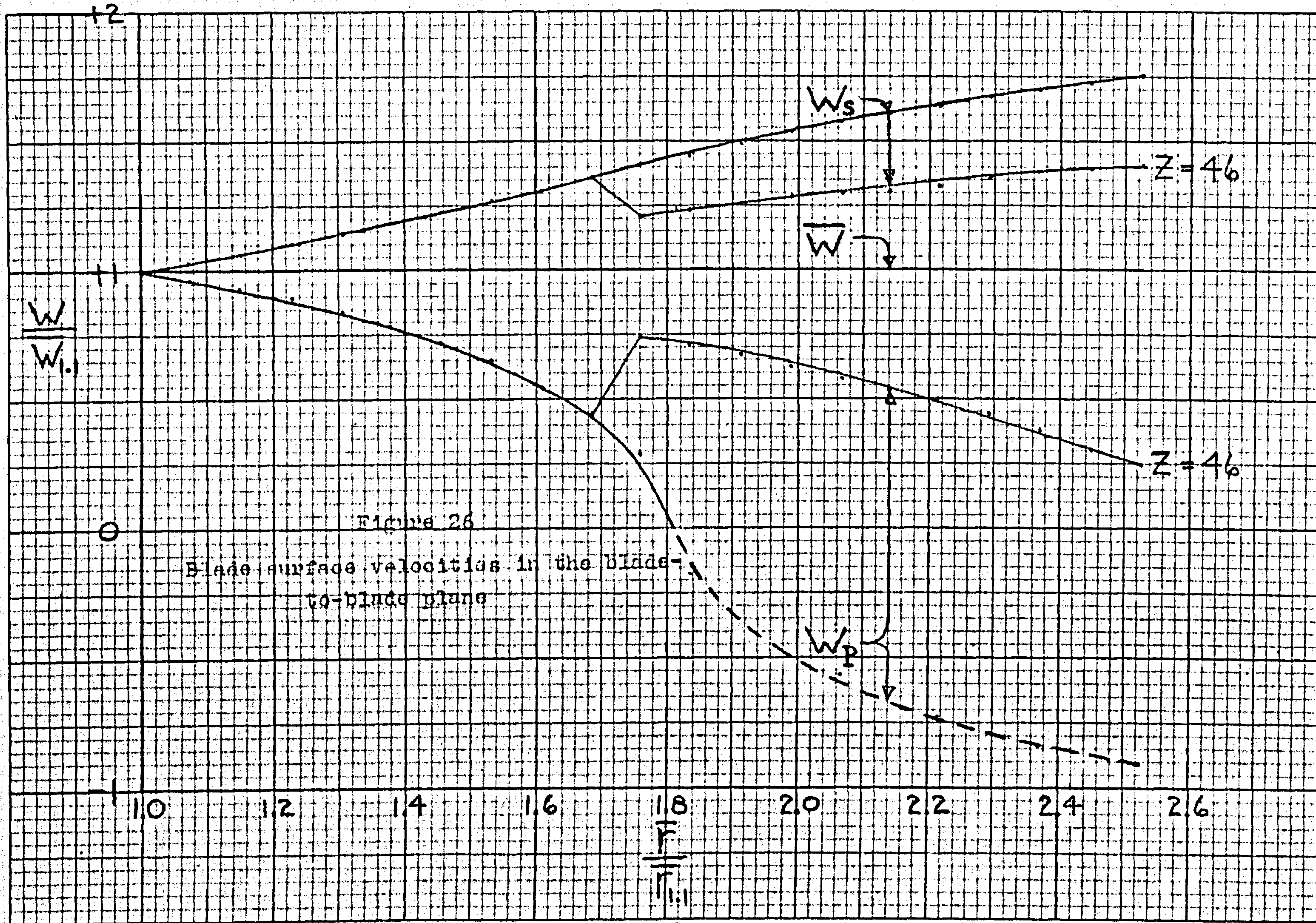

Figure 26

Blade surface velocities in the blade-to-blade plane

There are 5 important conclusions to be drawn from Figure 26.

1. The boundry layer on the blade suction surface is in no danger of separating as W_s is continually increasing.

2. The boundry layer on the blade pressure surface would separate due to the rapid deceleration of W_p at radius ratio 1.8 if it were not for the experimentally observed result that the boundry layer on the pressure surface does <u>not</u> separate under normal operation (reference 13, page 5).

3. W_p is negative (thus imaginary) from a radius ratio of approximately 1.8 to the impeller outlet. In general, a negative value of a blade surface velocity indicates an "eddy", or zone of stagnant air, which is attached to the blade. The eddy decreases the flow area of the channel and thus increases all relative velocities outside of the stagnant area.

4. There is an additional factor which has been neglected in computing Figure 26 - "slip". We have assumed complete guiding of the fluid by the impeller blades and it is well known that such is not the case. Near the impeller outlet the fluid deviates appreciably from the blade direction and, in effect, the flow acts as if the impeller had backward curved blades, rather than radial blades. The velocity triangles are as shown in Figure 27. "Slip" has the effect of <u>increasing</u> the relative velocity near the impeller outlet and thus <u>decreasing</u> the blade loading at the outlet (good).

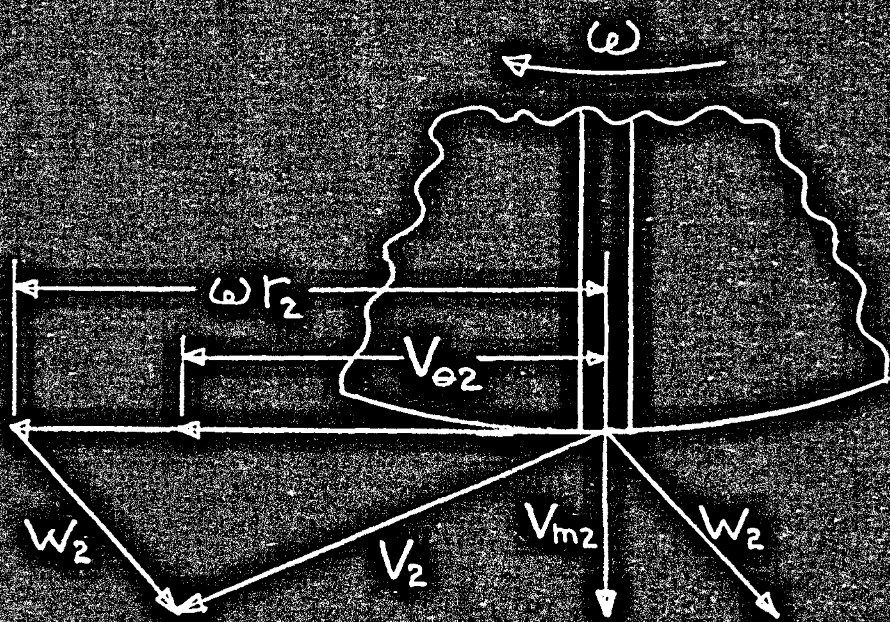

Figure 27

Impeller outlet velocity triangles

5. The great length of blade which shows negative velocity (W_p) in Figure 26 suggests using "splitter" blades which would extend from about radius ratio 1.7 to the outlet. This would eliminate the negative values of W_p and would insure "eddyless" operation (at the design condition). The curves marked "Z = 46" in Figure 26 are the calculated velocities using 46 blades from radius ratio 1.76 to the impeller outlet. For this impeller, splitter blades would certainly be an improvement.

By combining Figures 25 and 26, we obtain a quasi three-dimensional picture of velocities throughout the impeller. Figure 28 is an end view of the impeller showing the location of the velocities of Figures 25 and 26.

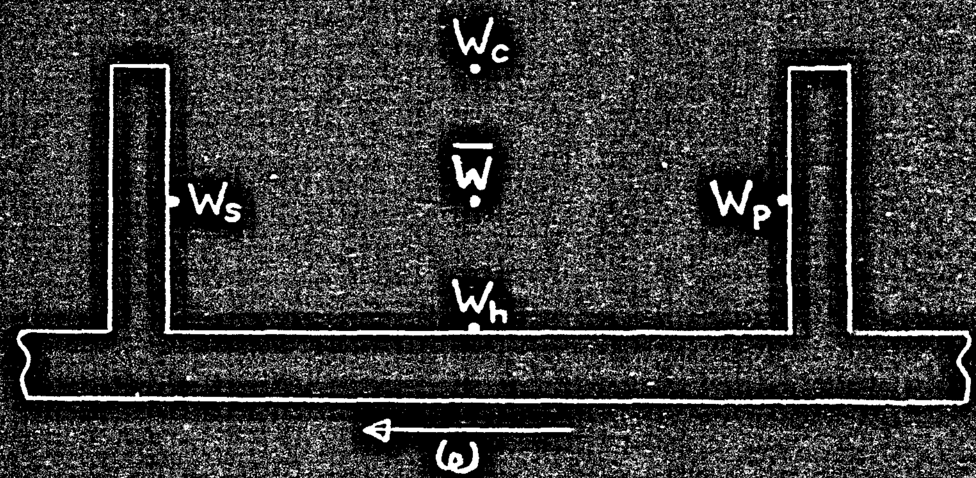

Figure 28
Quasi three-dimensional picture of impeller velocities

Figure 29 combines Figures 25 and 26 on one graph to show the relative magnitudes of the five velocities for this particular design.

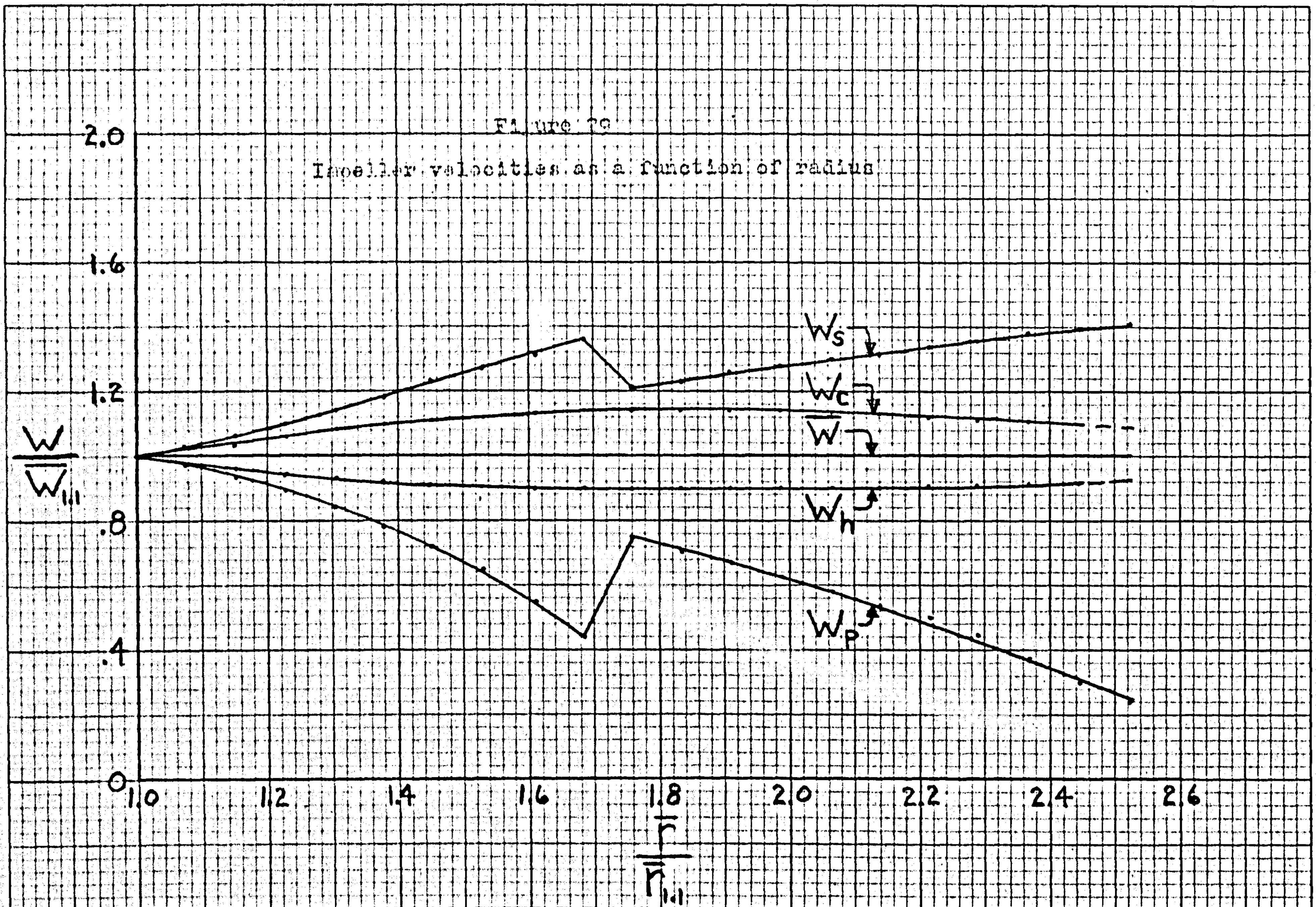

Figure 79

Impeller velocities as a function of radius

REFERENCES

1. R. A. Becker, "Introduction to Theoretical Mechanics" (McGraw-Hill).

2. F. B. Hildebrand, "Advanced Calculus for Engineers" (Prentice-Hall).

3. A. Stodola, "Stream and Gas Turbines" (McGraw-Hill).

4. Kenneth J. Smith and Joseph T. Hamrick, "A Rapid Approximate Method for the Design of Hub-Shroud Profiles of Centrifugal Impellers of Given Blade Shape." NACA TN 3399, 1954.

5. John D. Stanitz and Vasily D. Prian, "A Rapid Approximate Method for Determining Velocity Distribution on Impeller Blades of Centrifugal Compressors." NACA TN 2421, 1951.

6. Chung-Hua Wu, "A General Theory of Three-Dimensional Flow in Subsonic and Supersonic Turbomachines of Axial, Radial, and Mixed-Flow Types." NACA TN 2604, 1951.

7. Joseph T. Hamrick, Ambrose Ginsburg, and Walter M. Osborn, "Method of Analysis for Compressible Flow Through Mixed-Flow Centrifugal Impellers of Arbitrary Design." NACA Report 1082, 1950.

8. J. T. Hamrick, J. Mizisin, and D. J. Michel, "Study of Three-Dimensional Internal Flow Distribution Based on Measurements in a 48-Inch Radial Inlet Centrifugal Impeller." NACA TN 3101, 1953.

9. Ascher H. Shapiro, "The Dynamics and Thermodynamics of Compressible Fluid Flow," volume 1 (Ronald).

10. Joseph H. Keenan, "Thermodynamics" (Wiley).

11. N. R. Balling and V. W. Van Ornum, "Development of a Centrifugal Compressor for a Small Gas Turbine Engine." ASME paper 56-GTP-2.

12. E. S. Taylor, "The Centrifugal Compressor." Gas Turbine Laboratory, Massachusetts Institute of Technology.

13. Donald J. Michel, John Mizisin, and Vasily D. Prian, "Effect of Changing Passage Configuration on Internal Flow Characteristics of a 48-Inch Centrifugal Compressor, I - Change in Blade Shape." NACA TN 2706, 1952.

14. John D. Stanitz and Gaylord O. Ellis, "Two-Dimensional Compressible Flow in Centrifugal Compressors with Straight Blades." NACA Report 954, 1949.

15. S. D. Heron, "Some Elements of Gas Turbine Performance." Paper presented at SAE National Passenger Car, Body, and Materials Meeting, March 6-8, 1956.

16. John D. Stanitz, "Approximate Design Method for High Solidity Blade Elements in Compressors and Turbines." NACA TN 2408, 1951.

17. I. A. Johnsen and Ambrose Ginsburg, "Some NACA Research on Centrifugal Compressors." ASME Transactions, volume 75, 1953, pages 805-817.

18. Seymour Lieblein, "Theoretical and Experimental Analysis of One-Dimensional Compressible Flow in a Rotating Radial-Inlet Impeller Channel." NACA TN 2691, 1952.

19. John D. Stanitz, "Centrifugal Compressors." Contained in "Gas Turbine Lectures," June 29-July 10, 1953, Dept. of Mechanical and Industrial Engineering, University of Michigan, Ann Arbor, Michigan.

20. O. E. Balje, "Design of Radial Flow Turbines." Contained "Gas Turbine and Free Piston Engines Lectures," June 13-June 17, 1955, Dept. of Mechanical and Industrial Engineering, University of Michigan, Ann Arbor, Michigan.